



NATIONAL CENTER FOR EARTHQUAKE  
ENGINEERING RESEARCH

State University of New York at Buffalo



PB97-133508

# Retrofit of Non-Ductile Reinforced Concrete Frames Using Friction Dampers

by

R.S. Rao, P. Gergely and R.N. White

Cornell University  
School of Civil and Environmental Engineering  
Hollister Hall  
Ithaca, New York 14853-3501

Technical Report NCEER-95-0020

December 22, 1995

REPRODUCED BY: **NTIS**  
U.S. Department of Commerce  
National Technical Information Service  
Springfield, Virginia 22161

This research was conducted at Cornell University and was supported in whole or in part  
by the National Science Foundation under Grant No. BCS 90-25010 and  
the New York State Science and Technology Foundation under Grant No. NEC-91029.

## NOTICE

This report was prepared by Cornell University as a result of research sponsored by the National Center for Earthquake Engineering Research (NCEER) through grants from the National Science Foundation, the New York State Science and Technology Foundation, and other sponsors. Neither NCEER, associates of NCEER, its sponsors, Cornell University, nor any person acting on their behalf:

- a. makes any warranty, express or implied, with respect to the use of any information, apparatus, method, or process disclosed in this report or that such use may not infringe upon privately owned rights; or
- b. assumes any liabilities of whatsoever kind with respect to the use of, or the damage resulting from the use of, any information, apparatus, method, or process disclosed in this report.

Any opinions, findings, and conclusions or recommendations expressed in this publication are those of the author(s) and do not necessarily reflect the views of NCEER, or the National Science Foundation, the New York State Science and Technology Foundation, or other sponsors.



---

## **Retrofit of Non-Ductile Reinforced Concrete Frames Using Friction Dampers**

by

R.S. Rao<sup>1</sup>, P. Gergely<sup>2</sup> and R.N. White<sup>3</sup>

December 22, 1995

Technical Report NCEER-95-0020

NCEER Task Number 94-3101B

NSF Master Contract Number BCS 90-25010

and

NYSSTF Grant Number NEC-91029

- 1 Senior Engineer, Simpson, Gumpertz and Heger, Inc., Former Graduate Research Assistant,  
School of Civil and Environmental Engineering, Cornell University
- 2 Professor of Structural Engineering (deceased), School of Civil and Environmental Engineering,  
Cornell University
- 3 James A. Friend Family Professor of Engineering, School of Civil and Environmental Engineering,  
Cornell University

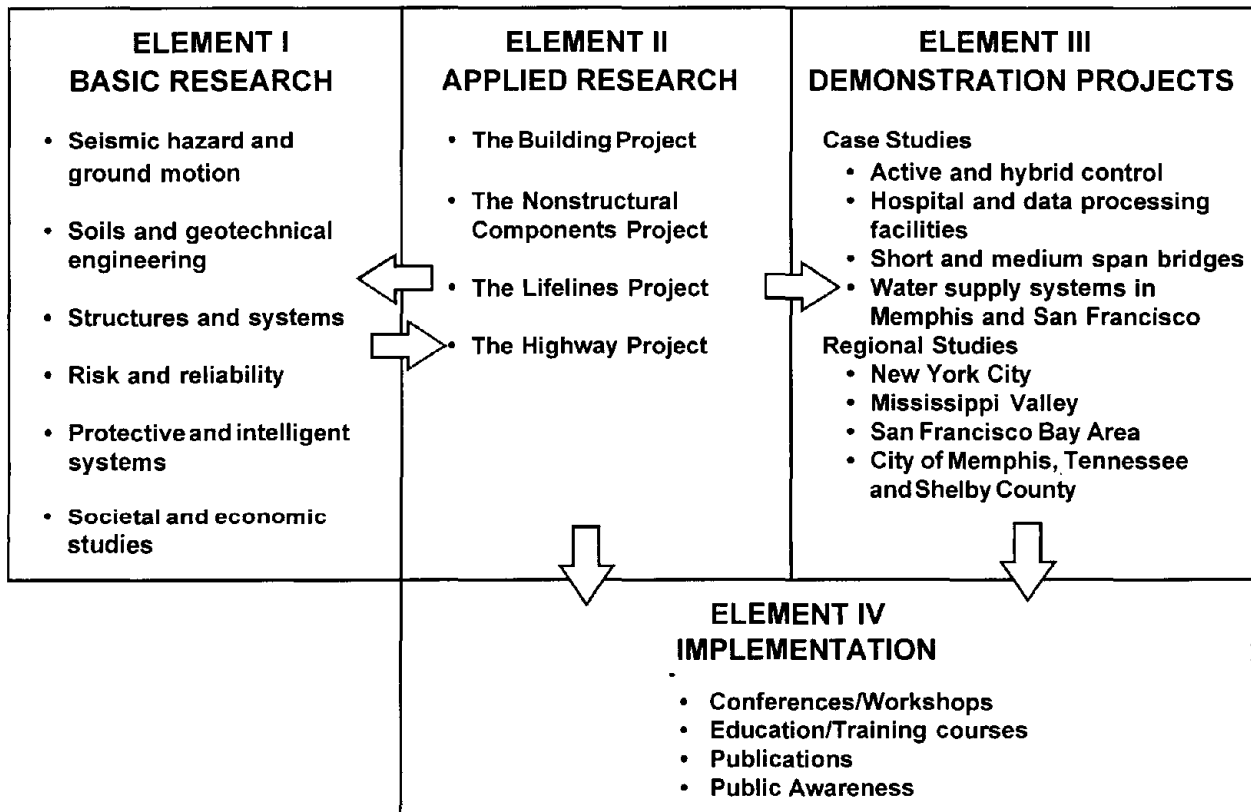
NATIONAL CENTER FOR EARTHQUAKE ENGINEERING RESEARCH  
State University of New York at Buffalo  
Red Jacket Quadrangle, Buffalo, NY 14261



## PREFACE

The National Center for Earthquake Engineering Research (NCEER) was established to expand and disseminate knowledge about earthquakes, improve earthquake-resistant design, and implement seismic hazard mitigation procedures to minimize loss of lives and property. The emphasis is on structures in the eastern and central United States and lifelines throughout the country that are found in zones of low, moderate, and high seismicity.

NCEER's research and implementation plan in years six through ten (1991-1996) comprises four interlocked elements, as shown in the figure below. Element I, Basic Research, is carried out to support projects in the Applied Research area. Element II, Applied Research, is the major focus of work for years six through ten. Element III, Demonstration Projects, have been planned to support Applied Research projects, and will be either case studies or regional studies. Element IV, Implementation, will result from activity in the four Applied Research projects, and from Demonstration Projects.



Research in the **Building Project** focuses on the evaluation and retrofit of buildings in regions of moderate seismicity. Emphasis is on lightly reinforced concrete buildings, steel semi-rigid frames, and masonry walls or infills. The research involves small- and medium-scale shake table tests and full-scale component tests at several institutions. In a parallel effort, analytical models and computer programs are being developed to aid in the prediction of the response of these buildings to various types of ground motion.

reinforced concrete buildings and a state-of-the-art report on unreinforced masonry.

The **protective and intelligent systems program** constitutes one of the important areas of research in the **Building Project**. Current tasks include the following:

1. Evaluate the performance of full-scale active bracing and active mass dampers already in place in terms of performance, power requirements, maintenance, reliability and cost.
2. Compare passive and active control strategies in terms of structural type, degree of effectiveness, cost and long-term reliability.
3. Perform fundamental studies of hybrid control.
4. Develop and test hybrid control systems.

*As stated above, NCEER's tasks in the area of protective systems are oriented toward evaluating the immediate applicability of innovative techniques, and finding their range of usability and limitations. A comprehensive study of evaluation of damping systems using shaking table studies and subsequent modeling has been completed and initial design recommendations were proposed at NCEER. This report takes further the friction damping devices and suggests engineering and economically feasible structural solutions and evaluates their performance. Moreover, design procedures based on capacity-demand spectra developed in numerous NCEER projects were extended to procedure specific design guidelines for friction dampers. The experience gained from this project will further enhance newer developments in seismic codes for retrofit of lightly reinforced concrete frames.*

## ABSTRACT

Recent earthquakes around the world have shown the disastrous effects of earthquakes on infrastructural facilities. The risks are particularly high in the eastern and central parts of United States, where most of the existing stock of buildings were designed without any consideration for seismic loads, and there is a potential for earthquakes to occur. In light of this, the aim of the research presented in the thesis was to propose and evaluate a practical seismic retrofit scheme for such structures. Earlier research had shown that the existing nonductile RC frames would undergo large drifts even under moderate earthquake loading. The proposed method aims to limit the drift levels without increasing the loading on the foundations. The proposed retrofit scheme involves the use of slotted bolt type friction dampers incorporated along with masonry infill walls. The proposed scheme has the advantage of being easy to install in an existing building and being economically realistic. The evaluation procedure for the scheme can be categorized into three parts: experiments, time history analyses and proposal of a design methodology. The scheme was experimentally evaluated using shake table tests on a 1/3rd scale one story one bay specimen. Under two contrasting ground motions, the wall-damper scheme exhibited different effects on the frame response, indicating the importance of ground motion characteristics on the effectiveness of the retrofit. An analytical model was used to simulate the test results. To further understand the effects of using friction dampers in multistory nonductile RC frames, nonlinear time history analyses were performed for a three bay three story nonductile RC frame. Nine different ground motions with two levels of loading were used. For each level of loading, the expected performance criteria in terms of maximum interstory drifts and maximum foundation loads were defined. The analyses showed that introducing the friction dampers improved the performance of the frame for the wide range of ground motions applied. The success of the retrofit scheme however

depends on the slip load setting in the friction dampers. From the analysis process it was determined that a large number of time history analysis runs would be required to obtain the optimum slip load setting. To make the design of friction damper retrofit schemes more acceptable for practicing engineers, a simplified design method, called the Inelastic Demand Spectrum (IDS) method, was proposed. For two different frames, a three story and a ten story frame, it was shown that the IDS method predicted the optimum slip load setting accurately. The method also provided interesting insight into the behavior of nonlinear structures under seismic loading.

To summarize, a practical and economical seismic retrofit scheme was proposed; the scheme was experimentally evaluated using shake table tests; several time history analyses were performed to study its effectiveness and a simplified design methodology was developed for obtaining the optimum slip load.

## TABLE OF CONTENTS

SECTION	TITLE	PAGE
<b>1</b>	<b>INTRODUCTION</b>	1-1
1.1	Motivation:	1-1
1.2	Objectives:	1-3
1.3	Scope and Organization of Report:	1-3
1.4	Review of Research on Existing Retrofit Methods and Damping Methods:	1-5
1.4.1	Conventional Retrofit Schemes:	1-5
1.4.2	Energy Dissipating Devices:	1-6
<b>2</b>	<b>A NEW CONSTRUCTIBLE RETROFIT SCHEME USING MASONRY INFILL AND FRICTION DAMPERS</b>	2-1
2.1	Selecting a Retrofit Scheme for Non-ductile RC Frames:	2-1
2.2	Proposed Retrofit Scheme using Masonry Infill and Friction Dampers:	2-4
2.3	Opinions From Leading Consulting Engineers on the Proposed Retrofit Scheme:	2-9
<b>3</b>	<b>EXPERIMENTAL EVALUATION OF PROPOSED RETROFIT SCHEME</b>	3-1
3.1	Cyclic Testing of Friction Dampers	3-1
3.1.1	Experimental Setup and Test Program for Cyclic Testing	3-1
3.1.2	Results	3-5
3.2	Shake Table Tests on the Proposed Damper Setup	3-5
3.2.1	Objectives	3-5
3.2.2	One Story Semi-rigid Frame	3-8
3.2.3	Installation of Retrofit Scheme	3-10
3.2.4	Ground Motions used in Tests	3-12
3.2.5	Experimental Setup, Instrumentation, and Data Acquisition System	3-15
3.3	Test Program for Shake Table Experiments	3-20
3.4	Results and Analytical Modeling of Tests on Bare Frame	3-21
3.4.1	Stiffness Test	3-21
3.4.2	Free Vibration Test	3-22
3.4.3	Impact Hammer Test	3-22
3.4.4	Dynamic Loading of Frame using Recorded Ground Motions	3-22
3.5	Shake Table Test Results for Frame with Retrofit	3-25
3.6	Interpretation of Test Results	3-27
3.7	Analytical Modeling of Wall-Damper Retrofit Scheme	3-36
3.7.1	Incorporating wall-damper model in IDARC 3.0	3-39

## TABLE OF CONTENTS (cont'd)

SECTION	TITLE	PAGE
<b>4</b>	<b>EVALUATION OF RETROFIT SCHEME FOR A THREE STORY NON-DUCTILE RC FRAME</b>	4-1
4.1	Introduction	4-1
4.1.1	Results from Earlier Tests and Analytical Studies	4-1
4.2	Defining Performance Objectives	4-6
4.2.1	Selection of Earthquake Loading	4-6
4.2.2	Defining Acceptable Response Limits	4-12
4.3	Modeling the Three Story RC Frame	4-17
4.4	Response with Proposed Retrofit Method	4-19
4.4.1	Design of Friction Damper Configuration	4-19
4.4.2	Results from Time History Analysis	4-21
4.5	Summary	4-39
<b>5</b>	<b>A NEW DESIGN PROCEDURE FOR RETROFITTING RC FRAMES WITH FRICTION DAMPERS</b>	5-1
5.1	Introduction	5-1
5.2	Existing design methods	5-1
5.2.1	Seismic design spectra for friction-damped structures [Filiatrault and Cherry (1990)]	5-1
5.2.2	Method proposed in ATC-33	5-5
5.2.3	Method Proposed by C. Li and A. Reinhorn	5-9
5.3	Proposed Design Procedure: Inelastic Demand Spectrum Method	5-10
5.3.1	Pushover analysis to construct the capacity curve	5-10
5.3.2	Equivalent linear SDOF system vs. nonlinear SDOF system	5-15
5.3.3	Inelastic Demand Spectra (IDS)	5-18
5.3.4	Retrofitting with Conventional Methods	5-21
5.3.5	Design of friction dampers for three story RC frame	5-23
5.3.6	Generalized Inelastic Demand Spectra	5-27
5.4	Summary	5-30
<b>6</b>	<b>EXAMPLE PROBLEM FOR DESIGN OF FRICTION DAMPER RETROFIT SCHEME USING THE INELASTIC DEMAND SPECTRUM METHOD</b>	6-1
6.1	Introduction	6-1
6.2	Definition of Retrofit Problem	6-1
6.2.1	Ten story nonductile RC frame	6-1
6.2.2	Earthquake Loading and Desired Performance Criterion	6-3
6.3	Design of Friction Dampers Using the Inelastic Demand Spectrum Method	6-4
6.4	Discussion	6-11

## TABLE OF CONTENTS (cont'd)

SECTION	TITLE	PAGE
7	<b>SUMMARY, CONCLUSIONS AND RECOMMENDATIONS FOR FUTURE RESEARCH</b>	7-1
7.1	Summary and Conclusions	7-1
7.2	Recommendations for Future Research	7-4



## LIST OF ILLUSTRATIONS

FIGURE	TITLE	PAGE
1-1	Summary of thesis objectives	1-1
2-1	Proposed retrofit scheme with masonry infill and friction damper	2-5
2-2	Added damping reduces base shear demand and accelerations.	2-7
2-3	Flow of forces through the wall-dampers under cyclic loading	2-8
2-4	Alternative scheme- replace walls with chevron bracing.	2-10
2-5	Possible installation schemes for friction dampers (part of questionnaire) contd....	2-11
2-5	Possible installation schemes for friction dampers (part of questionnaire) .....cont	2-12
3-1	Schematic Diagram of Friction Damper Specimens	3-2
3-2	Friction damper specimens used for cyclic testing	3-2
3-3	Schematic Diagram of Test Setup for Cyclic Testing on Dampers	3-3
3-4	Response of specimen SP1 to ten cycle tests	3-6
3-5	Results for 100 cycle test on friction damper samples	3-7
3-6	Dimensions and sections designed for shake table model	3-10
3-7	Stage 3 of installation of retrofit scheme	3-12
3-8 (a)	Side-view of test frame	3-13
3-8 (b)	Slotted bolt friction damper	3-13
3-8 (c)	View of bottom of frame column	3-14
3-8 (d)	Semi-rigid connection between beam and column	3-14
3-9(a)	Time history and response spectrum of Taft earthquake	3-16
3-9(b)	Time history and response spectrum of Pacoima earthquake	3-17
3-10	Instrumentation used in test	3-19
3-11	Schematic diagram of data acquisition system used in test.	3-19
3-12	Acceleration time history and PSD from free vibration test	3-23
3-13	Displacement time history and PSD from impact hammer test	3-24
3-14	Estimating frame stiffness from bare frame response	3-26
3-15	Idealized SDOF system	3-26
3-16	Measured pre and post slip stiffness	3-28
3-17(a)	Response of retrofitted frame to moderate level Taft motion	3-29
3-17(b)	Response of retrofitted frame to moderate level Pacoima motion	3-30
3-18(a)	Comparison of bare frame and retrofitted frame response (Taft)	3-31
3-18(b)	Comparison of bare frame and retrofitted frame response (Pacoima)	3-32
3-19(a)	Response spectrum interpretation for damper performance under Taft	3-34
3-19(b)	Response spectrum interpretation for damper performance under Pacoima	3-35
3-20(a)	Analytical modeling of retrofitted frame under Taft	3-37
3-20(b)	Analytical modeling of retrofitted frame under Pacoima	3-38

## LIST OF ILLUSTRATIONS (cont'd)

FIGURE	TITLE	PAGE
4-1	Details of the three story nonductile RC building	4-2
4-2	Process in a seismic evaluation-rehabilitation project	4-7
4-3	“Matching” response spectra for Taft (N21E) earthquake	4-12
4-4	Typical column shear force vs. interstory drift [Beres (1994)]	4-16
4-5	Pushover curve for three story frame	4-16
4-6	Target responses for two levels of earthquake loading	4-18
4-7	Response of three story frame to nine ground motions	4-20
4-8(a)	Response of three story frame with dampers to Earthquake No. 1	4-22
4-8(b)	Response of three story frame with dampers to Earthquake No. 2	4-23
4-8(c)	Response of three story frame with dampers to Earthquake No. 3	4-24
4-9	Effect of friction dampers for 500 year earthquake	4-25
4-10	Effect of friction for 2500 year earthquake	4-26
4-11	Displacement response of frame with and without retrofit under Taft (500 yr)	4-30
4-12	Drift response of frame with and without retrofit under Taft (500 yr)	4-31
4-13	Shear response of frame with and without retrofit under Taft (500 yr)	4-32
4-14	Wall-damper hysteresis under Taft (500 yr)	4-33
4-15	Influence of dampers on story hysteresis for Taft (500 yr)	4-34
4-16	Energy time history of frame with and without retrofit to Taft (500 yr)	4-36
4-17	Influence of slip load variation on RC hysteretic energy	4-37
4-18	Influence of slip load variation on maximum energies	4-37
5-1	Construction of design slip-load spectrum [Filiatrault and Cherry (1990)]	5-2
5-2	Capacity and demand curves for frame with friction dampers [ATC-33 50% submittal draft (1994)]	5-8
5-3	Corrected capacity curve for frame with friction dampers	5-11
5-4	Construction of Q-model [Saidi and Sozen (1981)]	5-11
5-5	Secant stiffness in one cycle	5-12
5-6	Constructing equivalent bilinear SDOF system	5-16
5-7	Comparison of spectral responses	5-17
5-8	Comparison of results from equivalent SDOF and MDOF time history	5-17
5-9	Constructing the Inelastic Demand Spectrum curve.	5-19
5-10	Inelastic Demand Spectra for 500 year Taft for different initial stiffness	5-20
5-11	Estimating response of frame with conventional retrofit	5-22
5-12	Friction damper arrangement for three story RC frame	5-22
5-13	Selecting the optimum damper setup	5-24
5-14	Response of structure for different damper settings	5-26
5-15	Evaluating the accuracy of using IDS method to select dampers setting	5-27
5-16	Generalized IDS curve using Miranda’s R factors	5-29
6-1	Dimensions of ten story RC frame	6-2

### LIST OF ILLUSTRATIONS (cont'd)

<b>FIGURE</b>	<b>TITLE</b>	<b>PAGE</b>
6-2	Capacity curve and equivalent bilinear curve for 10 story frame	6-7
6-3	Capacity curve and acceptable limit	6-8
6-4	IDS curves for $K(\text{initial}) = 1.5, 2.0$ and $3.0 K(\text{bare})$	6-8
6-5	Selecting the optimum bilinear SDOF	6-10
6-6	Pre-slip capacity curve for frame with dampers	6-10
6-7	Frame response for different slip load settings	6-12



## LIST OF TABLES

<b>TABLE</b>	<b>TITLE</b>	<b>PAGE</b>
Table 3-I	Torque Settings for 100 cycles test	3-4
Table 3-II	Summary of tests performed on bare frame	3-20
Table 3-III	Ground motions applied to frame with friction dampers	3-20
Table 4-I	Shake Table Tests by El-Attar (1991)	4-3
Table 4-II	Shake Table Tests by Bracci et. al. (1992)	4-3
Table 4-II	Analytical Results El-Borgi (1993)	4-4
Table 4-III	Results from Simplified Analysis [Beres (1994)];	4-4
Table 4-IV	Description of Selected Ground Motions	4-10
Table 4-V	PGA's for 500 year and 2500 year earthquake	4-11
Table 4-VI	Comparison of Analytical and Bracci et. al.'s Test Results	4-18
Table 6-I:	Section properties used for 10 story frame [Beres (1994)]	6-3



# SECTION 1

## INTRODUCTION

### 1.1 Motivation:

An area of increasing concern is the state of preparedness of the existing infrastructure facilities to withstand natural hazards. In areas considered as strong seismicity regions, the sense of urgency to prepare against earthquakes is higher. Considerable attention and effort has been devoted to evaluate the likely performance of structures (buildings, bridges, towers, etc.) when subjected to severe ground motions. Lessons learned from every major earthquake around the world clearly indicate that the economic and human losses resulting from an earthquake disaster can be immeasurable as seen from two recent earthquake events. Economic losses from the 1994 Northridge earthquake has been estimated to be of the order of tens of billions of dollars, while the January 17, 1995 Kobe (Japan) earthquake has left over 5000 people dead, 26000 people injured and more than 300000 people homeless, with losses in the hundreds of billions of dollars.

As research in earthquake engineering became more intense and widespread and from examination of structures after major earthquakes, seismic design has undergone fundamental changes. The beneficial aspects of providing ductility to absorb energy became more accepted. Due to these developments, modern structures have performed very well in recent earthquakes. However, there exist a large number of buildings (and bridges) which were designed with old detailing practices, thereby making them non-ductile. Many were designed without consideration for any significant lateral loading. Such building frames have been referred to as lightly reinforced concrete structures (LRC) or non-ductile RC frames. The ability of these structures to sustain severe

ground motion is suspect. Several researchers (discussed in Section 2) have investigated approaches to seismically retrofit such deficient structures.

Much of the evaluation and retrofit research, however, has been aimed mainly towards structures in regions of high seismicity. Recent research has revealed that many parts of eastern and central US are also vulnerable to earthquake hazard. Although major earthquakes have been recorded in these regions (St. Louis and Charleston), practically all of the structures in these regions were designed without any consideration for earthquake loading.

A research program was initiated under the auspices of NCEER (National Center for Earthquake Engineering Research), with the goal "to expand and disseminate knowledge about earthquakes, improve earthquake resistant design and implement seismic hazard mitigation procedures to minimize loss of lives and property". The emphasis was on structures in the eastern and central U.S. The program covers a wide range of aspects of earthquake engineering, including seismology, geotechnical engineering, structures and systems, risk and reliability, protective and intelligent systems, and societal and economical studies.

As part of the buildings project, an experimental and analytical research program was initiated at Cornell and SUNY (State University of New York) at Buffalo, to evaluate the seismic resistance of non-ductile frames and to study seismic retrofit schemes for these class of structures.

The research presented in this report is aimed towards developing a retrofit scheme for non-ductile RC frame structures. The retrofit scheme has to limit the drifts in the structure under moderate ground motions. The proposed scheme has to be such that the installation process leads to minimum disruption of activities for the occupants. Also

the scheme has to be made economical in order to be acceptable in moderate and low seismic risk zones, such as the eastern and central U.S.

## **1.2 Objectives:**

The objective of this research is to propose and evaluate a constructible retrofit scheme for non-ductile RC frames. The proposed scheme, as discussed in Section 2, involves using slotted bolt friction dampers placed in masonry infills. Scaled models of friction dampers were tested to study their energy dissipation characteristics. A 1/3 scale model of the retrofit scheme was constructed and tested on a shake table to model the dynamic characteristics of the wall-dampers. Analytical studies using non-linear time history analyses showed that retrofitting non-ductile RC frames with the proposed method would improve their performance for a wide range of earthquake loadings. An important aspect of retrofitting frames with friction dampers is to determine the slip load settings and determine the location of the dampers. A design method has been proposed to design the slip loads in friction dampers. The overall objectives and tasks of this project are summarized in figure 1-1.

In order to make the scheme more useful for practicing engineers, a simplified design method has also been proposed.

## **1.3 Scope and Organization of Report:**

The report has been divided into seven sections. An introduction to the subject matter, objectives and scope of the report are given in Section 1. Also, in Section 1, a brief summary of research in retrofit of buildings is presented. Conventional retrofit schemes and retrofit with supplemental damping devices are discussed. The proposed retrofit method is presented and described in Section 2, along with a discussion of the practical issues involved in seismic retrofit.

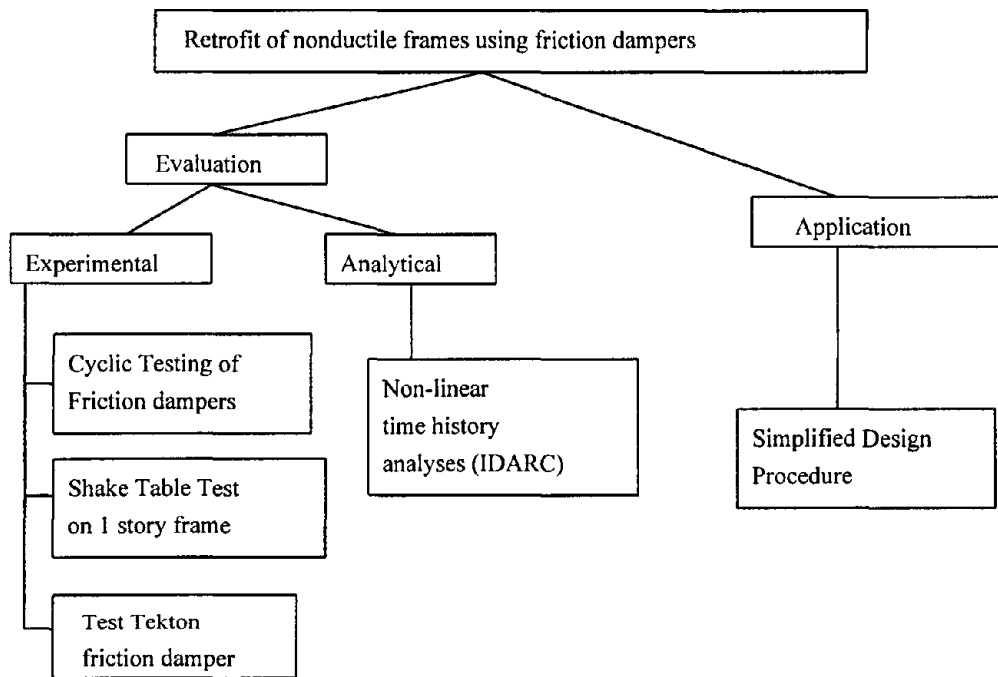


**FIGURE 1-1: Summary of the project objectives**

In the beginning of Section 3, cyclic testing of friction damper specimens is described and test results provided. Also in Section 3, details of the shake table test of the 1/3 scale steel frame with and without the retrofit scheme are presented, results from the tests are presented and examined, and analytical modeling of the frame and the wall-damper is provided.

A three story non-ductile RC frame was considered as an example frame for analytical studies. The frame with and without retrofit was modeled and non-linear time history analyses were performed using the computer program IDARC. Nine different ground motions were considered in the analytical study. Section 4 covers the analytical studies for this three story frame and also presents a discussion on selection of performance objectives. A design procedure, called the Inelastic Demand Spectrum method, is presented in Section 5. The method can be used as a preliminary design approach to

select the location of dampers and slip load settings in the friction dampers. An example design problem is included in Section 6. Summary, discussions, conclusions and ideas for future research are part of the concluding Section 7. In the section on future research, a novel modification of the friction dampers viz. multi-level dampers, is presented and some preliminary analytical results are presented.

#### **1.4 Review of Research on Existing Retrofit Methods and Damping Methods:**

In this section, various conventional retrofit methods evaluated by other researchers are briefly discussed. Also various supplemental damping methods used in seismic engineering are enumerated

##### **1.4.1 Conventional Retrofit Schemes:**

The conventional retrofit schemes most commonly used in practice can be categorized into jacketing of beams and columns, adding steel bracing and adding shear walls. Jacketing can be done either using concrete, steel and carbon fibers. Jacketing results in increased stiffness and strength of the frame. Also, jacketing is intended to improve the ductility of the structural elements. Adding steel bracing or shear wall increases the stiffness and strength of the structure.

Several experimental and analytical studies have been carried out to characterize the performance these retrofit schemes. Alcocer and Jirsa (1990) performed bidirectional cyclic loading tests on full scale beam column joints with and without jacketing. Bracci et. al. (1992) performed shake table tests on a 1/3 scale three story RC frame with columns jacketed and post tensioned. Engelhardt et. al. (1994) performed tests on large scale rectangular column specimens retrofitted with steel jackets. Katsumata et. al. (1987) investigated the retrofit method wherein the concrete column is wrapped with

carbon fibers in a spiral. The fibers were expected to provide confinement and increase the strength and ductility in the column.

One of the most common retrofit strategies used in practice is that of adding shear walls which are cast into existing frames. Ramirez, et. al. (1992) performed tests of frame strengthened by adding shear walls. Pincheira and Jirsa (1994) performed analytical studies for a twelve story RC frame retrofitted with RC walls.

Goel and Lee (1990) performed tests on a two story RC frame which was substantially damaged in earlier tests and then rehabilitated by adding steel bracing. Badoux and Jirsa (1990) investigated a steel bracing system for frames with deep beams and short columns.

As mentioned earlier, conventional retrofit schemes increase the frame stiffness which is intended to result in reduced displacements in the frames. Adding stiffness would cause a reduction in the period of the structure. This reduction in the period would cause a larger spectral acceleration demand on the structure resulting in higher lateral force demand and larger foundation loads. The other drawback of using conventional schemes is that the additional elements introduced in the frame i.e. jacketing, bracing or walls, need to be integrated with the existing structure in order to perform adequately. This can cause difficulty in installation and result in expensive connections.

#### **1.4.2 Energy Dissipating Devices:**

In light of the abovementioned drawbacks of conventional retrofit schemes, it is advantageous to use energy dissipating devices (EDD) for seismic retrofit. In recent years there has been a strong surge in research involving the use of EDDs. The EDDs are used to dissipate much of the input energy during a seismic event thereby reducing the energy demand on the structure. Several damping devices have been developed and

many of these have been used in practice. The types of damping devices are: friction dampers, viscoelastic dampers, fluid viscous dampers and hysteretic devices.

*Friction Dampers:* Devices dissipating energy through Coulomb friction have rectangular hysteresis under cyclic loading. The controlling factors are the coefficient of friction between the two materials and the normal force acting on the contact surface. Several devices have been developed that dissipate energy through friction. Grigorian and Popov (1994) proposed using slotted bolt connections (SBC) as part of diagonal bracing elements. Results from shake table tests indicated that SBCs, when placed in the chevron bracing configuration, are capable of dissipating a large amount of energy. A modified version of the slotted bolt friction damper was proposed by Pall and Marsh (1982). The dampers are placed in combination with X tension braces. The advantage of the configuration is that the stiffness is provided by tension action in the braces. The Pall friction device has been the subject of research of several researchers including Filiatrault and Cherry (1987), Pekau and Guimond (1991). The Pall friction device has been used in several field applications (Pall et. al. (1993)). Fitzgerald (1989) has studied slotted bolt connection friction dampers. Another damping device utilizing friction is the Energy Dissipating Restraint (EDR) from Fluor Daniel Inc. which has self centering capabilities. More recently, Tekton utilized cylindrical surface contact in their friction dampers. Constantinou, Reinhorn (1991) proposed the use of sliding friction for retrofitting bridge structures. One of the earlier commercially manufactured friction dampers was developed by Sumitomo Metal Ltd. Japan.

*Fluid Viscous Damper and Viscoelastic Dampers:* These devices have velocity dependent force response. The fluid viscous dampers operate on the principle of fluid flow through orifices specially shaped so as to produce damping forces proportional to the velocity. Constantinou and Symans (1993) investigated the use of fluid dampers for seismic response mitigation. Fluid dampers do not add stiffness to the existing

structure. Viscoelastic dampers consist of layers of viscoelastic material sandwiched between plates and configured to deform in shear. Viscoelastic dampers add stiffness and viscous damping to the system. Chang et. al. (1993) discuss some of the practical issues associated with the application of viscoelastic dampers to building structures for seismic performance enhancement. Based on shake table tests, it was inferred that adding viscoelastic dampers to structures can achieve a significant reduction of structural response even at high temperature.

*ADAS Devices:* Added Damping and Stiffness (ADAS) elements are mechanical devices which consist of X-shaped plates, which when cyclically loaded dissipate energy by inelastic deformations of those plates. Whittaker et. al. (1991) performed shake table tests on a moment resisting frame with ADAS devices mounted on chevron braces and showed the improved performance of the retrofitted frame.

A thorough experimental study and evaluation of a wide range of damping devices has been conducted at SUNY (Buffalo) (Li and Reinhorn (1995)). A 3 story RC frame was retrofitted with several types of dampers and subjected to different simulated ground motions. The results were analytically modeled using IDARC and the effectiveness of each of the damping devices was quantified.

In the next section a new retrofit scheme will be introduced to improve the performance of nonductile reinforced concrete frames.

## SECTION 2

### A NEW CONSTRUCTIBLE RETROFIT SCHEME USING MASONRY INFILL AND FRICTION DAMPERS

#### 2.1 Selecting a Retrofit Scheme for Non-ductile RC Frames:

As stated in Section 1, the objective of this research is to develop a seismic retrofit scheme for nonductile frames which would be relatively easy to install in an existing structure and also be economical. These nonductile frames, a large number of which were built in the central and eastern US in the 1950's through 1970's, were designed with little or no consideration for lateral loading and the detailing of reinforcement in the frames was such that these provided little confinement in columns or joints. Typical deficiencies in these frames can be enumerated as follows:

1. Low percentage of longitudinal reinforcement in columns.
2. Lapped splices of vertical column reinforcement located in the maximum moment region just above the construction joint at the floor level.
3. Widely spaced column ties which provide little confinement to the concrete.
4. Little or no transverse reinforcement within the joint region.
5. Discontinuous positive beam reinforcement with a 6 inch embedment length into the column.
6. Construction joints below and above the beam-column joint.
7. Columns having bending moment capacity less than the beam capacity

To evaluate the performance of such structures, a research program was initiated at Cornell and SUNY at Buffalo, under the auspices of the National Center for Earthquake Engineering Research (NCEER). Full scale beam-column joints were tested under cyclic loading by Beres (1994). Shake table tests were performed on model non-ductile RC frames by El-Attar (1991) and Bracci et. al. (1992). An analytical model for these non-ductile joint performance was developed by El-Borgi (1993), and was incorporated into a nonlinear analysis program (IDARC, Kunnath (1990)). Time history analyses were performed with several structures, to evaluate the performance of non-ductile frames to different types of ground motions. Based on these studies it was concluded that:

1. The pullout of positive reinforcement in the joint region resulted in high flexibility of the structures.
2. Because of their high flexibility, these frames would undergo large drifts under moderate level ground motions thereby possibly causing major non-structural damage. The higher flexibility of the structure however resulted in greatly reduced acceleration demand.
3. It was observed that the collapse mode of these frames results from soft story action i.e. hinging in the columns before the beams yield.

The objective of the retrofit program was hence to rehabilitate the frame to reduce the drifts in the frames. Limiting the drifts would reduce the nonstructural damage and also prevent hinging in the columns. The extent to which the drifts are to be reduced would depend on the design ground motion and the selected performance criterion. A discussion on the selection of design ground motions and the acceptable performance levels is provided in detail in Section 4.

Selecting the retrofit scheme depends on several factors. Bertero (1992) has summarized most of these factors. Some of these are listed below:

1. Level of seismic activity and sources of seismic hazards.
2. The main seismic hazards, given the vulnerability of the facility's whole system.
3. Type, function and age of facility.
4. The required levels of performance (serviceability, continuous operation, life safety) expected of the upgraded facility for different levels of ground motions and seismic hazards that can occur during the expected service life of the structure.
5. Architectural requirements.
6. Need to minimize disturbance to the occupants and operations of the facility during upgrading.
7. The availability of equipment and expertise for the field work.
8. Cost vs. benefits of the upgrading work, and the socio-economic impact on the community.

Other influencing factors not listed above are:

9. Influence of retrofitting on other components in the structure (e.g. foundations).
10. Availability of space around the existing structure.

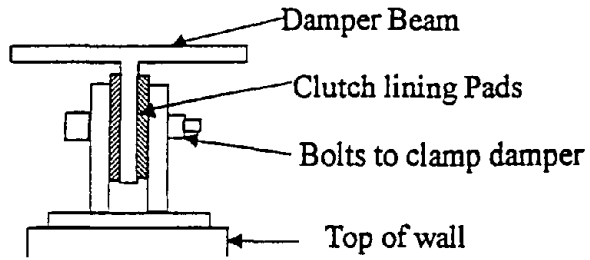
It can be summarized from the discussion in Section 2.2 that the conventional schemes lead to increasing loads on foundations, and also have problems in terms of installation, thereby making them expensive. There is hence a need to introduce a retrofit scheme that limits the load on the foundations and is easy to install. Since the method is aimed mainly towards structures in the central and eastern US, where the level of earthquake hazard awareness is low, the method has to be economically viable in order to be made more acceptable among the owners.

Hence the retrofit scheme to be proposed for non-ductile RC frames had to satisfy the abovementioned constraints.

## **2.2 Proposed Retrofit Scheme using Masonry Infill and Friction Dampers:**

Based on the discussions in Section 2.1 and the constraints imposed, a retrofit scheme using slotted bolt friction dampers set in a masonry infill wall is proposed. A schematic diagram of the proposed scheme is shown in figure 2-1. The scheme involves constructing a masonry infill wall with gaps on the sides and top of the wall. The force is transferred from the frame columns to the wall through a damper beam with slotted bolt friction dampers. Figure 2-1 also shows details of the friction dampers. The friction is provided by cold rolled steel rubbing against clutch lining pads. The tension in the high strength bolt controls the normal force acting on the surfaces and consequently the slip load in the dampers. Belleville washers help maintain constant tension in the bolt when the damper elements are moving.

The connection between the damper beam and the columns is designed hinged in order to avoid introduction of moments into the damper beam. The steps involved in installing the wall-dampers are described in Section 3, where the construction scheme for a 1/3 scale model of the retrofit scheme for dynamic testing is described in detail. Size of the damper beam and the connections would depend on the specific design



Sectional view of friction damper

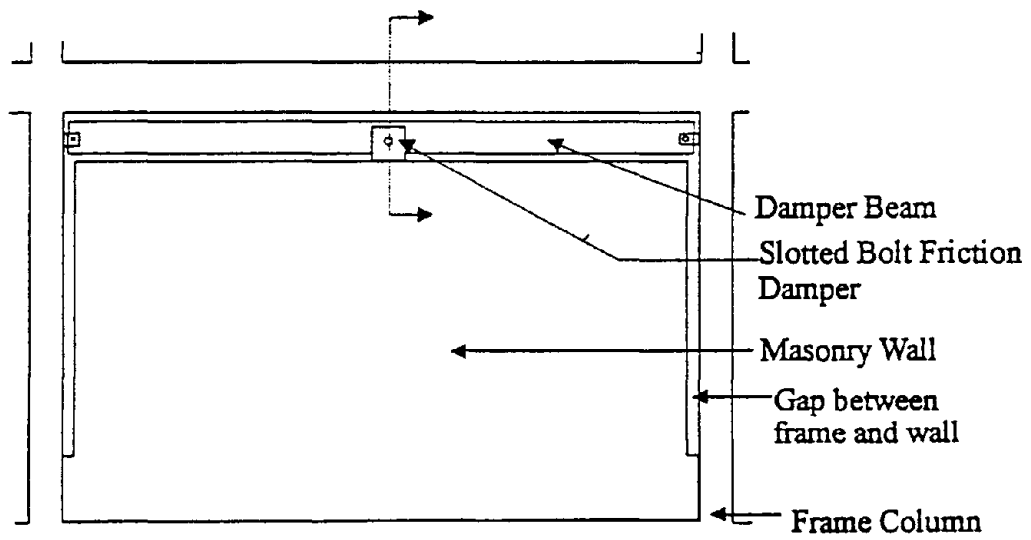
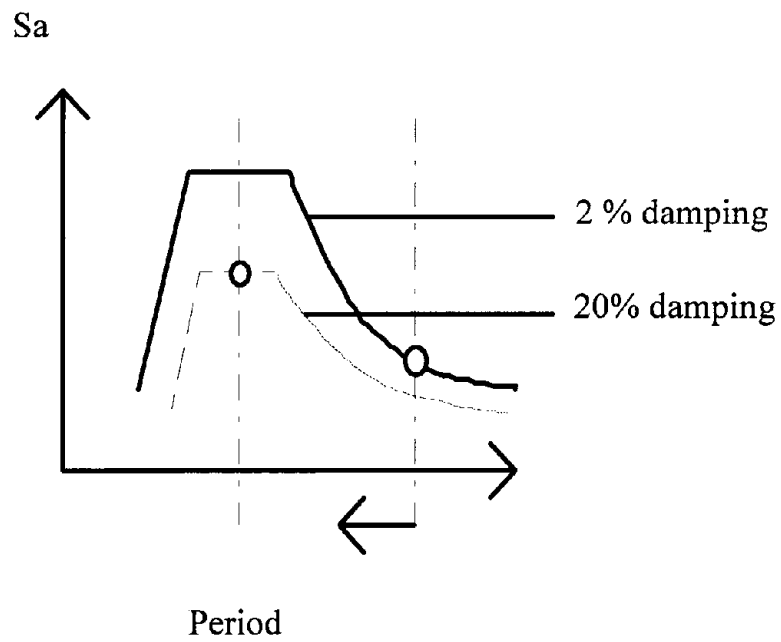


FIGURE 2-1: Proposed retrofit scheme with masonry infill and friction damper

conditions. Some of the advantages and salient features of the proposed scheme are discussed below:

1. Use of friction damper allows control over the extent of forces flowing to the foundations. Knowing the capacity of the existing foundations, the slip force in the dampers can be selected so as to limit the forces in the foundations. The wall damper system provides the required increase in stiffness and the dampers provide additional non-destructive energy dissipation which would reduce the displacements and limit the acceleration demand on the structure (see figure 2-2).
2. During the reversed cyclic loading, the flow of forces through the wall damper system can be kept purely compressive, as shown in figure 2-3. This allows for simpler connections between the damper beam and columns, and between the wall and the frame. Since connections have to transfer compression forces only, there is no need for drilling expansion bolts which would otherwise be required for connections transferring tension or shear type forces. As a result, the installation is less noisy and dusty and is expected to be more economical.
3. Use of a masonry wall allows for rapid construction and minimizes dust and noise during installation. As mentioned earlier, in a retrofit scheme, it is important to have mobility of the installation equipment and to cause the least amount of disturbance to occupants. Masonry walls can be built with very little space and maneuverability requirements in most situations. The wall can also serve as a partition wall. The wall may be reinforced and also anchored at the bottom, although the forces applied on the wall are limited by the dampers, hence limiting the extent of reinforcing and anchoring.



**FIGURE 2-2: Added damping reduces base shear demand and accelerations in comparison to conventional retrofit**

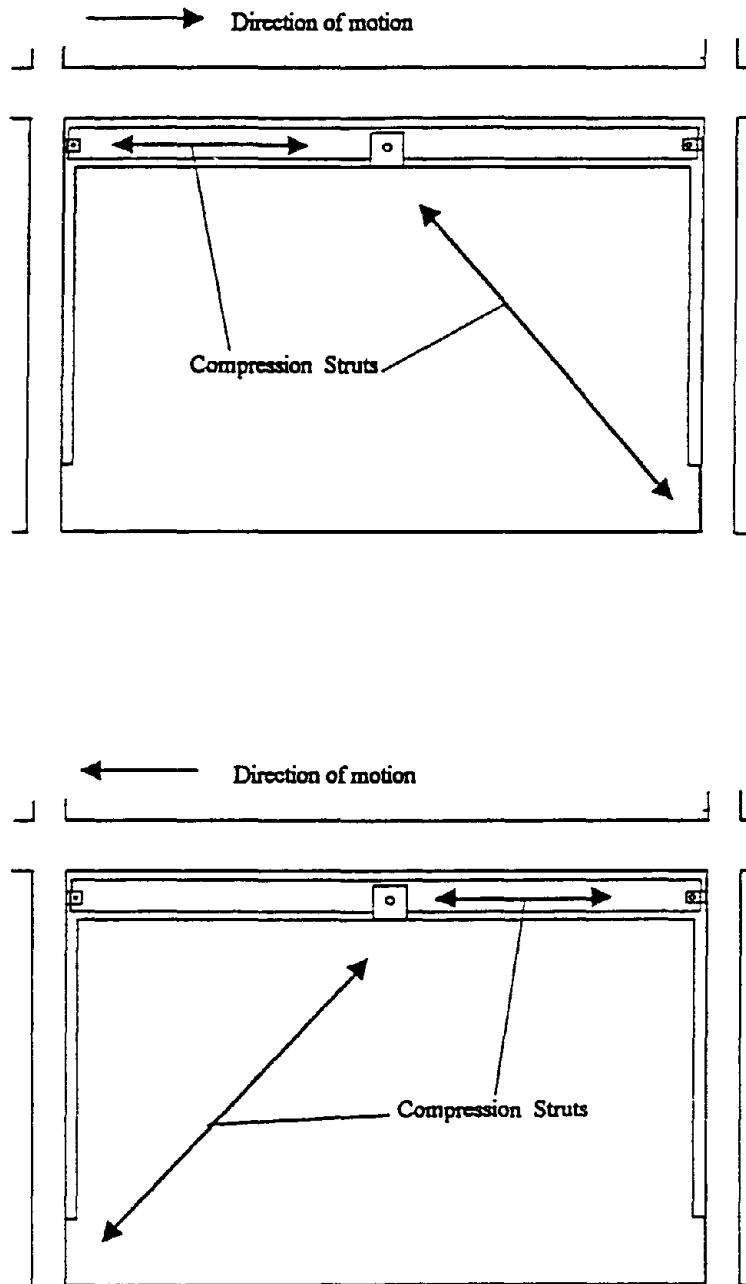


FIGURE 2-3: Flow of forces through the wall-dampers under cyclic loading

A limitation of the use of masonry infill is that the maximum force in the dampers is limited by the capacity of the masonry infill wall. If the design friction forces are large, several bays may need infills which may not meet the architect's requirements. In such situations, it is recommended that the masonry wall be replaced by K bracings.

Hence, the use of masonry infill with simplified connections results in an economical yet effective solution which increases the stiffness and damping and also satisfies the constraints imposed. The cost effectiveness of this scheme in comparison to other retrofit options needs detailed investigation. Another aspect of the wall-damper performance that would need a closer look, would be the possible uplift of the wall during the earthquake loading. To investigate this aspect, wall uplift measurements were taken during the shake table tests on the model wall-damper scheme. Test results indicate that the uplift is not large and does not hinder the performance of the dampers.

A possible modification to the installation scheme of friction dampers is to replace the wall with chevron steel bracing, as shown in figure 2-4. This approach may be needed if the wall is insufficient to provide the required pre-slip stiffness. The bracing sizes selected would control the pre-slip stiffness in the retrofitted frame. The positive features of having compression type connections are still retained in this modification.

### **2.3 Opinions From Leading Consulting Engineers on the Proposed Retrofit Scheme:**

As discussed above, the retrofit scheme proposed at Cornell was developed after considering several practical considerations involved in the retrofit problem. It was decided to further confirm the "constructibility " of the method, by seeking opinions from practicing engineers. Questionnaires were sent to seven leading consultants

actively involved in the retrofit business, of whom four responded. The questions asked and the general responses are summarized below:

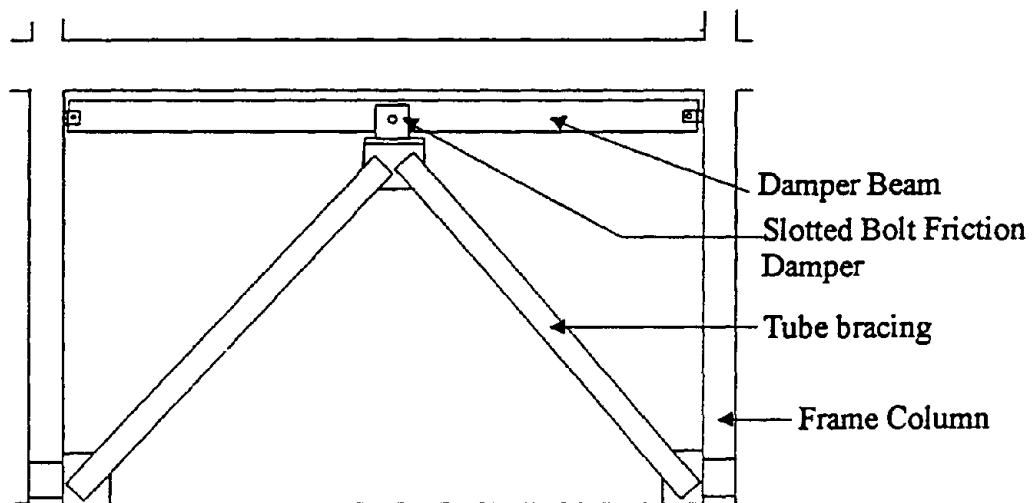
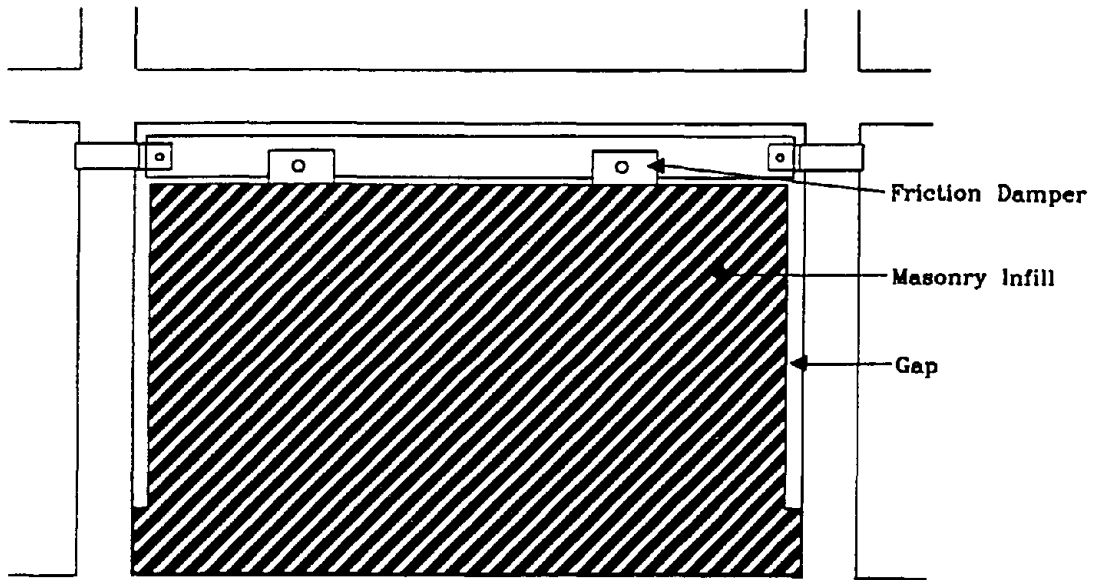
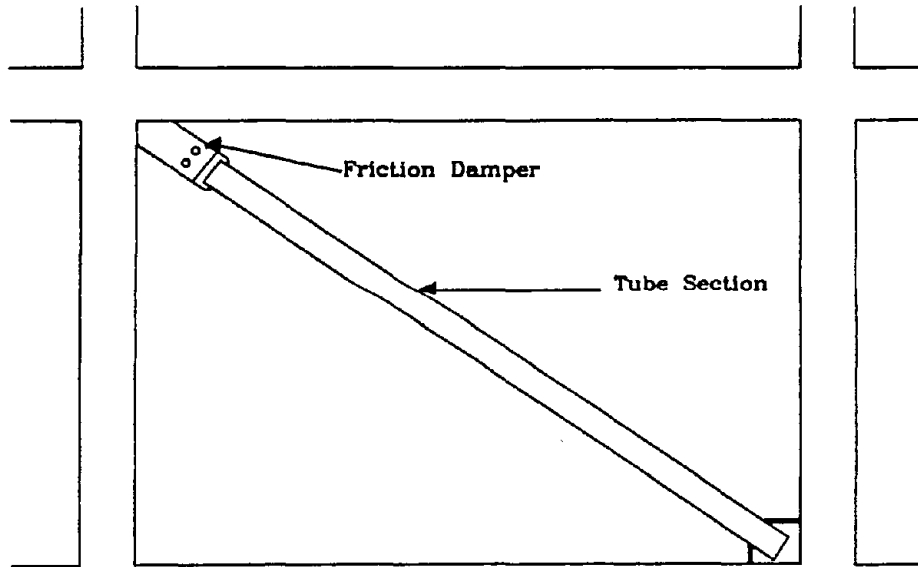


**FIGURE 2-4: Alternative scheme- replace walls with chevron bracing.**

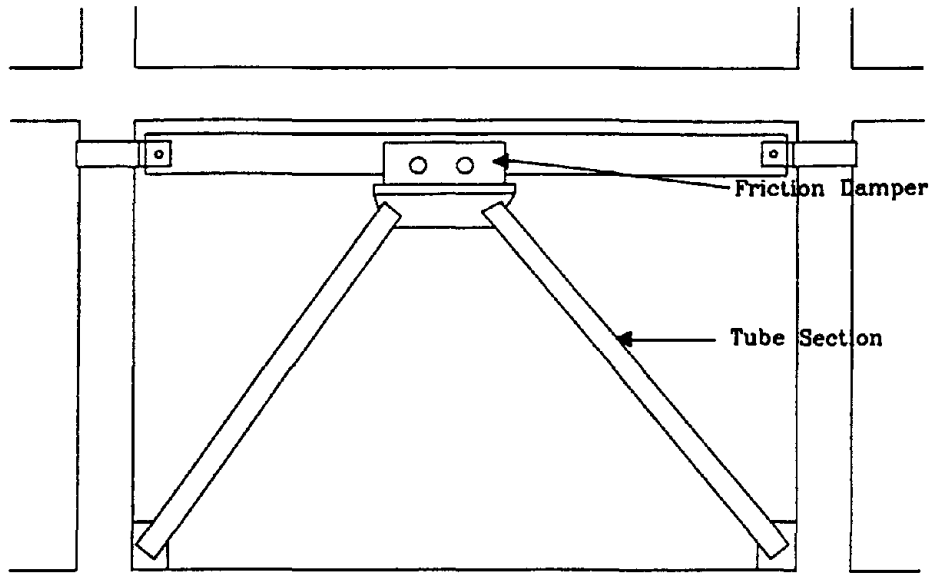


(a) Friction Dampers in Masonry Walls

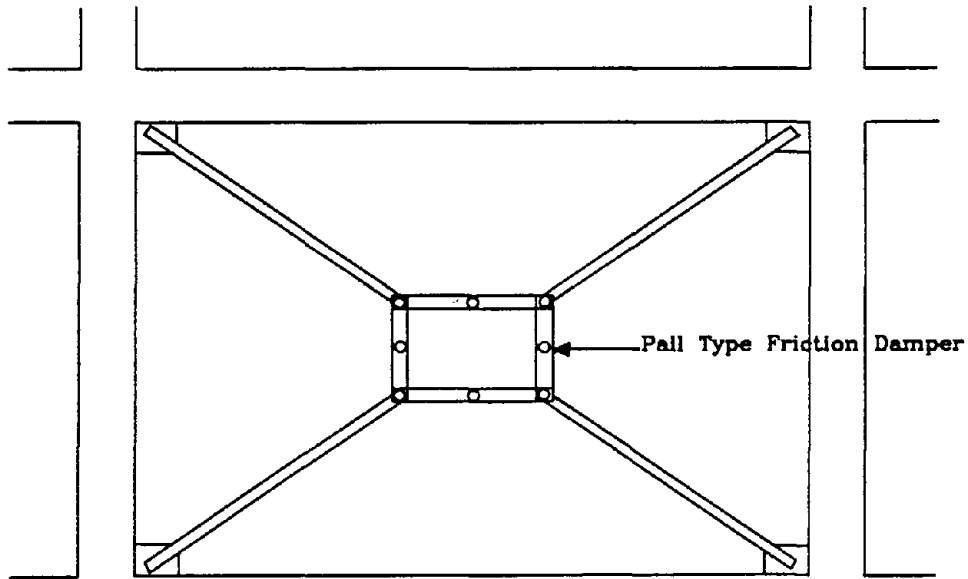


(b) Friction Dampers in Diagonal Bracings

**FIGURE 2-5: Possible installation schemes for friction dampers (part of questionnaire) contd....**



(c) Replacing wall in (a) with Tube Bracings



(d) Friction Dampers Proposed by Pall and Marsh

**FIGURE 2-5: Possible installation schemes for friction dampers (part of questionnaire) .....cont**

**Question 1:** Figures 2-5(a) through 2-5(d) below show various schemes for installation of friction dampers. Which method(s) would be best suited for a lightly reinforced concrete frame:

**Response:** Three of the four consultants decidedly favored the first two schemes (where the forces through the connections are of compression type). The fourth consultant felt that architectural and/or functional requirements would dictate the scheme to be selected. All the consultants suggested that if a masonry wall is used, it must be reinforced.

**Question 2:** Please provide your comments on the advantages and disadvantages of friction damper retrofit scheme as compared with

1. Solid infill walls
2. column and beam jacketing
3. steel bracing
4. other type of dampers

**Response:** Majority of the engineers found the friction dampers to be more advantageous to use. Solid walls were found to have problems of poor out-of-plane resistance and increased the base shear demand. One of the engineers, however, felt that if space is available and foundations are not compromised, infill walls are still the optimum retrofit choice. All but one of the consultants disapproved the jacketing scheme, as they found it expensive and disruptive. Steel bracing was found to be inadequate in terms of providing sufficient stiffness. Also, bracing would increase base shear and would cause problems with transferring loads at the connections. One of the consultants found other types of dampers, like viscoelastic dampers, to be considerably

more expensive. Another engineer felt that dampers need large drifts to be effective and it may not be possible to accommodate these large drifts in an existing structure. A third consultant suggested that there were no design tools which are easy to implement for friction dampers.

**Question 3:** Most retrofit schemes result in increasing the stiffness of the structure. This leads to increased base shear demand on the structure under seismic loading. Is overloading of foundations a frequent problem in retrofit design and what level of increased base shear and overturning moments can typically be allowed in the foundations?

**Response:** Three of the four consultants regarded the increase in base shear demand a potential problem in retrofit design. The level of allowed increased base shear would depend on the individual case. One of the engineers suggested a figure of 15-20%, while another suggested a 50-100% increase in the allowable bearing pressure. Another engineer felt that foundation stability and overturning problem was more severe for tall buildings than for low-rise structures.

There was a general endorsement from the consultant that the proposed scheme had advantages of constructability and in controlling foundation loads.

Another practicing engineer, who was consulted earlier during the research, had some useful comments on economic and constructibility considerations. He reiterated that dealing with a concept in general terms is difficult. Project specific conditions (will the building remain occupied during retrofit? Is the seismic retrofit part of a larger renovation project? How easy is access for renovation?) drive the economy of important decisions. The specific details of the retrofit, such as connections, depend greatly on the force demands. He further mentioned that the impact of infill walls on architectural considerations is also important. If the infilled wall is an exterior wall, for example,

waterproofing of the exterior wall will be required. Building gaps into the wall or between the wall and the surrounding concrete frame could complicate waterproofing; so such gaps must be minimized and simplified.



## SECTION 3

### EXPERIMENTAL EVALUATION OF PROPOSED RETROFIT SCHEME

#### 3.1 Cyclic Testing of Friction Dampers

As discussed in Section 2, the proposed retrofit scheme utilizes slotted bolt type friction dampers. A sectional view of the dampers is shown in figure 3-1. The damper consists of a central plate with clutch lining pad (coefficient of friction  $\mu_f = 0.4$ ) epoxied on both sides. The surfaces rubbing against the pads on either side are cold rolled steel surfaces with mill scale removed. To understand the performance of these dampers under repeated cyclic loading, a series of tests were performed where small scale specimens of the friction damper were manufactured and tested under dynamic cyclic loading. The tests were designed to study:

- a) the performance of the friction surfaces in the dampers when subjected to several cycles of motion.
- b) influence of bolt tension on the slip load
- c) influence of frequency of loading on the slip load

The tension in the bolt depends on the torque applied to the bolt. The torque applied to the bolt was used as a measure of the normal force applied to the friction surfaces. A torque wrench was used to measure the torque. The specimens used for the cyclic testing are shown in figures 3-1 and 3-2.

#### 3.1.1 Experimental Setup and Test Program for Cyclic Testing

A tension frame mounted with an actuator capable of applying sinusoidal loading was constructed for this test. Figure 3-3 shows a schematic view of the test setup.

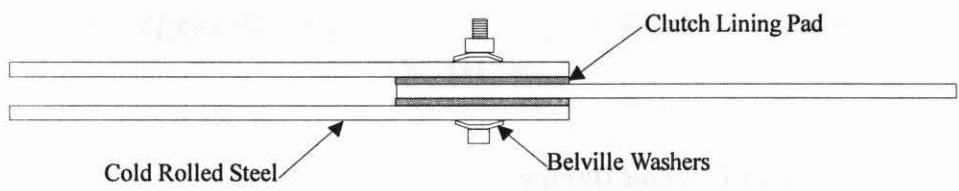


**FIGURE 3-1. Schematic Diagram of Friction Damper Specimens**

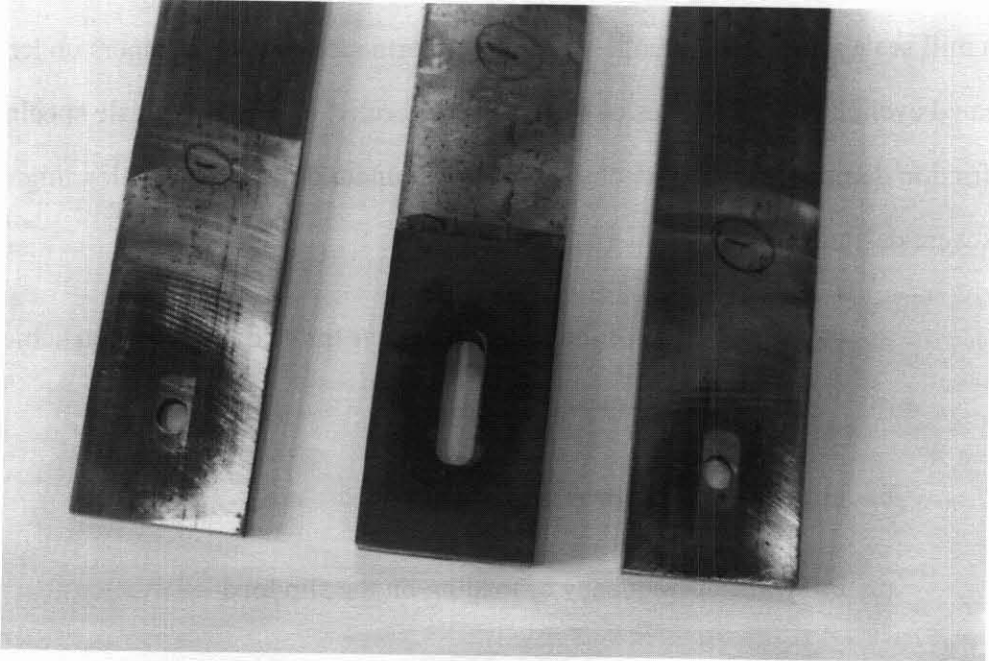


**FIGURE 3-2 Friction damper specimens used for cyclic testing**

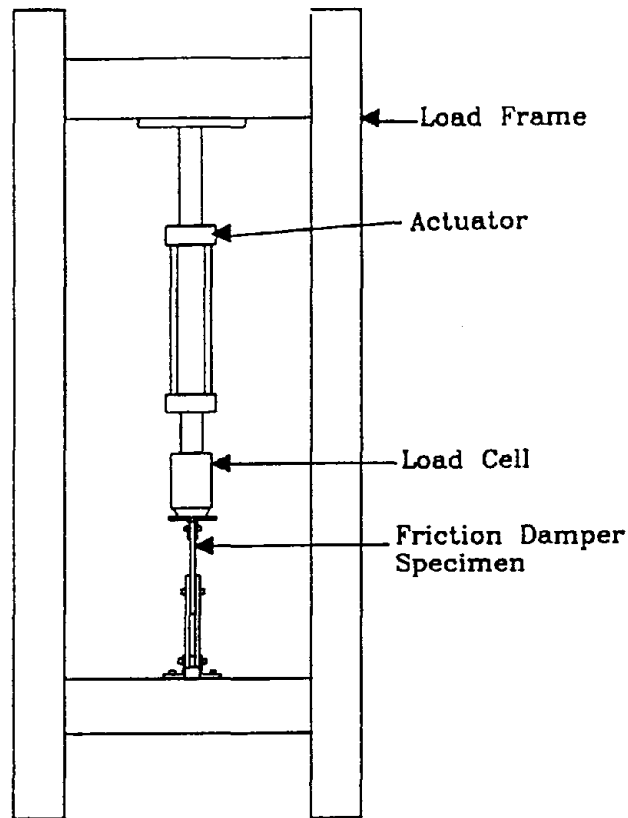


**FIGURE 3-3 Schematic Diagram of Test Setup for Cyclic Testing on Dampers**

The actuator used in the test has a stroke of 5 inches and a load capacity of 22.0 kips. A DCDT was used to measure the slip between the surfaces. A 286 IBM compatible with a DT2818 data acquisition card was used to read and store the data. The data acquisition software Labtech Notebook was used to store the data. The measured loads applied to the damper and the relative slip between the elements were measured at 20 hz. except for specimen SP5, where for the 2 hz. loading case, the data was collected at a rate of 40 hz.

Five dampers designated as SP1, SP2, SP3, SP4 and SP5 were tested. The cyclic loading applied in all the tests was displacement-controlled. The displacements applied to the specimens were sinusoidal signals with amplitude of 0.3 in. The test program is outlined below:

1. Specimens SP1, SP2, SP3 and SP4: Each specimen was subjected to 10 load cycles for eight different levels of torques. The values of the torques applied to the bolts were 25, 40, 60, 80, 100, 120, 150 and 180 in-lbs. All the cycles were applied at a frequency 0.5 hz. After applying the set of ten load cycles, each specimen was subjected to 100 cycles of loading at 1.0 hz. The torque settings for the specimens for the 100 cycle tests is shown in table 3-I. The 100 cycles test was performed to observe if there was any loss in slip load of the specimens when a large number of cycles are applied.
  
2. Specimen SP5 was subjected to 10 cycles at 0.5, 1.0, 1.5 and 2.0 hz. The torque applied to the bolts for these cases was 60 in-lbs. This set of tests was performed to investigate the influence of frequency of loading on the damper response.

**TABLE 3-I: Torque Settings for 100 cycles test**

Specimen No.	Torque Applied (in-lbs)
SP-1	120
SP-2	25
SP-3	180
SP-4	60

### **3.1.2 Results**

Figure 3-4 shows the load-displacement response of specimen SP1 for 10 cycle loading tests, with the eight different torque settings. The specimens showed repeated rectangular hysteresis for all the cases, with the slip loads increasing with the increase in torque applied to the bolt. The slip load for the specimens was taken to be the average of the slip loads observed in the two directions of loading. The torque vs. slip load relation was found to be fairly repeatable. Hence the torque applied to the specimens can be used as a convenient measure for obtaining a specific slip load.

Figure 3-5 shows the damper hysteresis for the four specimens, under the 100 cycle tests. It can be seen that even after 100 cycles of repeated loading there was very little change in slip loads between successive load cycles. The maximum loss of slip load was observed in specimen 4, where the difference in slip load between the first and the 100th cycle was less than 15 % of the maximum slip load value.

The slip load variation of the specimen SP5 at four different frequencies of loading is shown that the damper performance (i.e. slip loads) is essentially independent of the frequency of loading.

## **3.2 Shake Table Tests on the Proposed Damper Setup**

### **3.2.1 Objectives**

The proposed retrofit scheme in Section 2 has several novel features. Conceptually the wall-damper scheme should provide the desired increase in stiffness and added energy dissipation. However it is important to experimentally verify if the proposed scheme can deliver the desired characteristics. Another important claim made in Section 2 was the "constructability" of the scheme. Again it was necessary to verify if the scheme was indeed easy to install. To attain these objectives it was decided to perform dynamic tests on the shake table for a one story one bay model. To meet space requirements

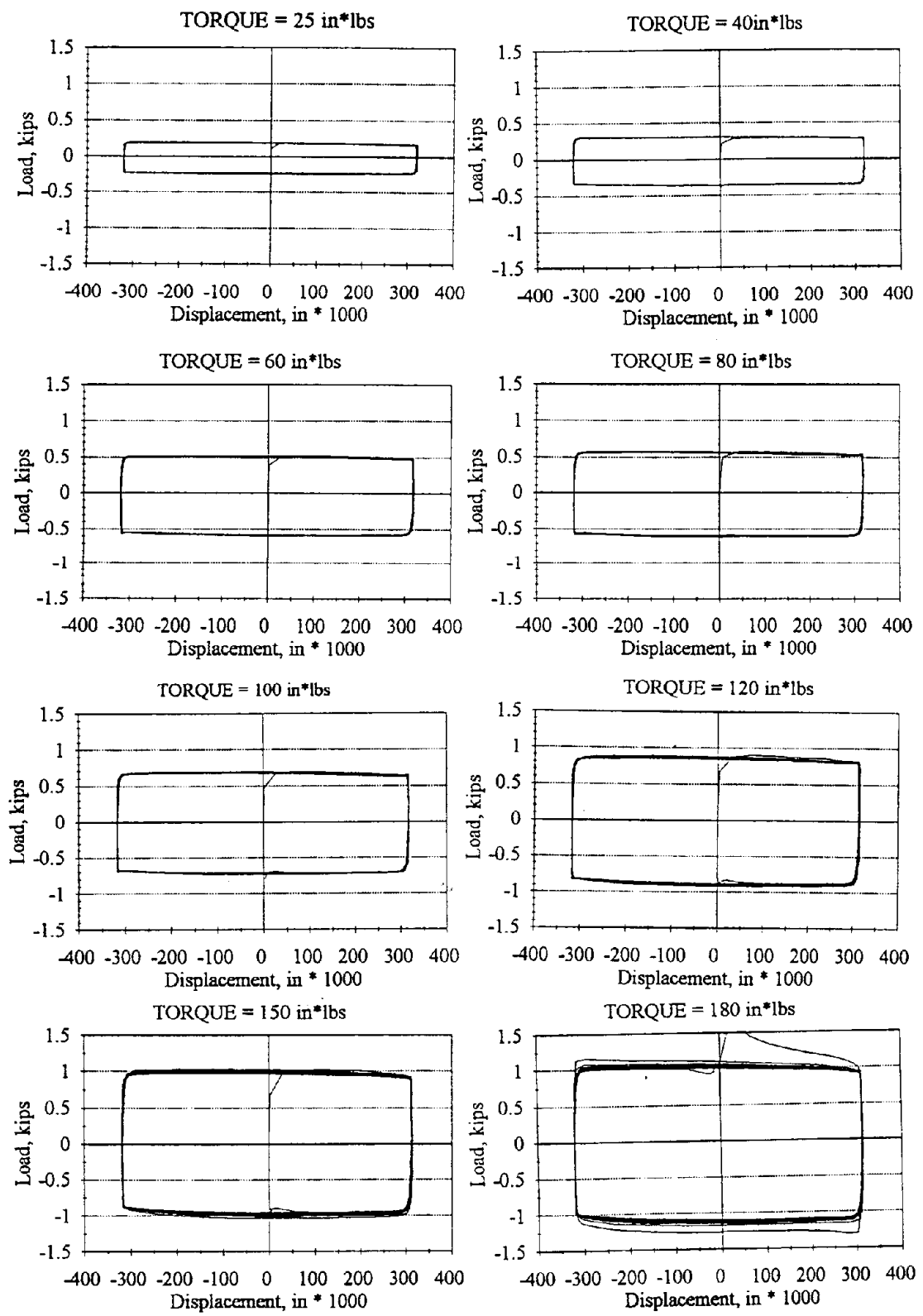


**FIGURE 3-4 Response of specimen SP1 to ten cycle tests**

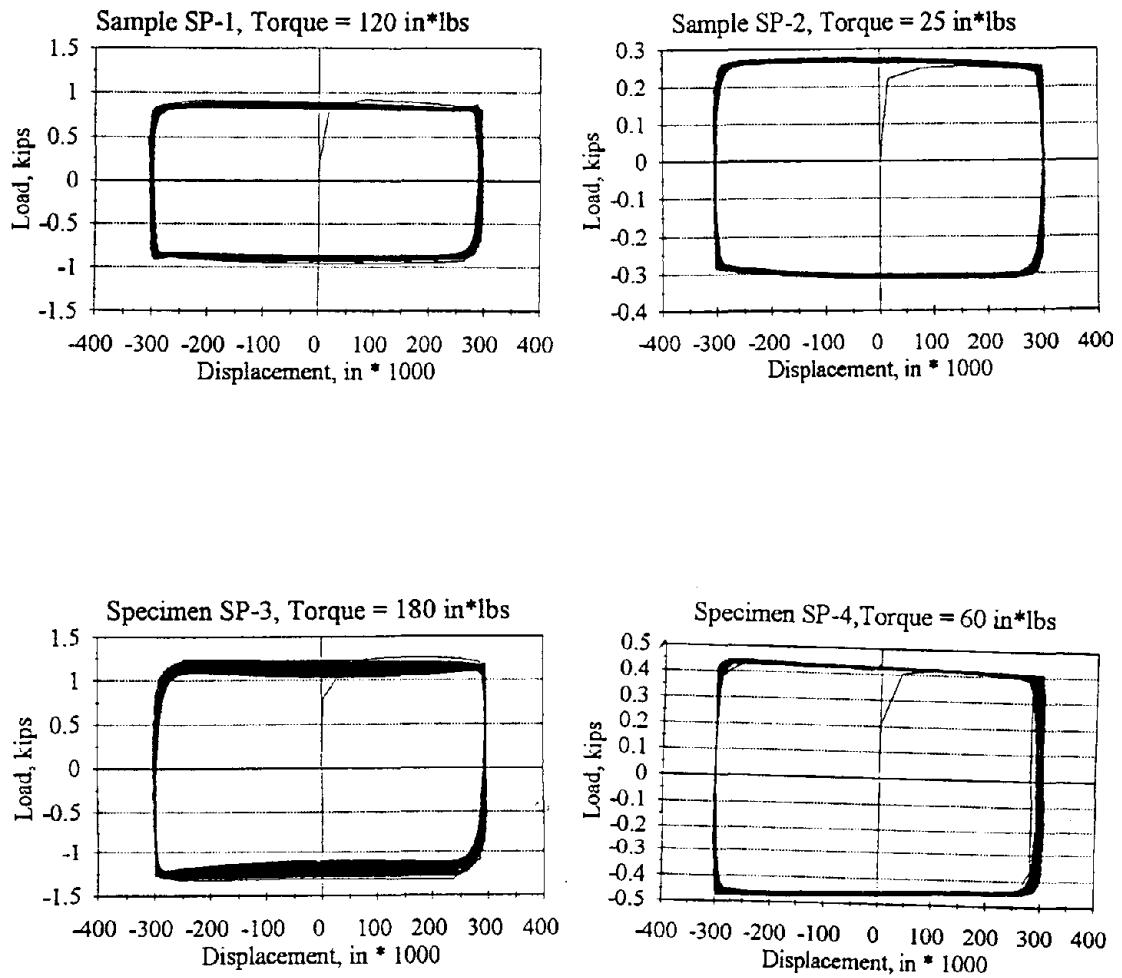


**FIGURE 3-5 Results for 100 cycle test on friction damper samples**

in the lab (on the shake table) the model was scaled to 1/3 the size of a bay in a typical full scale RC frame.

Another objective of these tests was to quantitatively characterize the hysteretic properties of the retrofit scheme. Tests on the 1/3 scale model of the wall-damper scheme along with dimensional analysis would be used to predict the properties of the full scale retrofit setup. Hence the response of the wall-damper must be isolated from the overall system response. With this in mind, it was decided to use a steel frame. The steel frame can be characterized as a linear system and hence its effect can be easily removed from the overall measured response, to get the wall-damper properties. Use of a concrete frame would complicate the situation, since the behavior of the RC frame would be nonlinear, hence making the process of identification of damper properties very complex. Moreover, several tests had to be carried out, with different damper settings. Use of the steel frame allows repeated testing, since no degradation is expected in the frame as long as the demand is kept within its linear range.

Details of the frame and the experimental setup on the shake table are described in Section 3.2.2. Selection of the ground motions is discussed in Section 3.2.3. Results from the tests, interpretation of results and analytical modeling are described in Section 3.3.

### **3.2.2 One Story Semi-rigid Frame**

As mentioned in the previous subsection, a one story one bay steel frame would be used in the shake table tests with the dimensions being 1/3 the typical bay size for a full scale RC frame. A typical bay was selected based on the three story RC frame designed and tested by Bracci et. al. (1992). The loading on the frame to be used to calculate story mass (dead load plus 25% of live load) was calculated to be 0.16 kips/sq. ft. The size of the bay is 18 ft by 12 ft. Hence, the dimensions the 1/3 scale model frame must be 72

inches wide and 48 inches, and the total simulated mass must be 5.72 kips. It must however be borne in mind that the shake table tests were not aimed towards modeling the internal bay of the three story RC frame per se; instead, the three story frame was used as a relative measure for selecting the model properties.

The proper mass in the model was achieved by placing lead blocks in a wooden box on top of the frame. To prevent free movement of the blocks during the dynamic tests, the blocks were placed such that they fit the box dimensions. It was decided to place three layers of lead blocks in the box. The total weight of the model was then calculated to be  $W = 3.86$  kips.

The frame was designed such that it remained elastic when maximum estimated drifts were reached. Also, the members had to bear the dead load and the dynamic loads. The member sizes were further restricted by the smallest section sizes available from the supplier.

The objective of the tests was to study the influence of the wall-damper scheme on the response of the frame. To be able to "improve" the frame response, the model frame must be "deficient" to start with. Hence it was necessary to make the frame flexible. This was done by introducing top and bottom seat angles (semi-rigid) connections at the beam column joint. Also, the bottom of the columns were provided with hinge connections. To prevent the stiffness of the box from stiffening the entire frame, vertical saw cuts were made in the box, such that the stiffness of the box sides was greatly reduced.

Based on these design considerations, the details of the steel frame model are shown in figure 3-6. Wooden side-supports were used to prevent accidental out-of-plane motion in the frame during the tests. Lubricated bearings were placed between the box and the side supports to minimize friction.

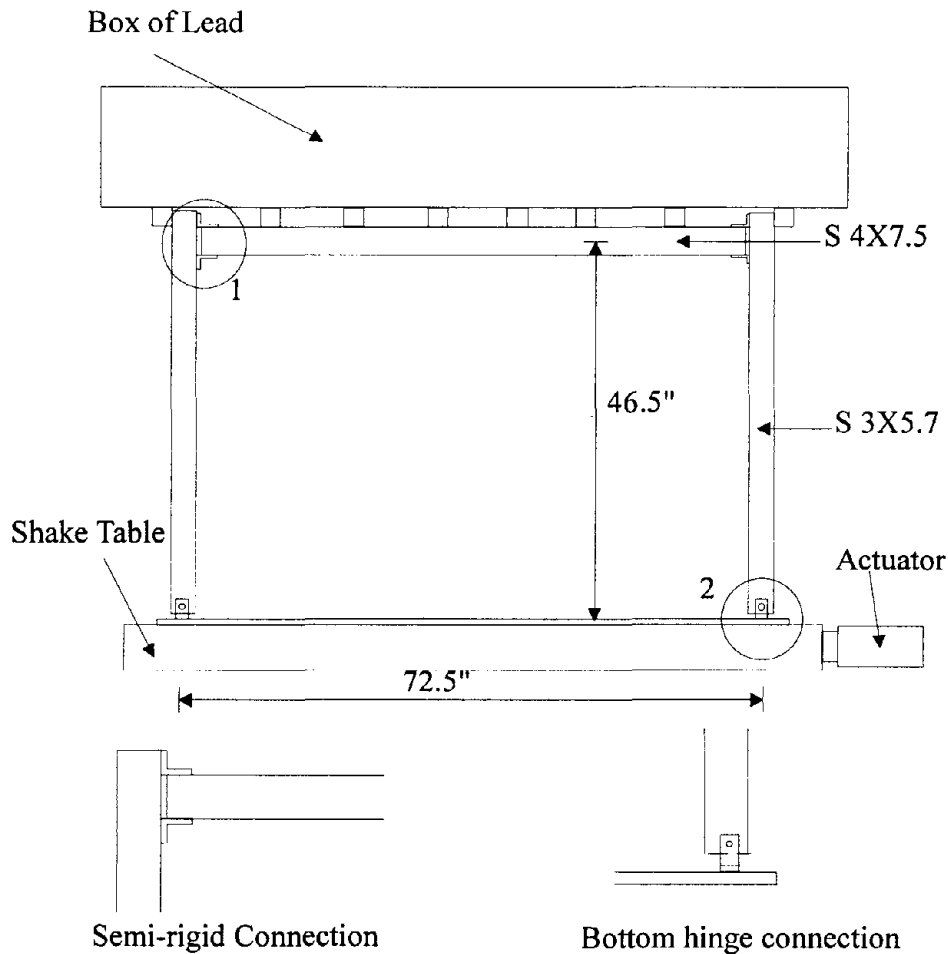


**FIGURE 3-6 Dimensions and sections designed for shake table model**

### 3.2.3 Installation of Retrofit Scheme

In this section, the installation procedure for the wall-damper scheme is described. The peculiar configuration of the proposed retrofit scheme necessitates the use of a specific set of operations. These operations, although straightforward from the construction standpoint, must follow a certain sequential order. The procedure outlined here must also be followed in the installation of full scale schemes in practice. The masonry wall was erected leaving appropriate amount of space on the sides and the top of the wall. A gap of 1 inch was left on the sides since drifts larger than 0.4 inches were not expected in the frame. The contact area between the column and the wall at the bottom was kept at

three blocks (six inches) high. This provided sufficient space for the column part above to deform flexurally without interference from the wall contact area. An important part of this stage is to place threaded rods at the top of the wall, where the dampers are to be placed. The rods were placed "loosely".

The damper beam was introduced along with the cold rolled steel plates already clamped to the beam. The beam ends were attached to the column through shoulder bolts to obtain hinge connections at the ends of the damper beam. The threaded rods at the top of the wall were then pulled up and connected to the base of the cold rolled steel plates. A useful aspect of this installation procedure was that the cold rolled steel and clutch pad surfaces in the friction damper are clamped together before being mounted onto the frame. As a result, in the field situation, the damper can be tested to give the desired slip load before being brought to site. Hence, a manageable size test setup would be required to set the damper slip load. In the final stage, the space between the damper base plate and the wall was covered with temporary forms and filled with grout. Some space must be left at the top to allow for pouring the grout and placing the vibrator. A schematic view of the retrofitted frame, after the installation of the wall-dampers is shown in figure 3-7. A wooden block was clamped in place between the damper beam and the frame beam. The function of the block was to transmit the vertical component of the force from the wall diagonal strut to the frame beam. This should prevent any uplift or rocking of the wall. In practice, for a RC frame, the damper beam can be placed such that the top flange is touching the bottom of the concrete beam, thereby transmitting the vertical force and avoiding the need for a block.

The above installation procedure was rather straightforward and was done using standard construction equipment and labor. Hence, the proposed retrofit scheme does indeed have the "constructability" feature which was claimed in Section 2.

Figures 3-8(a) through 3-8(d) show pictures of the shake table setup after the retrofit scheme had been installed. Figure 3-8(a) shows the side view of the retrofitted frame, while Figure 3-8(b) gives a closer view of the friction damper connection at the top of the wall. In Figure 3-8(c), the contact area between the wall and the column is seen along with the hinge connection provided at the bottom of the column. The top and

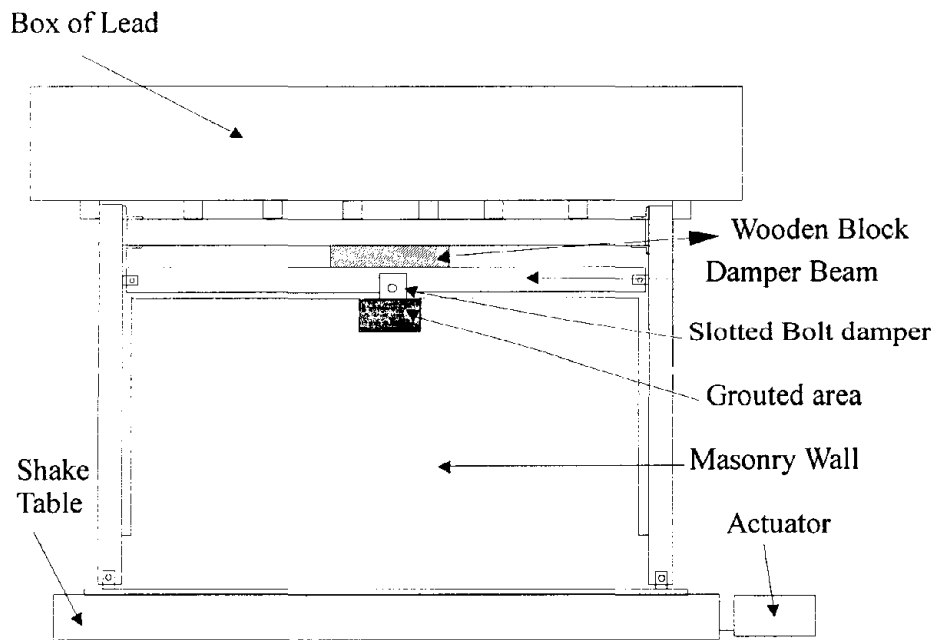


**FIGURE 3-7: Final Stage of installation of retrofit scheme**

bottom seat angle type semi-rigid connection between the beam and the column and the hinge connection between the damper beam and the column is shown in figure 3-8(d).

### 3.2.4 Ground Motions used in Tests

It was decided to use two recorded earthquakes as input motions for the shake table tests. The two records used were the Kern County Earthquake of 1952, measured at the Taft Lincoln school tunnel (S69E component) and San Fernando 1971 earthquake measured at Pacoima Dam (S74W component). For brevity, these earthquake motions

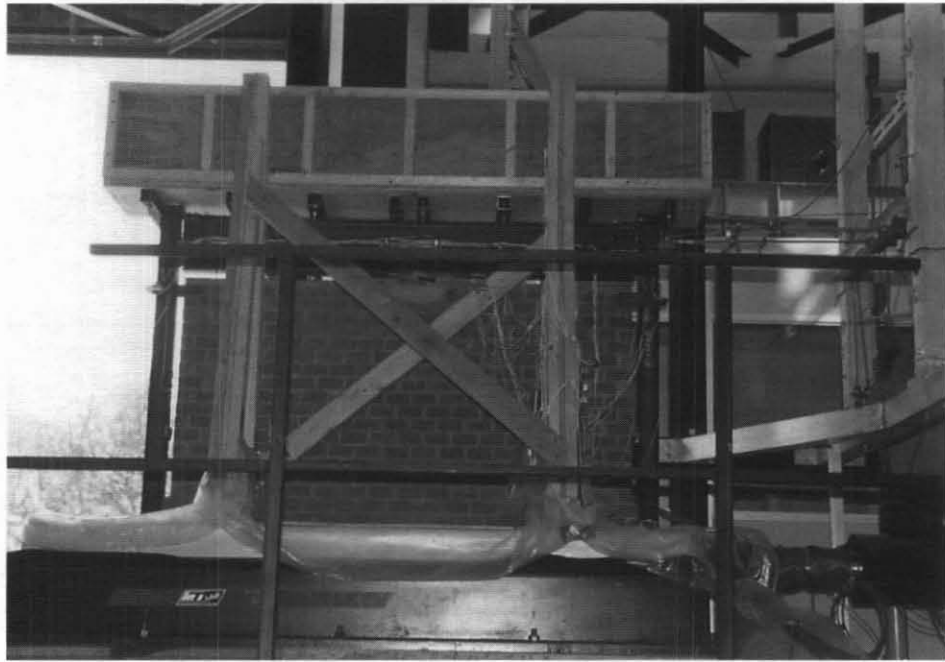


**FIGURE 3-8 (a) Side-view of test frame**

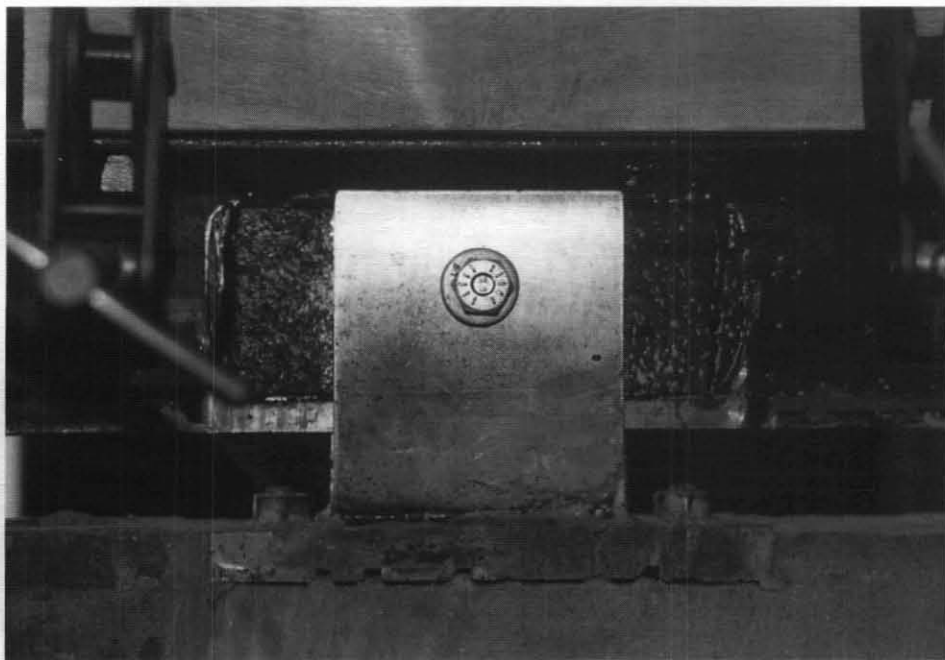


**FIGURE 3-8 (b) Slotted bolt friction damper**

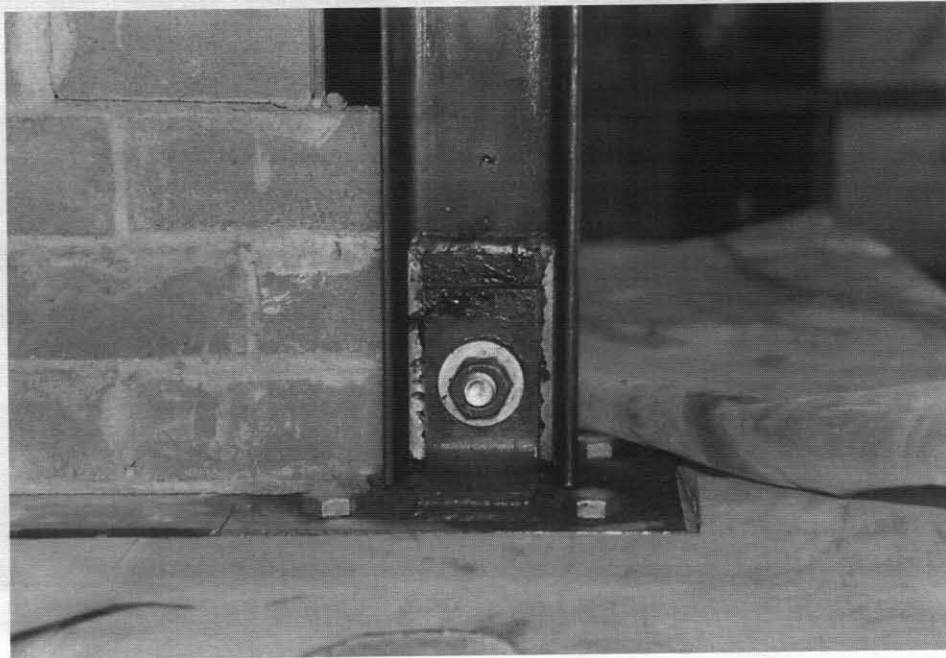


**FIGURE 3-8 (c) View of bottom of frame column**

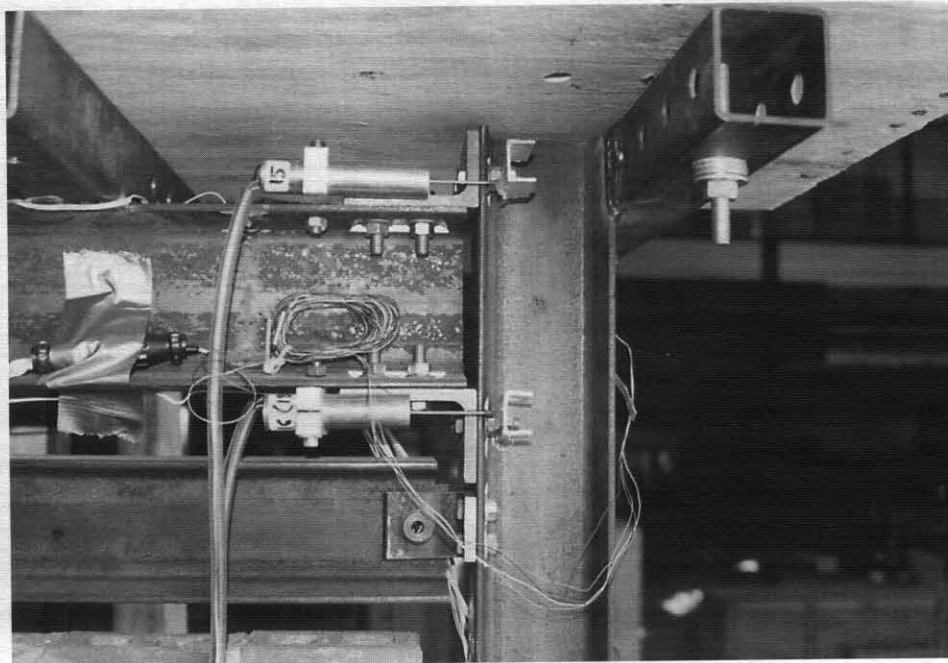


**FIGURE 3-8 (d) Semi-rigid connection between beam and column**

will be referred to as Taft and Pacoima motions respectively, in this report. The time histories of the acceleration records and the 2% damping acceleration response spectra for these ground motions are shown in Figure 3-9(a) and (b). The ground motions selected represent two contrasting types of earthquake loading. The Taft motion is characterized by a gradual buildup of acceleration followed by intense ground motion. The acceleration response spectrum is distributed over a wide range of periods. The Pacoima motion, on the other hand, is more sporadic with the intense motion being confined to a shorter time frame. It was postulated that the friction dampers would be less effective for Pacoima type motions. This is because the phenomenon of damping gets effective through energy dissipation and hence some cycles of loading are required before the effect of damping is felt. However, for impulse-like motions, the peak comes suddenly; hence it is likely that the dampers may not be able to damp out these peaks.

For a 1/3 scale testing the input motion was scaled such that the peak accelerations can be reproduced. As a result, the time had to be scaled to  $1/\sqrt{3}$ .

### **3.2.5 Experimental Setup, Instrumentation, and Data Acquisition System**

The overall setup of the frame on the shake table is shown in figure 3-10. The details of the shake table, instrumentation used to measure the frame response to simulated motions and the data acquisition system used to digitize and store the data are described below:

#### **Cornell University Shake Table**

Some of the salient features of the Cornell University shake table are outlined here. A more detailed description of the equipment, table control system, limitations and the dynamic characterization is provided by El-Attar (1991).

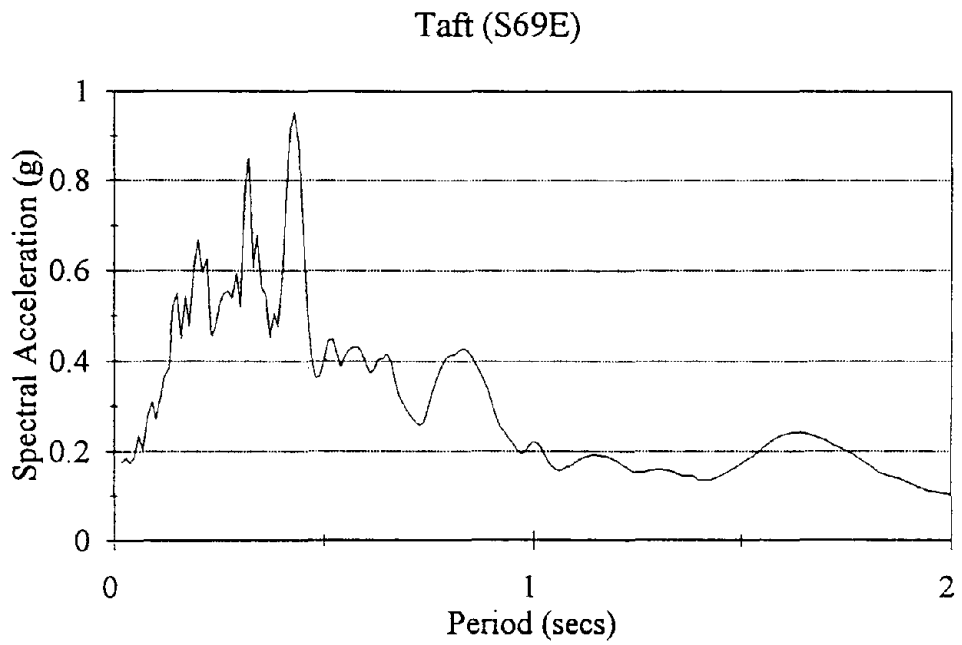
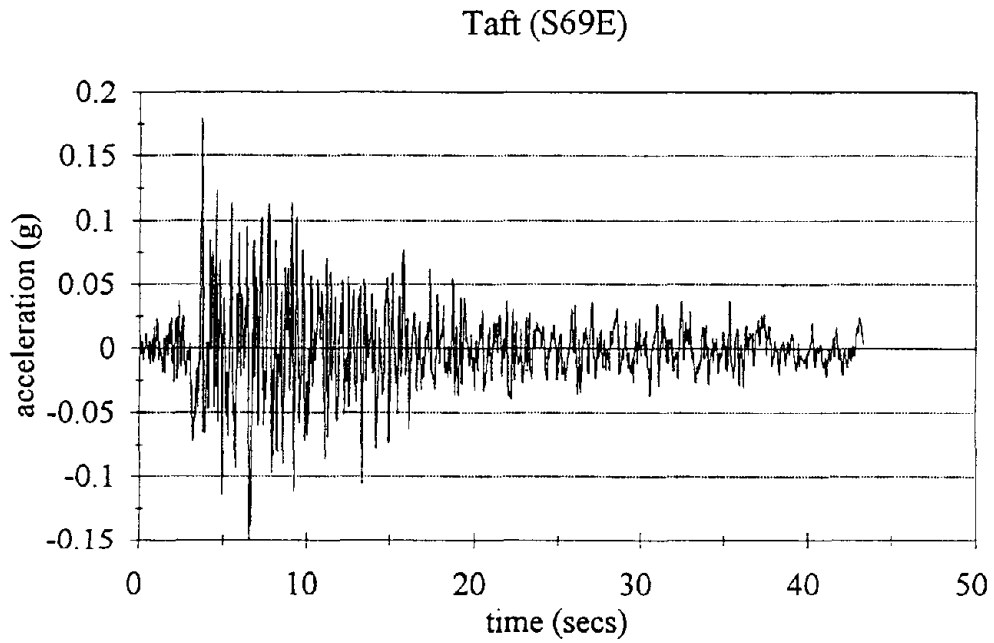


**FIGURE 3-9(a) Time history and response spectrum of Taft earthquake**

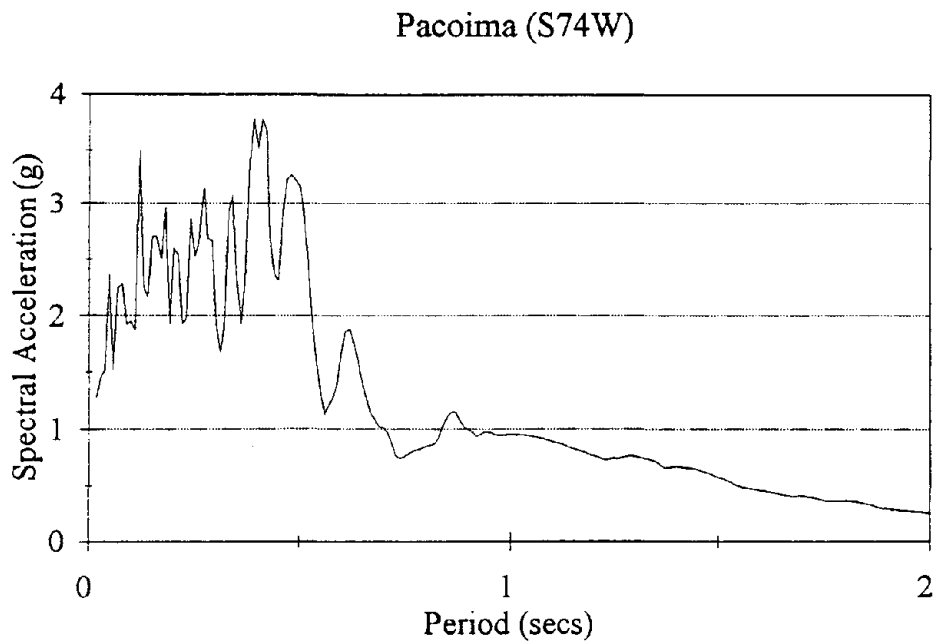
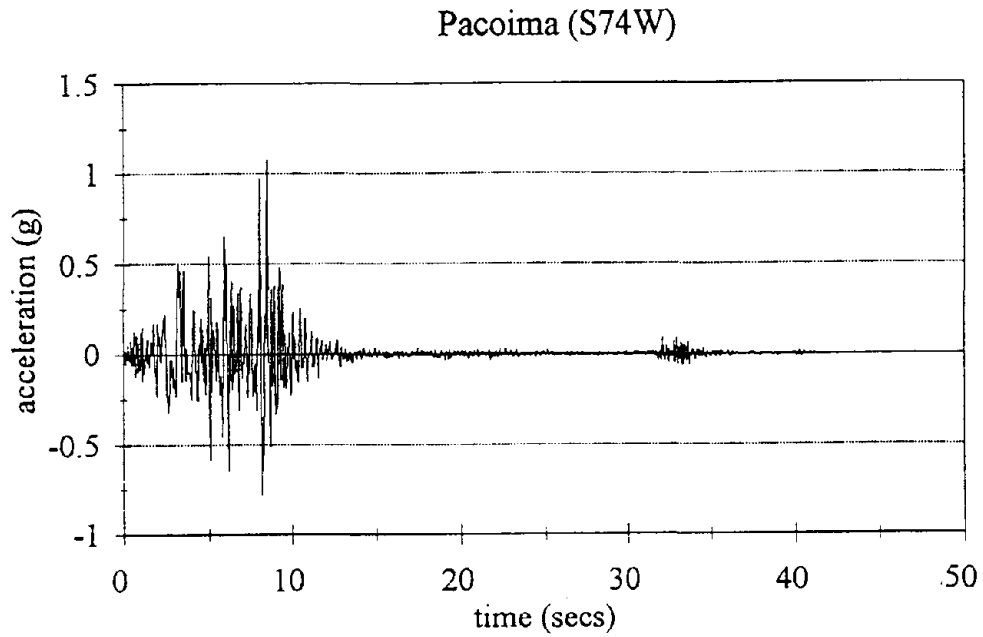


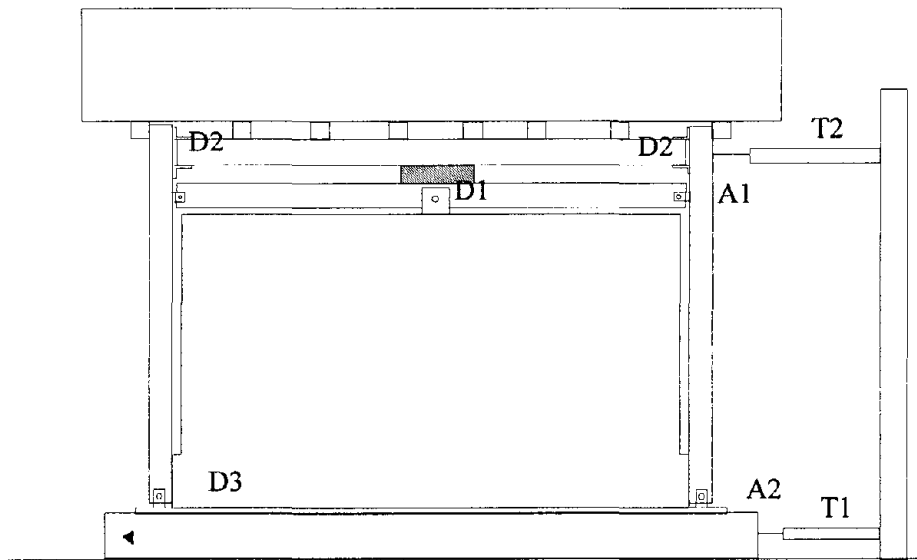
**FIGURE 3-9(b) Time history and response spectrum of Pacoima earthquake**

The shake table consists of a 4 inch thick aluminum plate, 5 feet by 7 feet in plan area. The plate moves on a polished granite block, with a thin oil film used as a lubricant. The table has one degree of freedom which is in the longitudinal direction. The hydraulic actuator driving the table has a stroke of 6 inches, with a capacity of 14.0 kips and static capacity of 21.0 kips. The table operates with a closed loop displacement control using L.A.B. (model 8830) servo-controller. A reference frame has been built next to the table to mount instruments to measure displacements of the specimens mounted on the table. Maximum vertical load on the shake table must not exceed 20.0 kips, and the maximum overturning moment uniformly distributed on the table must not exceed 125 kip-ft. Maximum dynamic force applied by the driving actuator is 14.0 kips. For the tests performed in this research, the demand on the table was well below its limitations.

### **Instrumentation**

In figure 3-10, the locations of the various instruments are shown. Temposonics were used to measure displacements of the table and the top of the frame. Table and frame accelerations were measured by using accelerometers. DCDTs were used to measure the relative displacement of the friction damper surfaces and to measure the uplift of the wall. To study the relative rotations between the beam and columns, a pair of DCDTs were placed at each joint. Also, 20 strain gages were used to measure the moments at various sections in the beams and columns and to measure the force in the beams. However, the instrumentation of primary use were the table and frame temposonics, table and frame accelerometers and DCDT to measure the damper slip

A schematic view of the data acquisition system is shown in figure 3-11.



- D1: DCDT to measure slip
- D2: DCDT pairs to measure relative rotation
- D3: DCDT to measure wall uplift
- T1: Tempesonic to measure table displacement
- T2: Tempesonic to measure frame displacement
- A1: Accelerometer to measure frame acceleration
- A2: Accelerometer to measure table acceleration

**FIGURE 3-10 Instrumentation used in test**

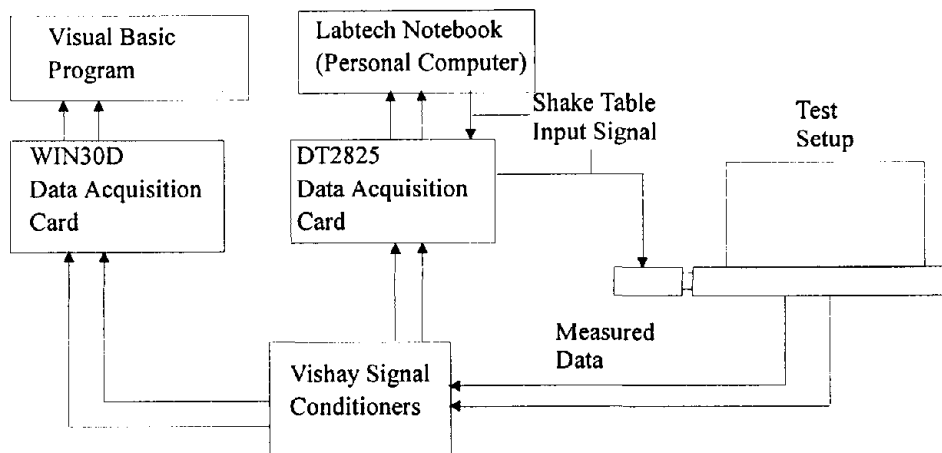


**FIGURE 3-11 Schematic diagram of data acquisition system used in test.**

**TABLE 3-II: Summary of tests performed on bare frame**

Ground Motion	Designation	Peak Ground Acceleration
Taft S69E	Taft1	0.0723g
Taft S69E	Taft2	0.1445g
Pacoima S74W	Pacoima1	0.0742g
Pacoima S74W	Pacoima2	0.1416g

**TABLE 3-III: Ground motions applied to frame with friction dampers**

Ground Motion	Designation	Peak Ground Acc.	Torque in bolts
Taft S69E	Taft2_50	0.1104g	50 in-lbs
Taft S69E	Taft2_100	0.1104g	100 in-lbs
Pacoima S74W	Pac2_50	0.1172g	50 in-lbs
Pacoima S74W	Pac2_100	0.1270g	100 in-lbs

### **3.3 Test Program for Shake Table Experiments**

In this section, an outline of the tests performed on the shake table with the bare steel frame and the frame with wall-damper installed is presented:

1. Three preliminary tests were performed on the frame to obtain its stiffness and natural frequency. The tests performed were: (a) Stiffness test (b) Free vibration test and (c) Impact hammer test.

2. The bare steel frame was subjected to two levels of Taft and Pacoima ground motions. Table 3-II presents a summary of the tests performed on the bare frame. The levels of the earthquake motions applied were kept low, in order to prevent any damage to the frame.

3. After the wall-damper was installed, low level Taft ground motions (PGA around 0.07g) were applied with six different torque settings applied to the damper bolts. The aim of these tests was to characterize the slip load of the wall-damper for different torque levels applied on the bolt. The torque settings applied in this series of low level loadings were 0, 25, 50, 75, 100 and 125 in-lbs.

4. In the next stage, moderate level Taft (PGA around 0.11g) and Pacoima motions (PGA around 0.12g) were applied. For each earthquake two damper settings were used (see table 3-III).

### **3.4 Results and Analytical Modeling of Tests on Bare Frame**

The bare steel frame was expected to stay in the linear range for the set of earthquakes to be applied to it. As mentioned earlier, the main objective of the tests on the bare frame was to obtain the frame's dynamic characteristics and to be able to model its behavior, analytically. Results from these tests and the analytical modeling details are presented below:

#### **3.4.1 Stiffness Test**

In this test a known amount of lateral force was applied to the frame, and the displacement of the frame was measured. A total of 100 lbs was applied on the pulley mechanism, using lead blocks. From the maximum observed displacement, the initial estimated stiffness of the frame is

$$K = \frac{\text{lateral force}}{\text{displacement}} = \frac{0.1 \text{ kips}}{0.05 \text{ in}} = 2.0 \text{ kips/in.}$$

### **3.4.2 Free Vibration Test**

In the free vibration test, the frame was pulled back using a cable and turnbuckle, and then suddenly released by cutting the cable. The free vibration of the top of the frame was measured. The displacement response of the frame to the free vibration test is shown in figure 3-12(a). Also shown in figure 3-12(b) is the power spectral density of the displacement response. The distinct spike observed at 2.78 hz. corresponds to the free vibration frequency of the bare frame. This corresponds to a natural period of 0.36 secs.

### **3.4.3 Impact Hammer Test**

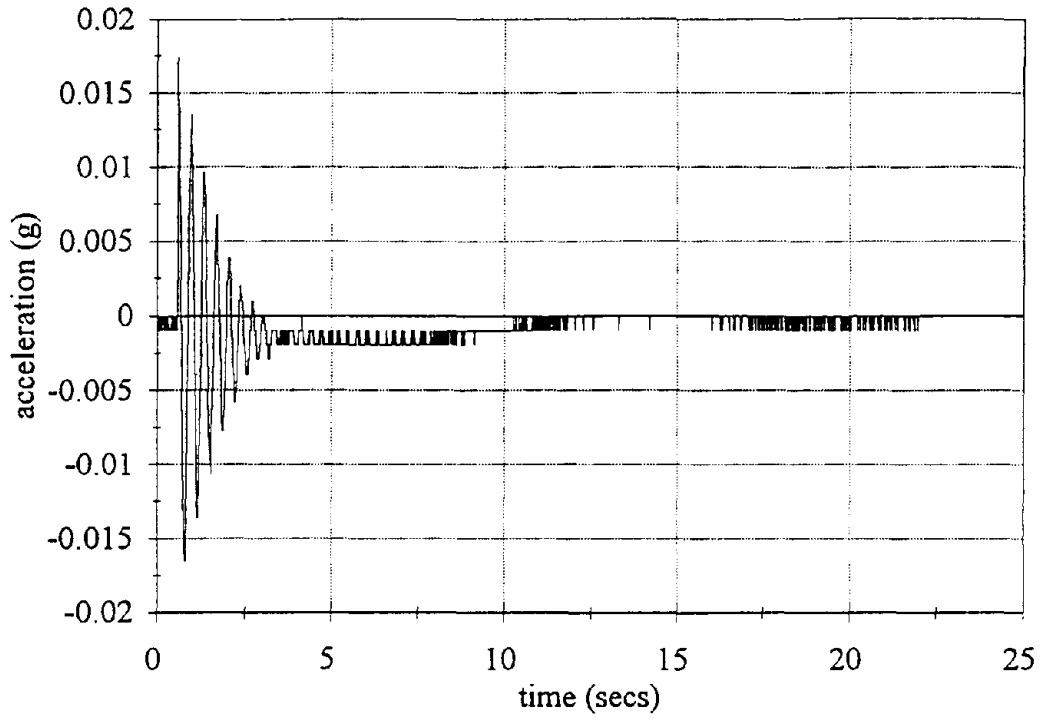
The impact hammer test involves, as the name suggests, applying an impulse load to the frame by impacting with a hammer. The displacement response of the frame to the impulse loading is shown in figure 3-13(a). As in the free vibration test, the power spectral density plot of the response was used to estimate the natural period of the frame. The power spectral density plot in figure 3-13(b) shows a spike at 2.92 hz. which indicates a natural period of 0.34 secs.

### **3.4.4 Dynamic Loading of Frame using Recorded Ground Motions**

Table 3-II outlines the set of ground motions applied to the bare frame. The drift in the frame is calculated by subtracting frame displacement from table displacement. Shear in the frame was calculated by multiplying the frame accelerations times the simulated mass.

$$\text{Drift} = \text{mass displacement} - \text{table displacement}$$

$$\text{Shear} = \text{mass acceleration} * \text{mass}$$



Power spectral density of accerelation

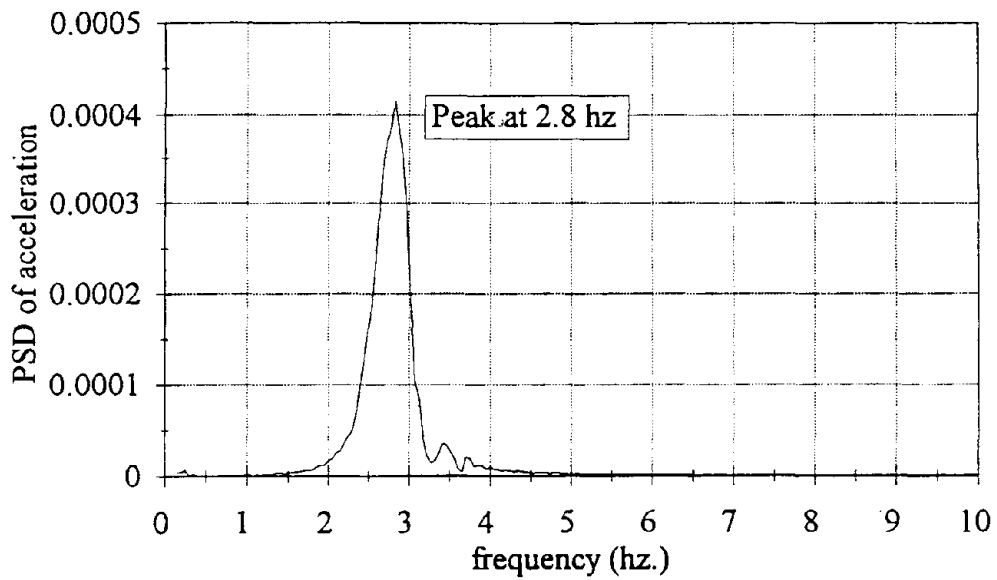
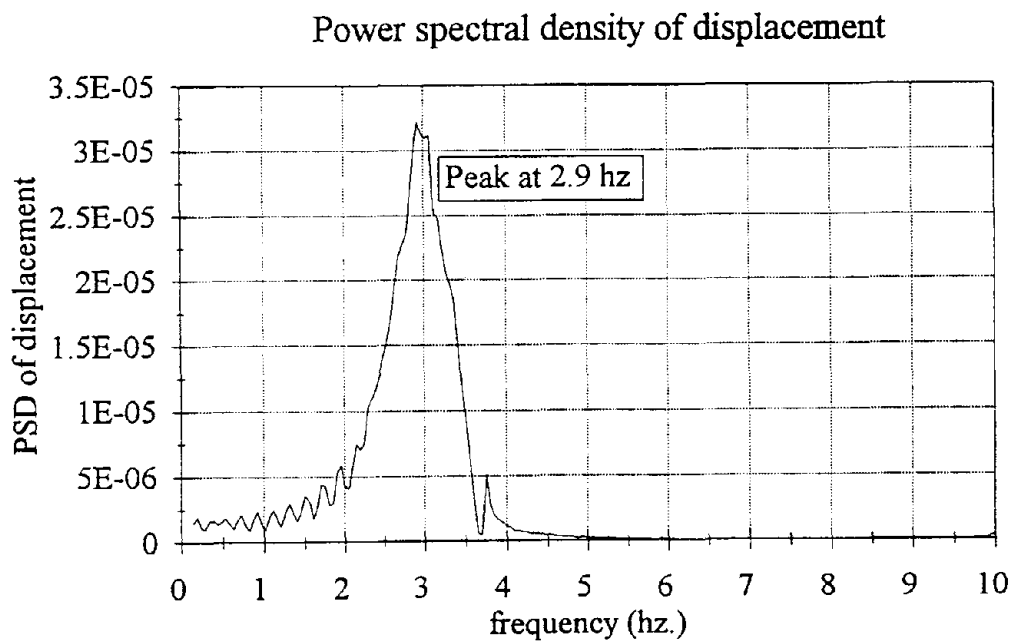
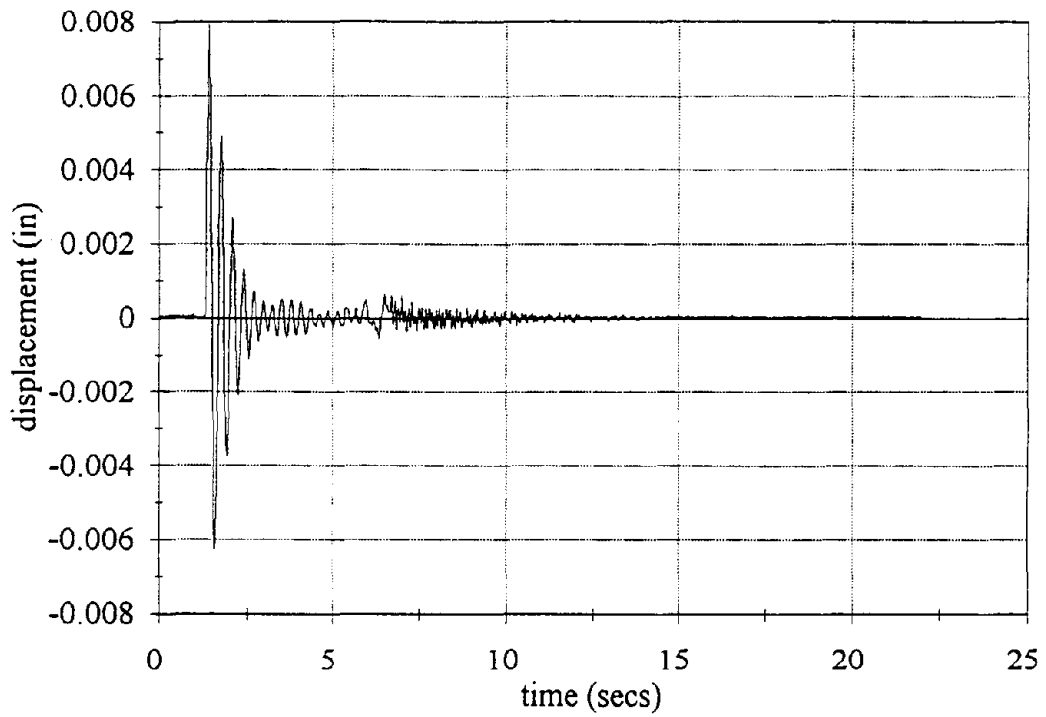


FIGURE 3-12: Acceleration time history and PSD from free vibration test



**FIGURE 3-13: Displacement time history and PSD from impact hammer test**

The response of the frame in shear-drift domains are shown in figure 3-14 for the Taft ground motion. It can be observed that the frame response is restricted to the linear range for the level of excitations used. From the shear-drift response of the frame, the stiffness of the frame can be estimated, as shown in figure 3-14, giving  $K = 2.5$  kips/in. The frame can hence be modeled as a linear oscillator with a small viscous damping (see figure 3-15). The properties defining the single degree of freedom (SDOF) system are its period and viscous damping. The mass of the system is known to be 3.86 kips. After considering several period and damping properties, the following values were found to best match the experimentally obtained time history response:

Period of frame  $T_f = 0.38$  secs.

Damping  $\xi$  (% of critical) = 4 %

Considering the idealized mass of the model to be 3.86 kips, the frame stiffness is calculated to be:

Frame stiffness  $K_f = 2.7$  kips/in

### **3.5 Shake Table Test Results for Frame with Retrofit**

In this section, results from the tests performed on the frame retrofitted with the wall-dampers are presented. The retrofitted frame was first subjected to a set of low level Taft earthquakes (PGA around 0.07g), for six different torque settings of 0, 25, 50, 75, 100 and 125 in-lbs. These set of tests provided a means of studying the variation in the slip load in the damper with change in applied torque. The force in the damper was calculated by subtracting the shear in the frame from the total shear in the system. The shear in the frame was calculated by multiplying the frame drift with estimated stiffness of the frame. The stiffness of the frame was estimated from the post-slip stiffness observed in the hysteresis of the retrofitted frame (figure 3-16).

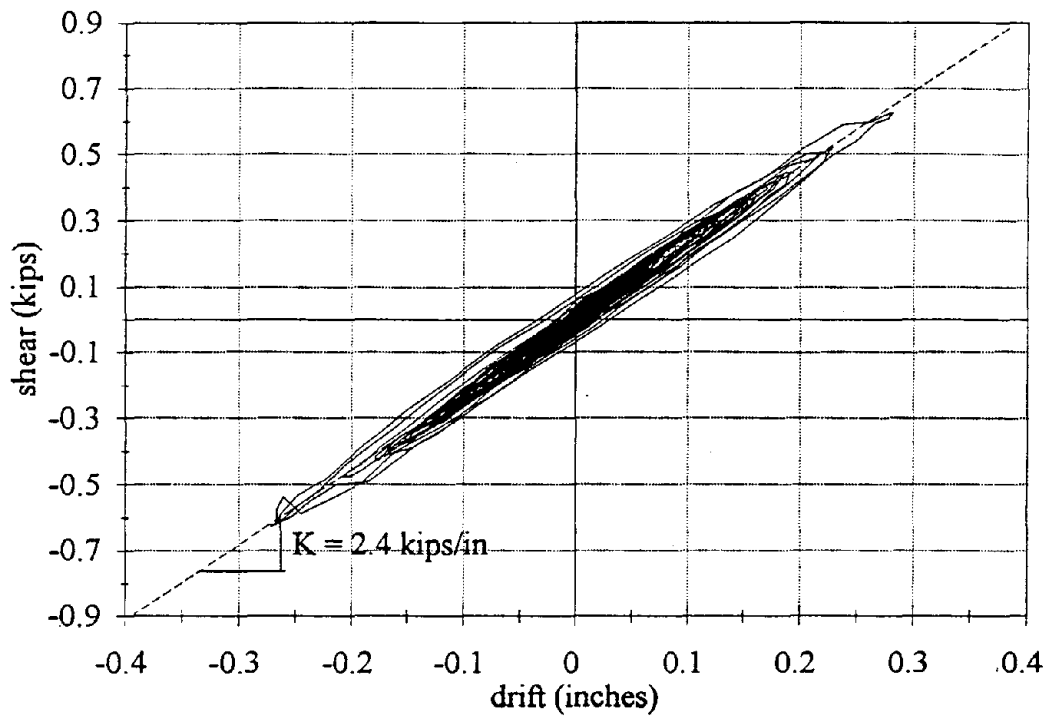


**FIGURE 3-14: Estimating frame stiffness from bare frame response**

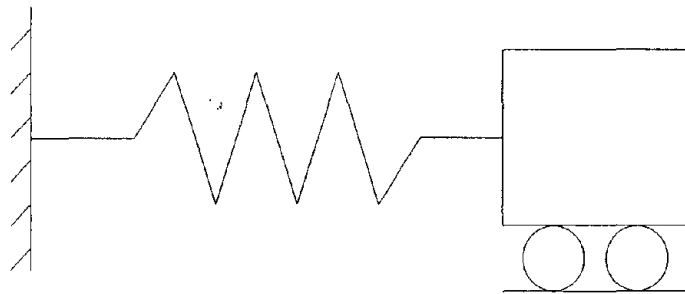


**FIGURE 3-15: Idealized SDOF system**

The stiffness of the frame was estimated to be 2.5 kips/in, which is very close to the estimates made in Section 3.4. Hence the force in the damper can be calculated to be:

$$F_D = F_{\text{base}} - K_{\text{frame}} * \text{drift}$$

where  $F_D$  = force in the damper

$F_{\text{base}}$  = total shear in the frame

$K_{\text{frame}}$  = stiffness of the bare frame

In the next step, moderate level Taft (PGA around 0.11g) and Pacoima (PGA around 0.12g) motions were applied to the frame with the dampers. For each earthquake, two damper settings were selected. The ground motions used and the damper settings are specified in table 3-III. For each of the tests, time history of the frame drift, frame shear and the frame response in story shear -story drift plane are plotted in figures 3-17(a) and (b) for the Taft and Pacoima ground motions, respectively. The wall uplift measured near the column base was less than 0.025 inches.

### **3.6 Interpretation of Test Results**

An important aspect of these tests is to compare the performance of the frame with and without the dampers and thereby study, experimentally, the influence of the added wall-damper system. It must be noted that the ground motions generated by the table are not easily repeatable. Hence to study the response of the frame with and without the dampers for the same ground motion, the bare frame response was estimated from the analytical SDOF model of the bare frame. As described in Section 3.4, the bare frame can be analytically represented by a SDOF system with  $T = 0.38$  s, and damping of 4% of the critical value. In figures 3-18(a) and (b), the response of the frame with friction dampers (torque = 100 in-lbs) is compared with the analytically estimated response for

the bare frame, for Taft and Pacoima ground motions respectively. For Taft ground motion, the dampers are successful in reducing the maximum drifts as well as the maximum total shear in the frame. However in the case of the Pacoima earthquake, introducing the dampers resulted in an increase in the maximum base shear and maximum drift response. This effect can be explained based on the frequency distribution of the ground motion as well as the time history nature of the input ground motions. One of the reasons why the dampers were ineffective in reducing the frame response when the Pacoima ground motion was used, was that the Pacoima motion is characterized by an impulsive motion with the peak arriving very early in the earthquake time history. The damping effect needs a few cycles of energy dissipation to be able to be effective in reducing peaks, and hence is ineffective in mitigating the early peak.

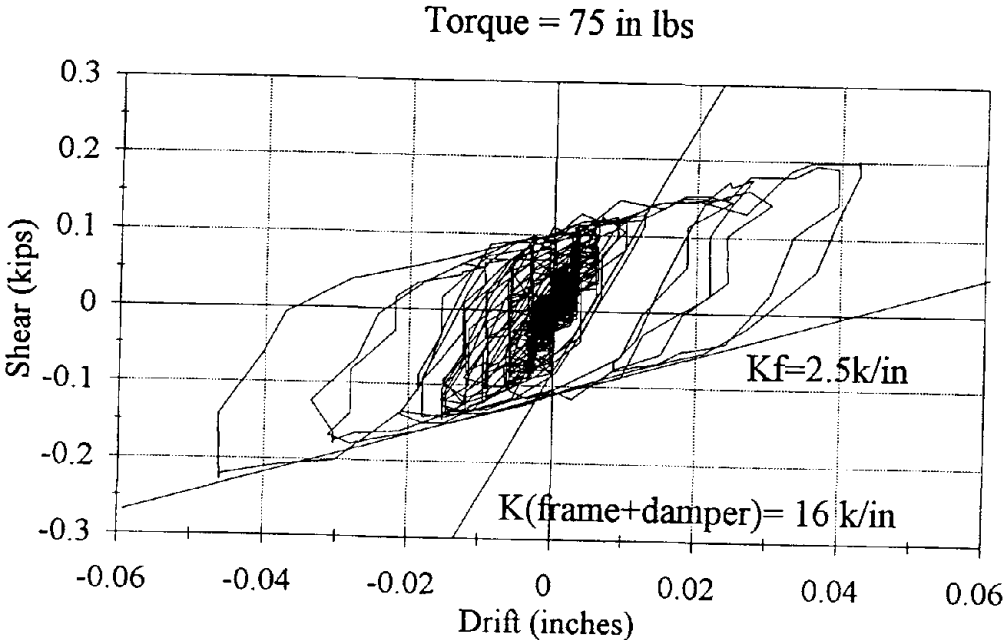


**FIGURE 3-16: Measured pre and post slip stiffness**

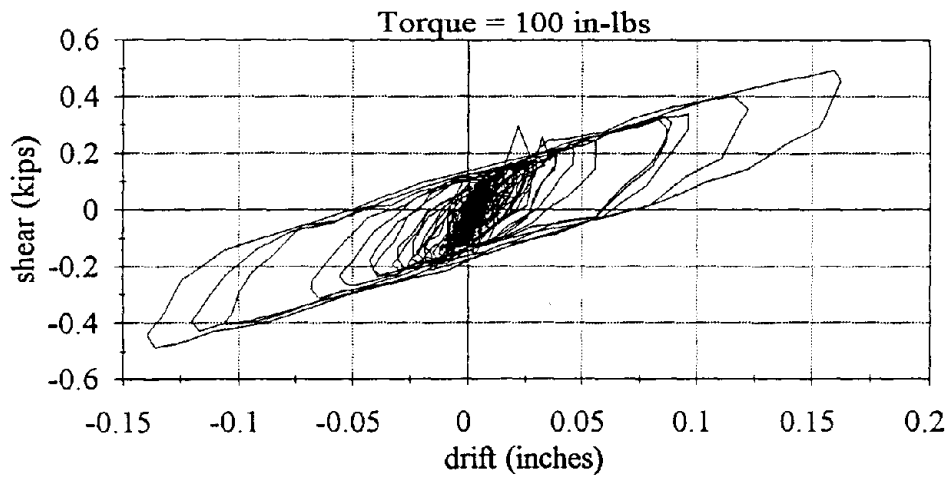
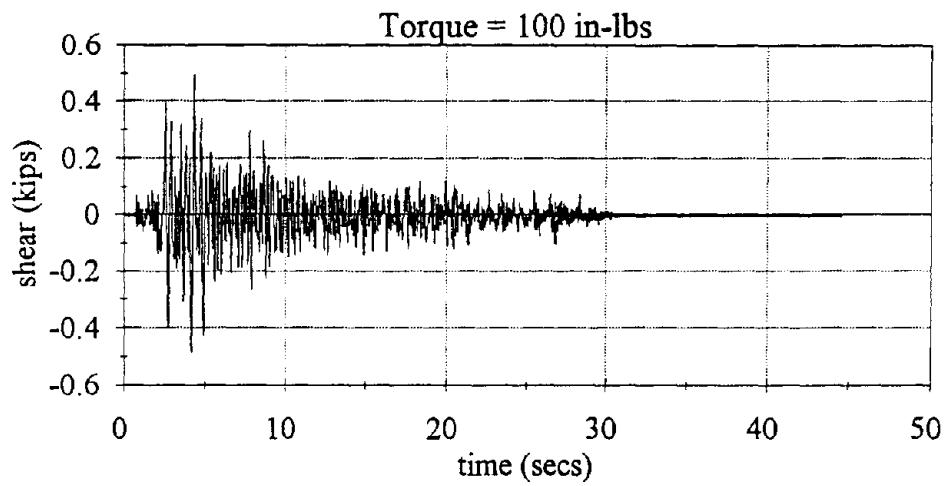
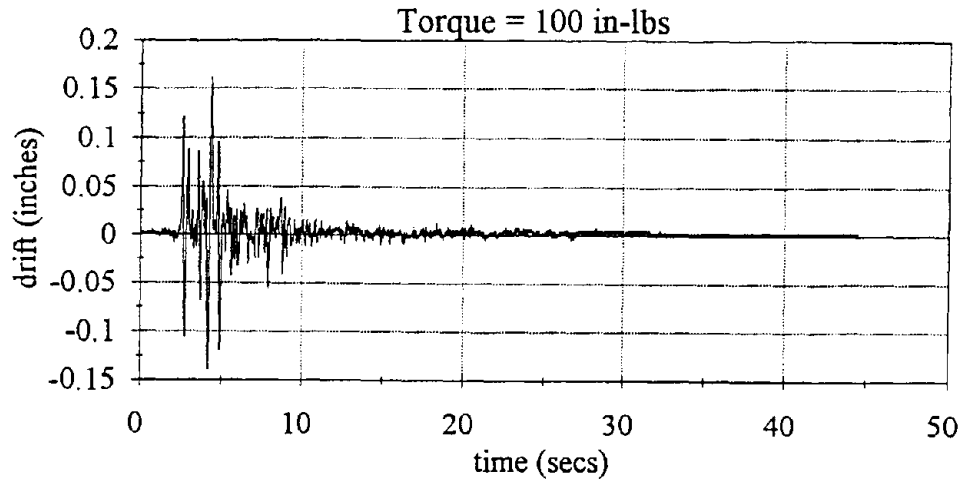


**FIGURE 3-17(a): Response of retrofitted frame to moderate level Taft motion**

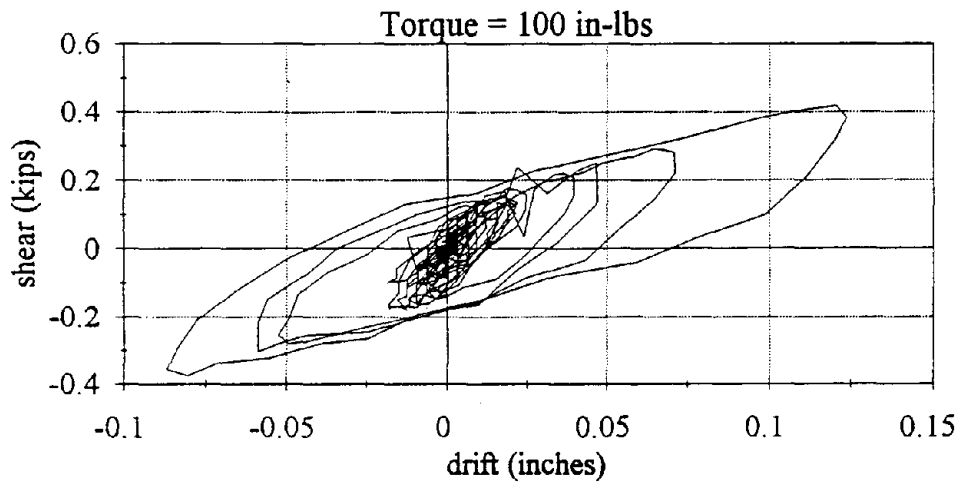
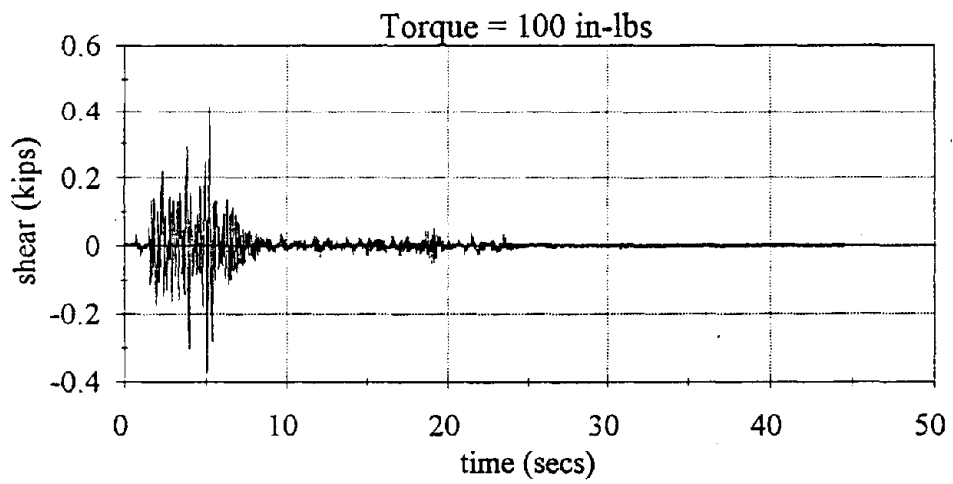
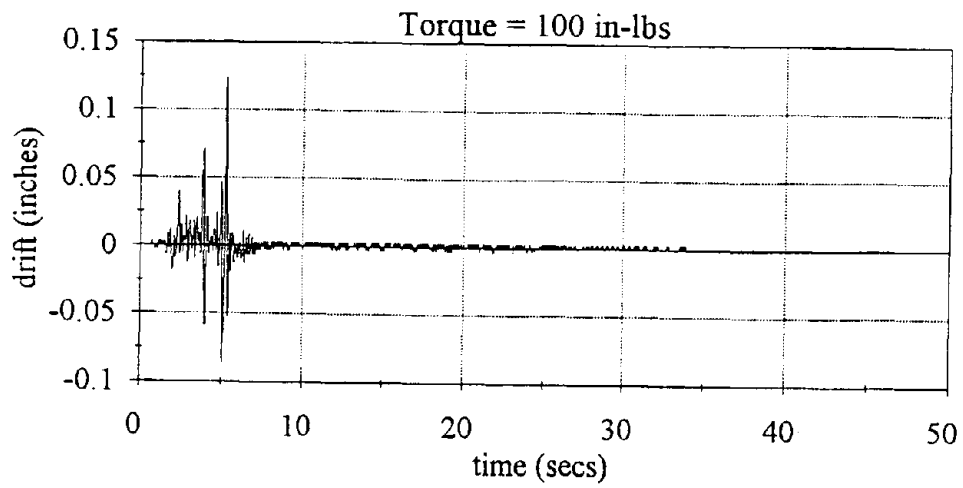


**FIGURE 3-17(b): Response of retrofitted frame to moderate level Pacoima motion**

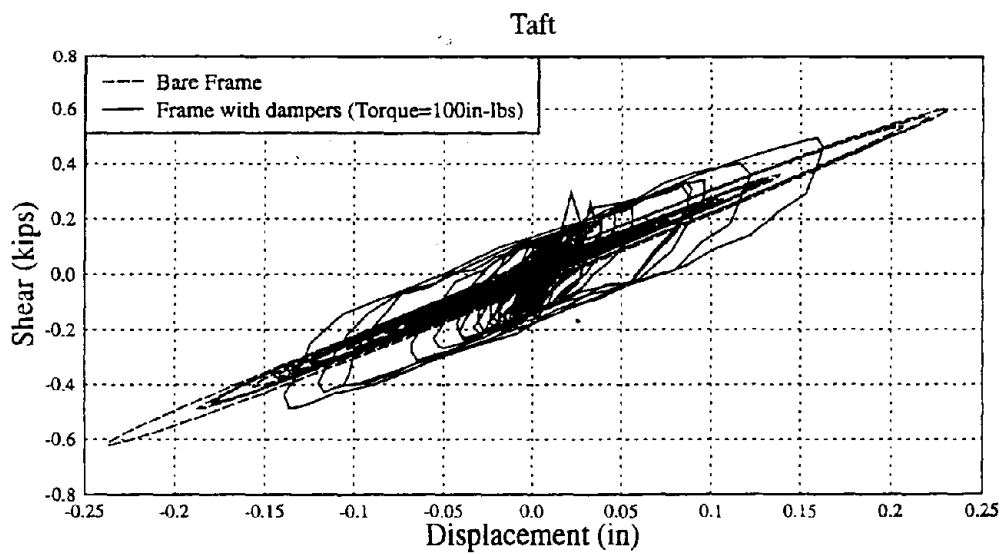
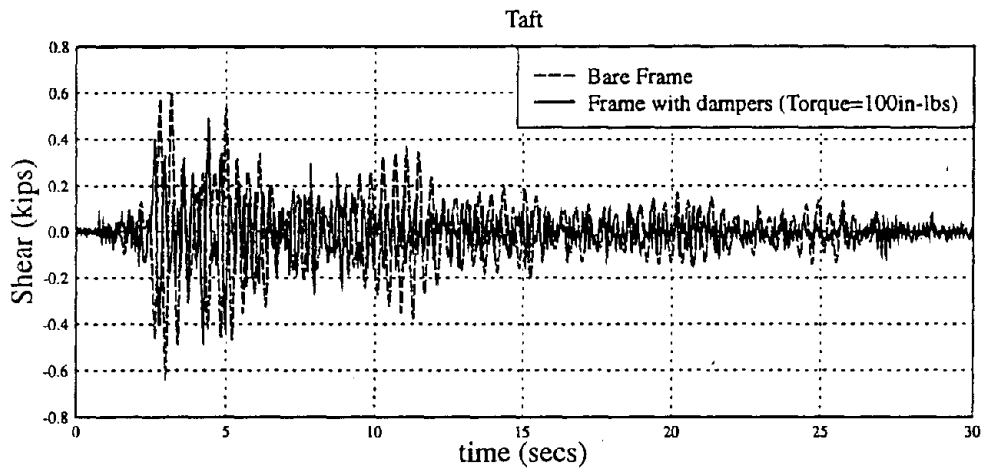
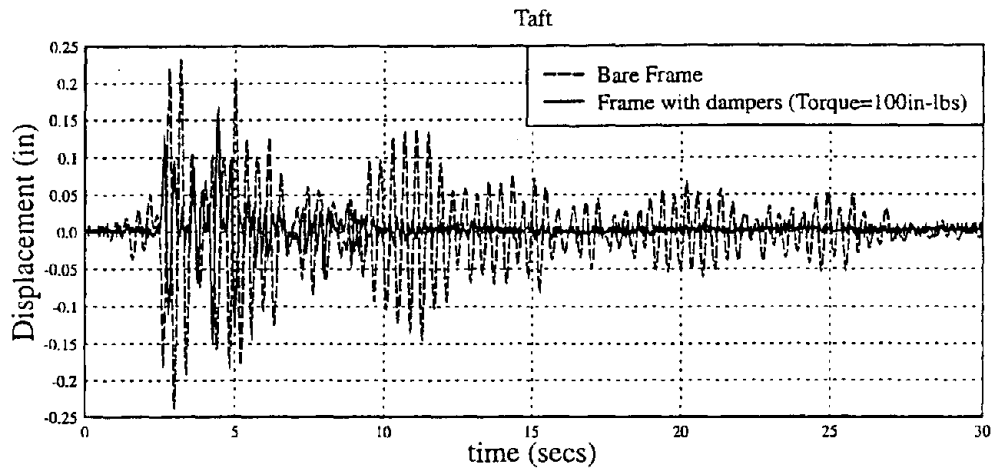


**FIGURE 3-18(a): Comparison of bare frame and retrofitted frame response (Taft)**

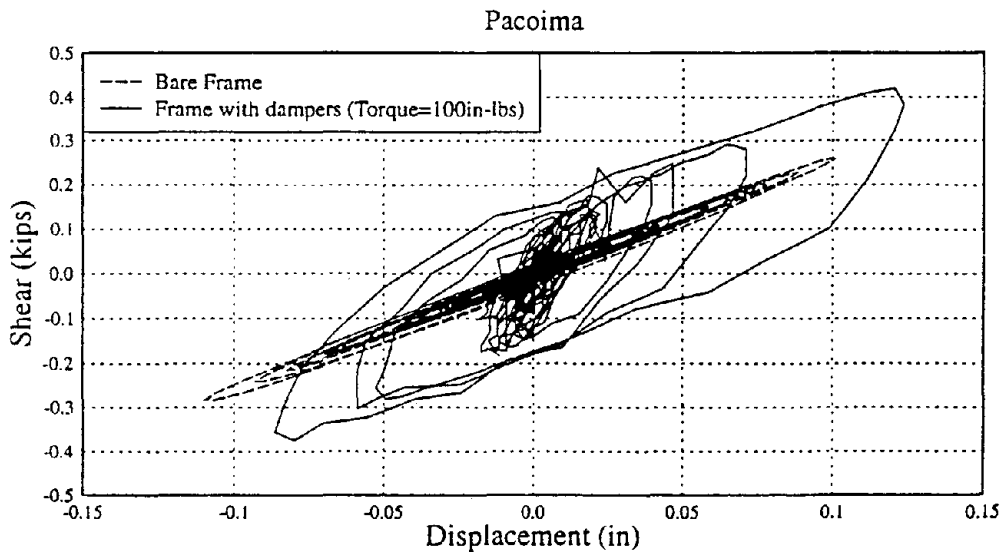
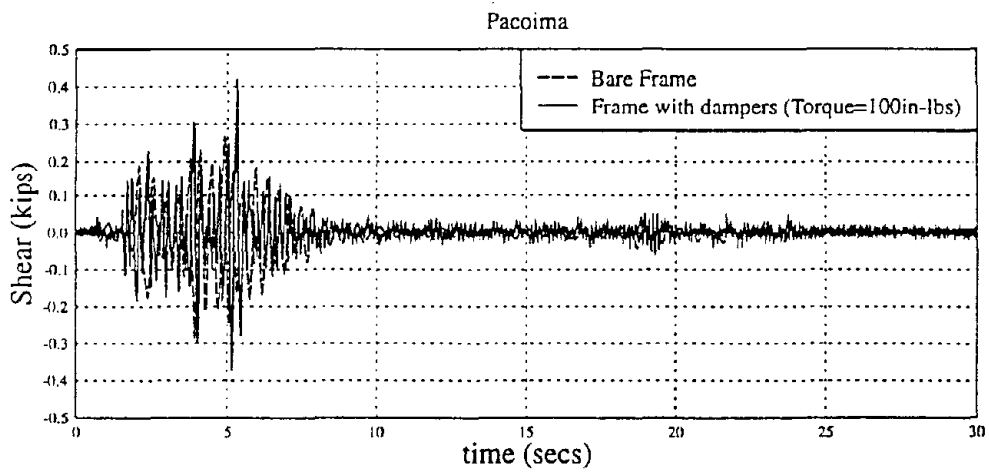
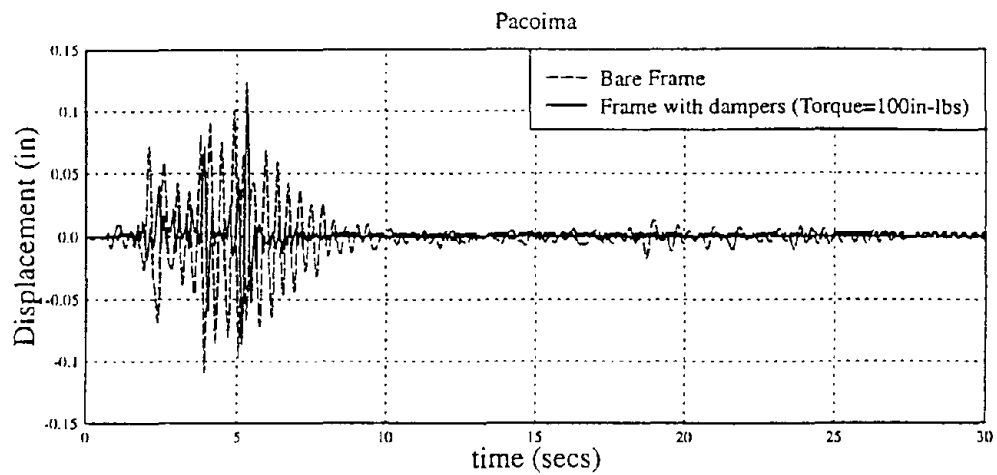


**FIGURE 3-18(b): Comparison of bare frame and retrofitted frame response (Pacoima)**

However, as seen in figure 3-18, although the maximum response is not reduced, the later part of motion is damped effectively. However for both the earthquake loadings, the dampers were successful in providing excellent energy dissipation characteristics.

The frequency content of the input motion and the natural period of the structure can strongly influence the effectiveness of added stiffness and damping. The influence of the dampers can be better visualized using the response spectrum plotted in the spectral acceleration - spectral displacement plane. Feeman (1992) introduced the representation of plotting the response spectrum in  $S_a$ - $S_d$  plane, which has been widely used in recent publications (Reinhorn et. al. (1995), ATC-33). In figure 3-19(a), the maximum drift and accelerations of the frame with and without the dampers for Taft2\_100 motion are plotted along with the response spectra of the ground motion. Figure 3-19(a) indicates that stiffening the structure by introducing the wall dampers pushes the structure to a position on the response spectrum where there is smaller displacement demand on the system. The added damping reduces the total acceleration and hence the total shear on the frame, and also the drifts are further reduced. By matching the maximum response of the friction damped frame with an equivalent viscous damping, it can be interpreted from figure 3-19(a) that the friction damper provided an equivalent of 12% viscous damping.

The response of the friction-damped frame and the bare frame in the acceleration- drift domain when subjected to Pacoima motion (designation Pac2\_100) is shown in figure 3-19(b). Here it can be seen that the frame is so located on the response spectrum that stiffening it up increases the displacement and the acceleration demand. Additional damping is not sufficient to bring down the total displacement and shear demand. For the friction-damped frame, the equivalent viscous damping was 8.5% as calculated from response spectrum fitting. Hence it can be concluded that the natural period of the structure in relation to the frequency content of the input ground motion determines

whether adding walls with friction dampers would be effective in reducing the frame response.

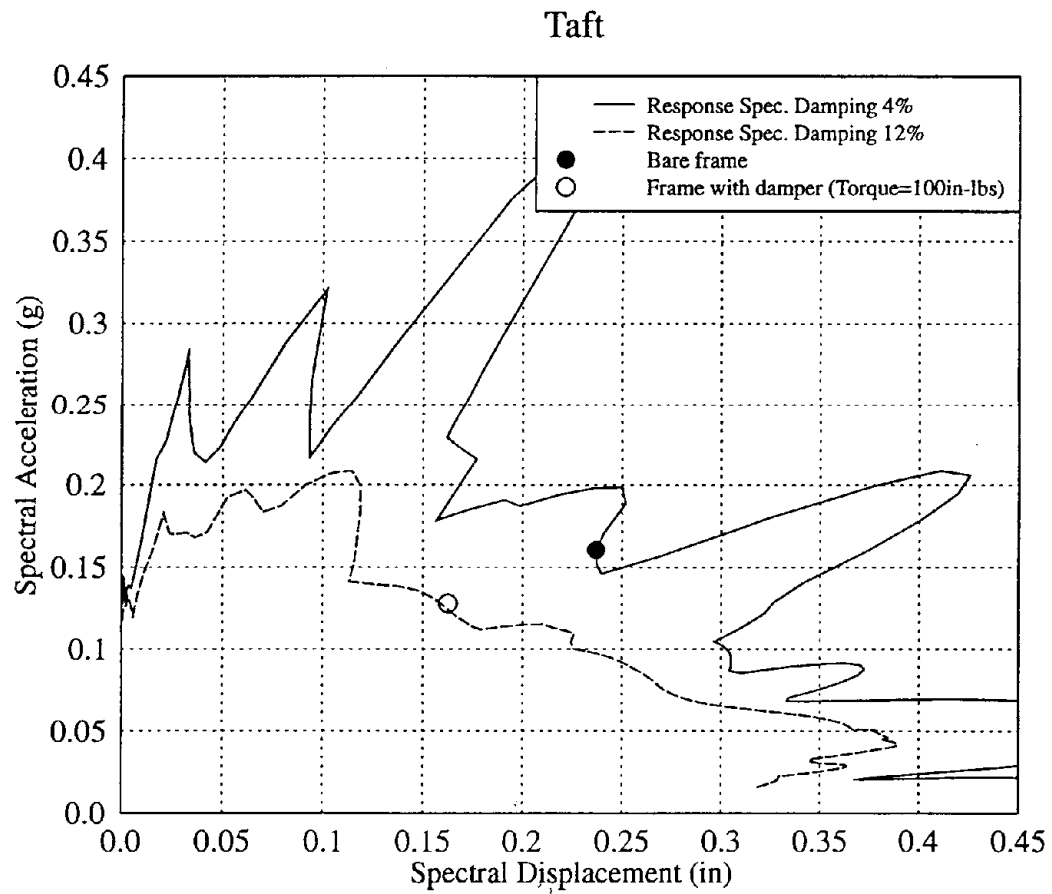


**FIGURE 3-19(a): Response spectrum interpretation for damper performance under Taft**

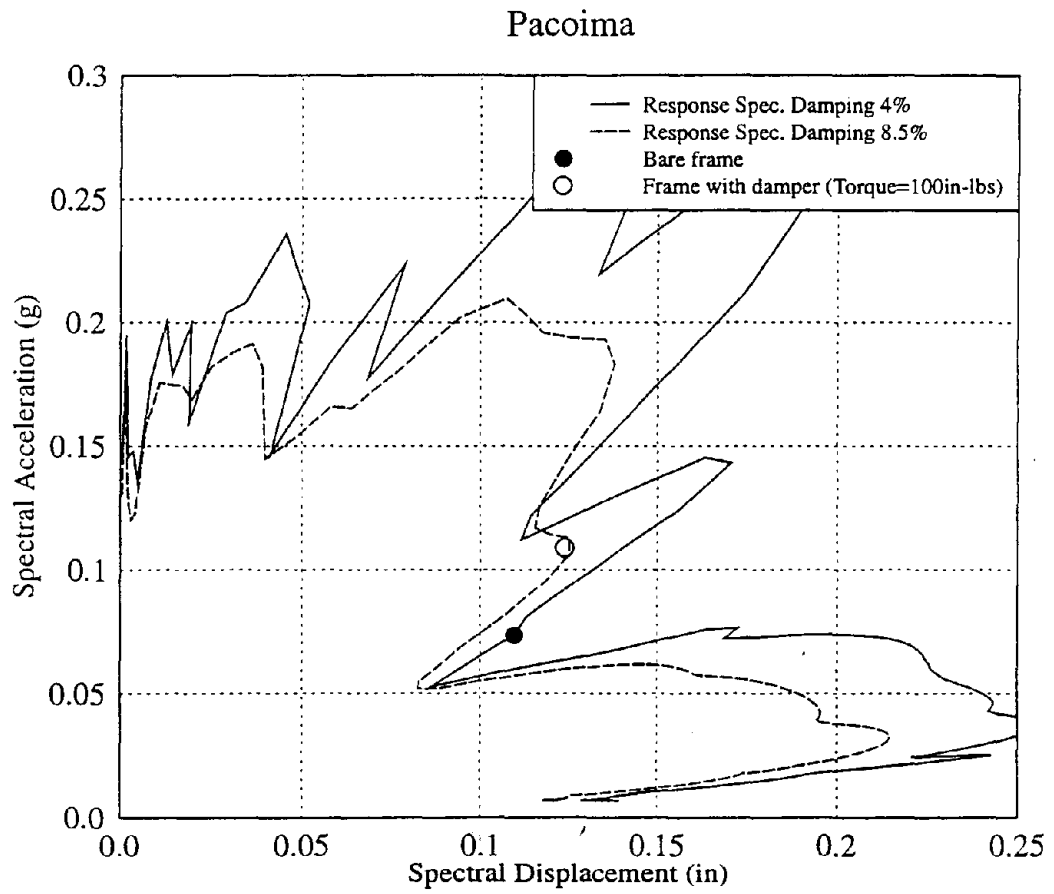


**FIGURE 3-19(b): Response spectrum interpretation for damper performance under Pacoima**

### 3.7 Analytical Modeling of Wall-Damper Retrofit Scheme

One of the main objectives of this experimental program was to characterize the wall-damper setup. To be able to analytically study the performance of full scale structures when retrofitted with the wall-damper scheme, it is first necessary to be able to analytically model the response of the simple model used in the shake table experiment. The overall response of the frame with the dampers is a combination of the response of the linear frame and the nonlinear wall-damper. From the known stiffness of the frame, and the pre-slip stiffness of the wall-damper and the slip load, the entire system can be idealized as a bilinear SDOF spring. The initial stiffness of the bilinear spring is the sum of the frame and wall stiffnesses and the post-slip stiffness represents the stiffness of the frame. The properties of the bilinear spring that provided the best match with the experimental results are:

$$K_{\text{pre-slip}} = 16.0 \text{ kips /in}$$

$$K_{\text{post-slip}} = 2.5 \text{ kips /in}$$

In figure 3-20(a) and (b), the measured displacements and shears for the frame with dampers, for Taft and Pacoima motions, are compared with the corresponding values obtained from time history analysis of the above mentioned bilinear spring. It can be seen that the frame response is fairly well predicted by the idealized SDOF bilinear spring. Based on the properties of the overall system, the initial stiffness of the wall-damper can be calculated to be:

$$\begin{aligned} K_{\text{pre-slip of wall-damper}} &= K_{\text{total}} - K_{\text{frame}} \\ &= 16.0 - 2.5 = 13.5 \text{ kips/in} \end{aligned}$$

Based on this, the initial stiffness of the full scale wall-damper system can be estimated.

Hence the pre-slip stiffness of the full scale wall-damper scheme must be

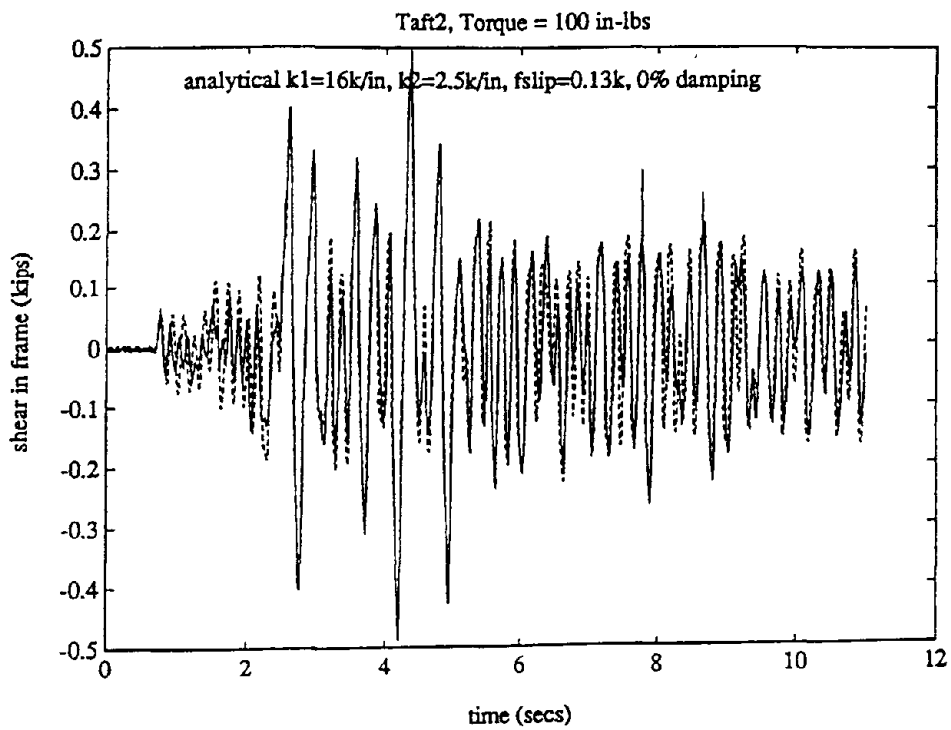
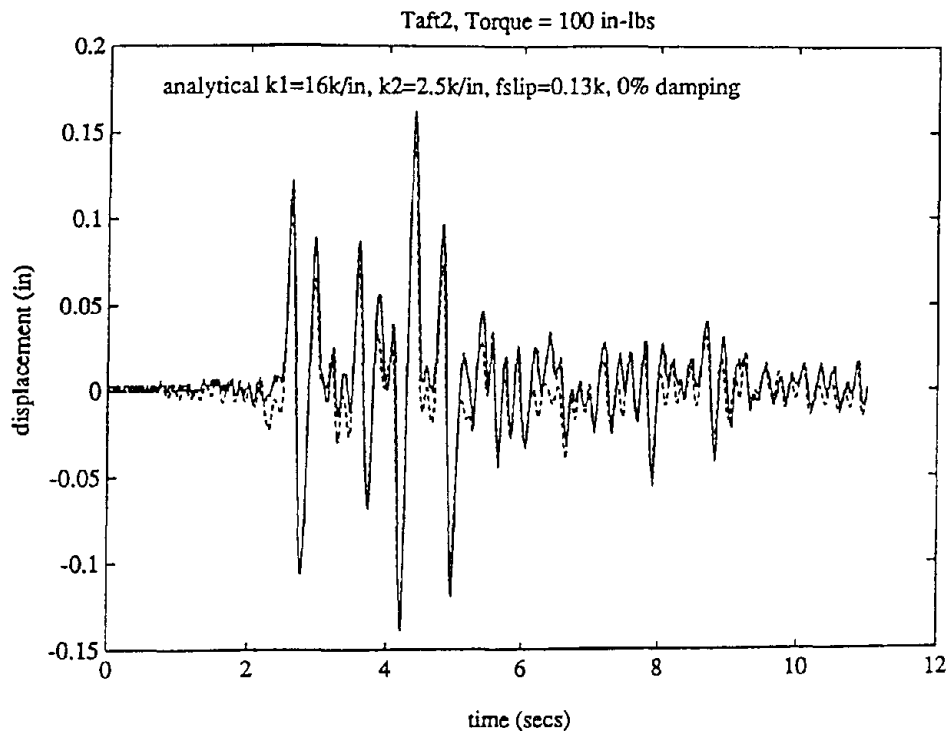


**FIGURE 3-20(a): Analytical modeling of retrofitted frame under Taft**

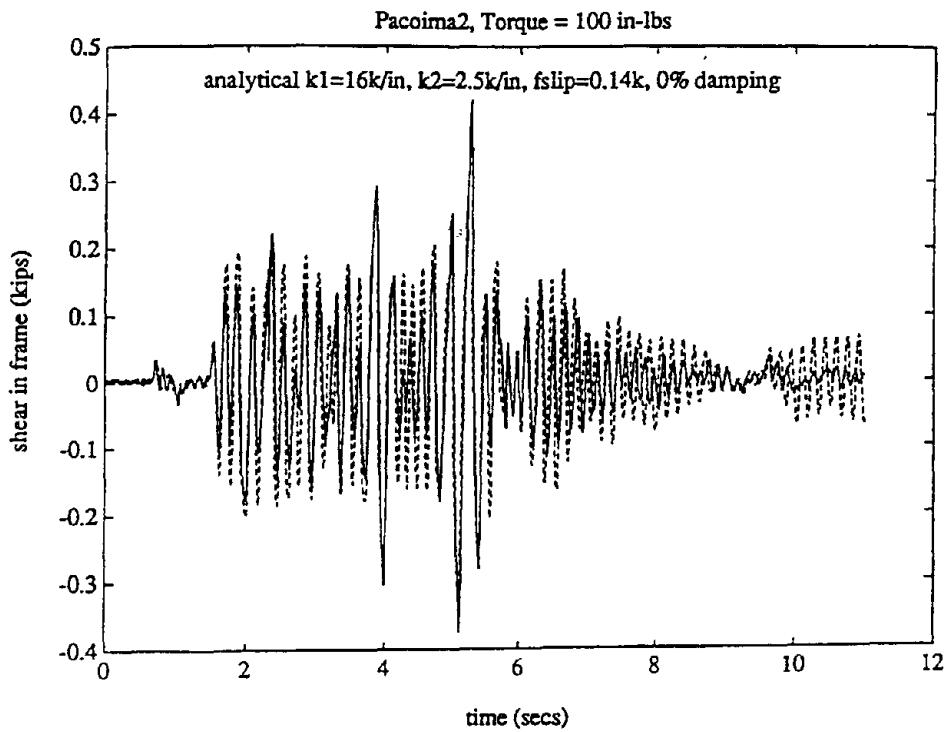
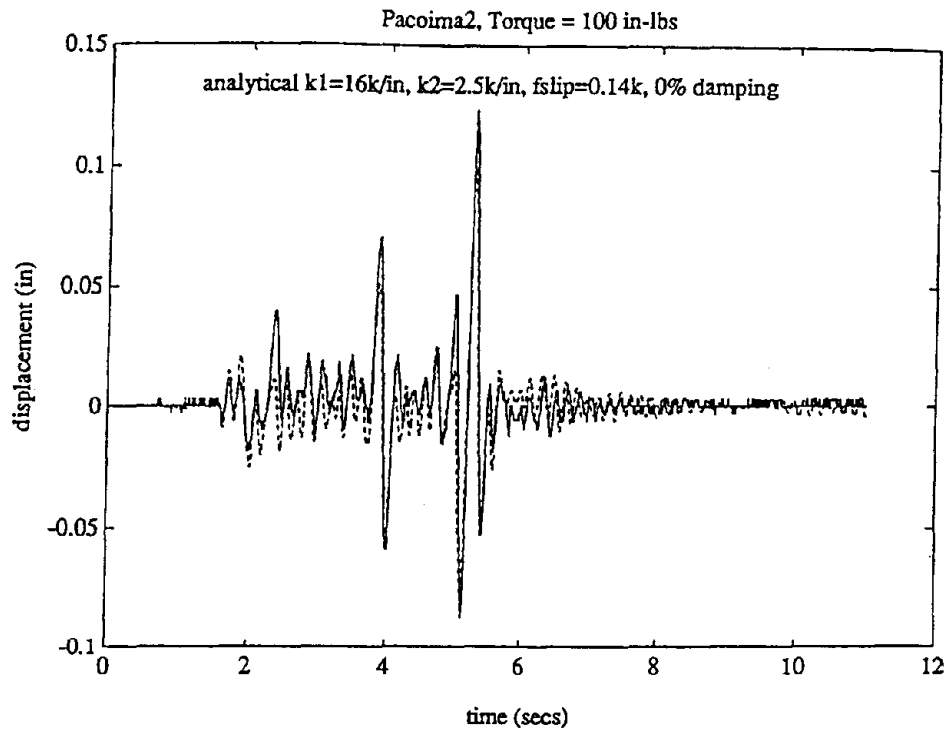


**FIGURE 3-20(b): Analytical modeling of retrofitted frame under Pacoima**

$$\begin{aligned}
 K_{\text{full scale}} &= K_{\text{model}} * \text{scale} \\
 &= 13.5 * 3 \text{ kips/in}
 \end{aligned}$$

It must be recalled that though the model frame was scaled to 1/3rd the dimensions of a typical bay of a RC frame, the masonry blocks used were of 1/4 scale. Hence the total stiffness of the overall full-scale wall-damper system would be:

$$\begin{aligned}
 K_{\text{full scale}} &= K_{\text{model}} * 3 * 4 / 3 \\
 &= 13.5 * 4 = 54.0 \text{ kips/in}
 \end{aligned}$$

Since the experiment model is distorted due to the use of 1/4 scale blocks, the stiffness calculated above is an estimate of the prototype wall's pre-slip stiffness. Hence the hysteretic behavior of the wall-damper system must be modeled as a system with rectangular hysteresis.

### **3.7.1 Incorporating wall-damper model in IDARC 3.0**

The next stage of the research involves extensive analytical studies to evaluate the effect of placing wall-dampers on the response of non-ductile RC frames when subjected to a wide variety of ground motions. A nonlinear analysis software IDARC 3.0, developed at SUNY-Buffalo [Kunnath (1990)], was used to model the RC frame. Salient features of the program are:

1. A trilinear envelope curve is used to model nonlinear moment curvature of beams and columns, and the shear force - shear strain behavior of shear walls.

2. A three parameter hysteretic model is used capture the response of RC elements under cyclic loading. Using these parameters, strength degradation, stiffness degradation, and pinching effects can be accounted for.
3. The shear wall is modeled as a shear spring in series with a flexural spring.

To model the wall-damper scheme, the flexural spring was selected to have a very large stiffness. Hence, the properties of the shear spring determine the overall wall response. In order to model the rectangular hysteresis of the damper, a new hysteretic model subroutine was added to the program, since the three parameter hysteretic model cannot simulate the required hysteresis. Details of the nonlinear analyses are given in Section 4.

## **SECTION 4**

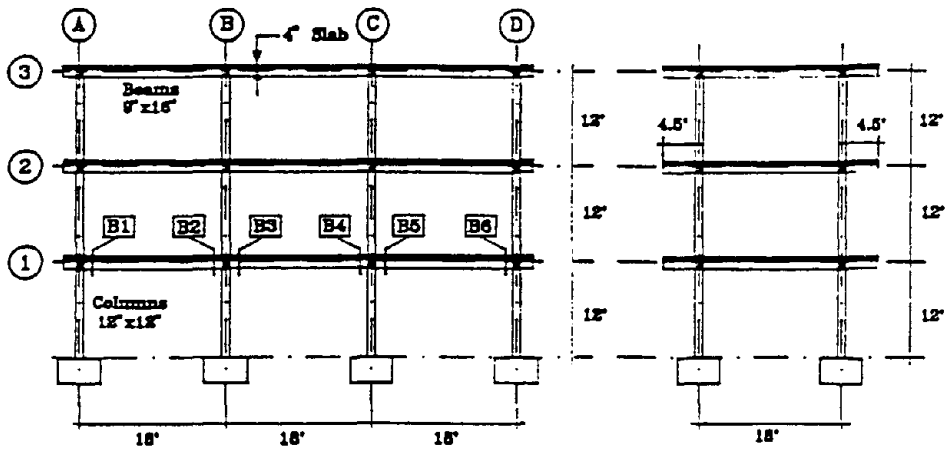
### **EVALUATION OF RETROFIT SCHEME FOR A THREE STORY NON-DUCTILE RC FRAME**

#### **4.1 Introduction**

The proposed retrofit scheme was dynamically tested in a scaled shake table experiment, and shown to be effective in providing additional stiffness and energy dissipation. The earlier section (Section 3) provides the description and discussion on the test program. Results of an analytical investigation to study the effectiveness of the retrofit scheme for a three story non-ductile RC frame are presented in this section. As mentioned in Section 1, several analytical studies and tests conducted at Cornell and SUNY (Buffalo) used a slice of a three story three bay RC frame. The same frame will be used in this Section to study the effectiveness of the proposed retrofit method. Details of the frame are shown in figure 4-1. The structure has reinforcement details conforming to pre-1970 construction, details of which are described in Section 2. The three story frame is considered to be a fairly representative structure, since most existing buildings are three stories high or less.

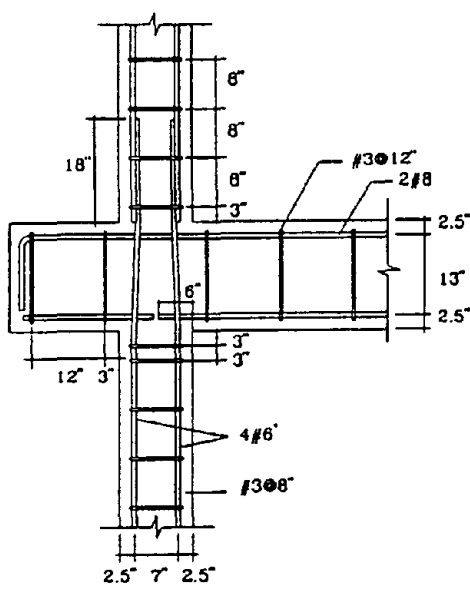
#### **4.1.1 Results from Earlier Tests and Analytical Studies**

El-Attar (1991) performed shake table tests on a 1/8 scale model of the three story frame. The frame was subjected to four levels of Kern County Earthquake (Taft Lincoln school Tunnel, 1952, S69E component). The peak ground accelerations of the four scaled motions were 0.05g, 0.18g, 0.35g and 0.8g. Peak inter-story drift (as % of story height) and base shear (as % of weight of the structure) response of the model for the first three ground motions are given in table 4-1. The structure collapsed under the 0.8g earthquake due to the formation of hinges in the first story columns. However, the structure would most likely have collapsed under a 0.4g to 0.5g PGA Taft earthquake.

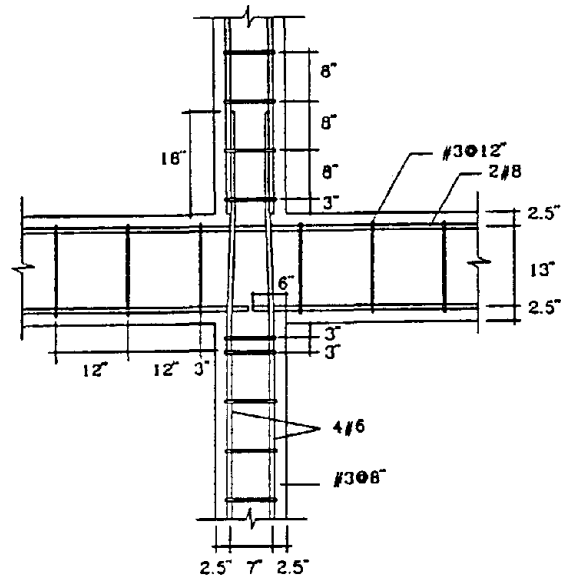


(a) Elevation.

(b) Sideview.



(b) Exterior Joint.



(a) Interior Joint.

FIGURE 4-1: Details of the three story nonductile RC building

Similar shake table tests were performed on a 1/3 scale model of the three story frame at SUNY [Bracci et. al. (1991)], with the applied ground motion being the N21E component of Kern County (Taft Lincoln school tunnel) earthquake having PGAs of 0.05g, 0.2g, and 0.3g. Peak response values for the test are presented in table 4-II. For the tests by Bracci et. al., under the severe earthquake loading (PGA=0.3g), considerable amount of inelastic deformation occurred in all the stories of the frame. Yielding in the first story columns indicated that soft story collapse mechanism was in development. These observations were found to be consistent with those made after tests by El-Attar.

**TABLE 4-I Shake Table Tests by El-Attar (1991)**

Earthquake	Max. Story Drift (%)	Max. Base Shear (%)
Taft S69E PGA=0.05g	0.18	2.3
Taft S69E PGA =0.18g	1.87	8.53
Taft S69E PGA = 0.35g	2.63	9.43

**TABLE 4-II Shake Table Tests by Bracci et. al. (1992)**

Earthquake	Max. Story Drift (%)	Max. Base Shear (%)
Taft N21E PGA=0.05g	0.28	6.5
Taft N21E PGA=0.2g	1.33	15.2
Taft N21E PGA=0.3g	2.24	15.3

Pessiki et. al.(1990) and Beres (1994) performed cyclic load tests on full scale beam column joints with various reinforcement configurations. In all 34 interior and exterior

joint specimens were tested. El-Borgi (1993) modeled the behavior of these connections using a smoothed hysteretic model. The model so developed was incorporated into a modified version of IDARC. El-Borgi utilized the model to analytically study the performance of the three story frame under various earthquakes. The dimensions of the sections for the three story frame used by El-Borgi were larger than those for the frame used by El-Attar and Bracci et. al.. The results obtained from the analyses are given in table 4-III.

Beres used the capacity spectrum method to predict the response of the three story frame of El-Borgi to various ground motions (see table 4-IV). It must be noted that in all the tests and analytical studies, only the bare frame without walls was considered.

**TABLE 4-III Analytical Results El-Borgi (1993)**

Earthquake	Max. Story Drift (%)	Max. Base Shear (%)
Taft S69E PGA=0.02g	0.09	5.6
Taft S69E PGA=0.2g	0.85	17.6
Taft S69E PGA=0.35g	1.48	21.3

**TABLE 4-IV Results from Simplified Analysis [Beres (1994)];**

Earthquake	Max. Story Drift (%)	Max. Base Shear (%)
Taft S69E PGA=0.2g	1 to 1.2	18 to 21
Taft S69E PGA=0.35g	1.8	25

Comparisons of the experimental and analytical responses of the three story frame by various investigators yields the following conclusions:

1. Bracci et. al.'s tests resulted in lower story drifts, but higher base shear coefficients when subjected to moderate and severe earthquakes. Due to weight limitations in the shake table actuators, live load was not considered for mass similitude for Bracci et. al.'s tests. As a result, the frame used in El-Attar's test was more flexible, which could explain the difference in results. Also, it must be noted that different components of Taft earthquake were used in the two tests. However, for both tests it was found that while the structure survived the severe earthquake (defined as 0.35g Taft), the drifts in the structure were large (1.33% and 1.87% respectively for Bracci et. al.'s and El-Attar's tests), even for moderate earthquake (0.18g). Hence, apart from partial structural damage, severe non-structural damage would be expected for moderate level earthquakes.

2. From the analytical studies performed on the stiffer three story frame, El-Borgi found much lower drift values for 0.2g and 0.35g Taft ground motions, and also a lower value for the period of the frame, in comparison to test results. In contrast Beres, using the capacity spectrum method, predicted larger drifts and damage levels for 0.2g and 0.35g Taft. Also the estimated period of the structure by Beres was much higher.

3. It must be noted that one cannot expect a good match between the shake table tests by El-Attar and Bracci et. al. and analytical predictions by El-Borgi and Beres, since the structure used by the latter was stiffer. The column sizes in the frame used by Beres and El-Borgi were 16"X16" as opposed to the 12"x12" column sizes used in the frames tested by El-Attar and Bracci et. al.. Also, for the shake table tests, ground motions were applied in sequence, as a result, changing the characteristics of the structure after each run.

It can be concluded in general that the three story frame displayed sufficient ductility at the joints to survive large drift levels. However, the structure was very flexible, resulting in large displacement responses even for moderate level ground motions. To control the extent of non-structural damage, the structure needs to be retrofitted.

## **4.2 Defining Performance Objectives**

In the studies described above, story drifts, story shears and damage indices were used to characterize the response of the structure to various ground motions, but there were no clearly defined acceptability limits. A realistic structural evaluation-rehabilitation project would involve the five or six steps shown in figure 4-2. Following the steps shown in figure 4-2, it is necessary to define the earthquake loading

### **4.2.1 Selection of Earthquake Loading**

There is no general consensus about defining the design ground motions. Several measures including peak ground or spectral acceleration, peak ground velocity, spectral intensity, and input energy. have been suggested as earthquake demand parameters. While each of the parameters has its own merits and drawbacks, there is no simple method to relate these parameters with the possible severity of the earthquake for a given geographical region. It was decided to instead use the procedure suggested in ATC-33 (50 % complete draft) for defining the earthquake loading and performance criterion.

The ATC-33 document (“Guidelines and Commentary for the Seismic Rehabilitation of Buildings”) is a product of the program sponsored by the Federal Emergency and Management Agency (FEMA) to prepare a set of technically sound, nationally applicable and influential guidelines for the seismic rehabilitation of buildings. At present a 50% complete draft has been prepared for review by the Seismic Rehabilitation Advisory Panel. The document is provided in three volumes: Volume I-

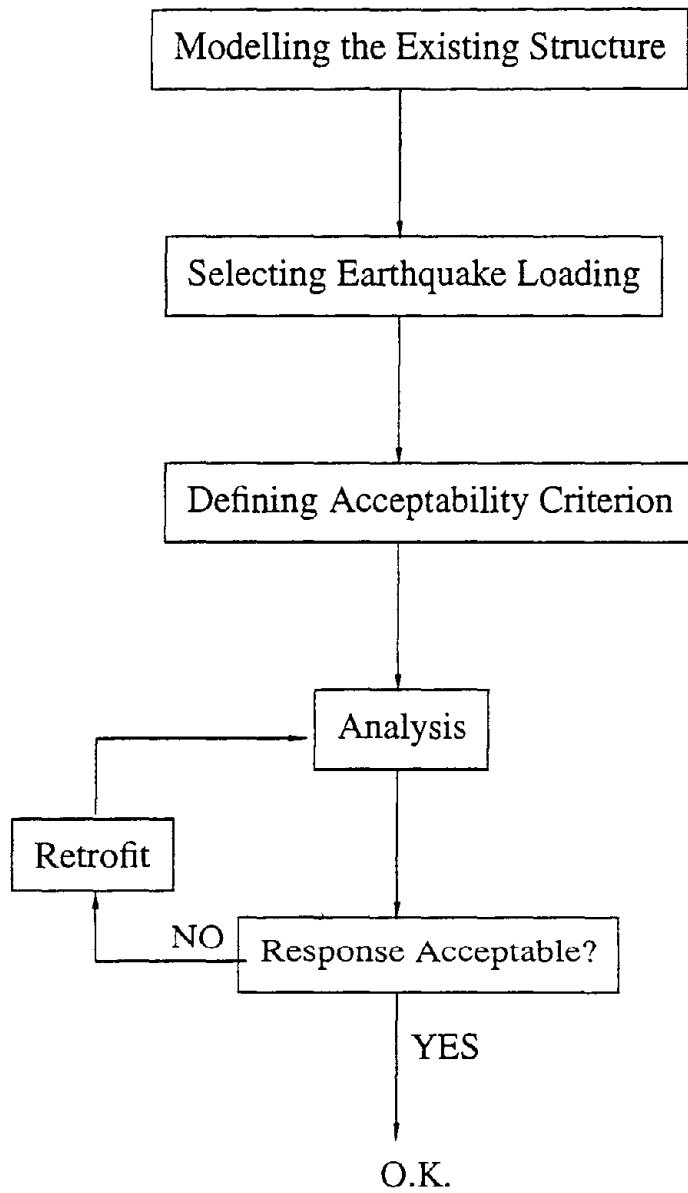


**FIGURE 4-2: Process in a seismic evaluation-rehabilitation project**

Guidelines, Volume 2-Commentary and Volume 3-Model Buildings Applications.

References have been made to several parts of the ATC-33 50% complete draft.

The earthquake loading is defined by two levels of ground motions with return periods of 500 years and 2500 years respectively. The loading so defined with the corresponding acceptable responses (defined in the next section) forms the performance objective. The ground motion for each return period was specified using a design spectrum with 5% damping. The design spectrum was constructed from NEHRP'94, where the variation of  $S_a$  (spectral acceleration) with period is shown below:

$$C_{sm} = \frac{1.2 C_v}{T^{2/3}} \quad (R = 1)$$

$$C_{sm} \leq 2.5 C_a$$

$$C_{sm} = \frac{3C_v}{T^{4/3}} \text{ for } T > 4.0\text{s}$$

and for soil profile types D, E and F

$$C_{sm} = C_a (1.0 + 5.0T) \text{ for } T < 0.3\text{s}$$

ATC-33 (50% draft) gives values of  $A_a$ (effective peak acceleration) and  $A_v$  (effective peak velocity-related acceleration) for different regions which are adopted from NEHRP. These values are for a return period of 475 years. From charts in ATC-33 (50% draft) values for  $A_a$  and  $A_v$  can be extrapolated for other return periods. Further, the coefficients  $C_a$  and  $C_v$  used in the above equations can be obtained for different soil types. For this research, the primary region of interest is the Eastern and Central US cities such as Boston, St. Louis (Missouri), Charlotte (North Carolina) and Memphis (Tennessee), which lie in zone 3 of the NEHRP maps; these were chosen as representative locations. Also it was decided to consider sites with stiff soils (soil type C). For time history analysis, either artificial ground motions can be constructed to match the design spectrum or recorded ground motions can be scaled until the response

spectrum of the recorded motion approximates the design spectrum. For this study it was decided to use nine recorded earthquakes with different characteristics as the input ground motions. The wide range of earthquakes used would serve as a test for the performance of the retrofit scheme. Tso et. al (1992) noted that A/V (ratio of peak ground acceleration (PGA) to peak ground velocity (PGV)) can be used to classify earthquakes. Low A/V ratio reflects ground motions with long duration and with energy in the low frequency range. High A/V ratios were found to represent ground motions with short duration and energy in the high frequency range. Also ground motions recorded near small or moderate earthquakes had higher A/V values, while earthquakes with low A/V values were large earthquakes measured at large distance from the epicenter. Tso et. al. (1992) classified earthquakes into three categories having A/V ranges as follows:

- Category 1:  $A/V < 0.8\text{g/m/s}$
- Category 2:  $0.8\text{g/m/s} \leq A/V \leq 1.2\text{g/m/s}$
- Category 3:  $A/V > 1.2\text{g/m/s}$

Three earthquakes were selected from each of the three categories. Details of the earthquakes selected are given in table 4-V. However in real-life design, the earthquakes selected should reflect the site conditions and would fall in only one of the three A/V categories.

**TABLE 4-V Description of Selected Ground Motions**

Earthquake No.	Earthquake	PGA g	A/V, g/m/s
1	Longbeach (N51W)	0.097	0.41
2	Lower California (S00W)	0.16	0.77
3	Michoacan Mexico City (S00E)	0.1033	0.65
4	Imperial Valley (S00E)	0.348	1.04
5	Kern County (Taft N21E)	0.156	0.99
6	San Fernando (N90E)	0.211	1.0
7	Parkfield (N85E)	0.434	1.70
8	Pacoima (S74W)	1.075	1.86
9	Nahanni (N10E)	0.9752	2.112

As mentioned earlier, the earthquakes selected were scaled until their response spectra “matched” the design spectra defined for return periods of 500 years and 2500 years. The response spectrum is considered to have “matched” the design spectrum when the following conditions are satisfied:

$$Avg\left(\frac{S_a(RS)}{S_a(DS)}\right) > 1.0 \quad \text{for all } T$$

and  $Avg\left(\frac{S_a(RS)}{S_a(DS)}\right) > 1.0 \quad \text{for } T = 1.0 \text{ to } 2.5s$

**TABLE 4-VI PGA's for 500 year and 2500 year earthquake**

Earthquake No.	Earthquake	PGA g (500 yr)	PGA g (2500 yr)
1	Longbeach (N51W)	0.093	0.174
2	Lower California (S00W)	0.268	0.498
3	Michoacan Mexico City (S00E)	0.076	0.141
4	Imperial Valley (S00E)	0.237	0.441
5	Kern County (Taft N21E)	0.262	0.485
6	San Fernando (N90E)	0.223	0.41
7	Parkfield (N85E)	0.495	0.921
8	Pacoima (S74W)	0.464	0.858
9	Nahanni (N10E)	0.73	1.351

The period range of 1.0s to 2.5s was selected since the three story frame was expected to be in this range, before and after cracking/yielding take place. figure 4-3 shows the response spectrum “matching” for the Taft earthquake for a 500 year return period. Table 4-VI shows the PGAs for 500 year and 2500 year return periods for the nine earthquakes obtained by matching their response spectra. The earthquake loading for the structure is hence defined.

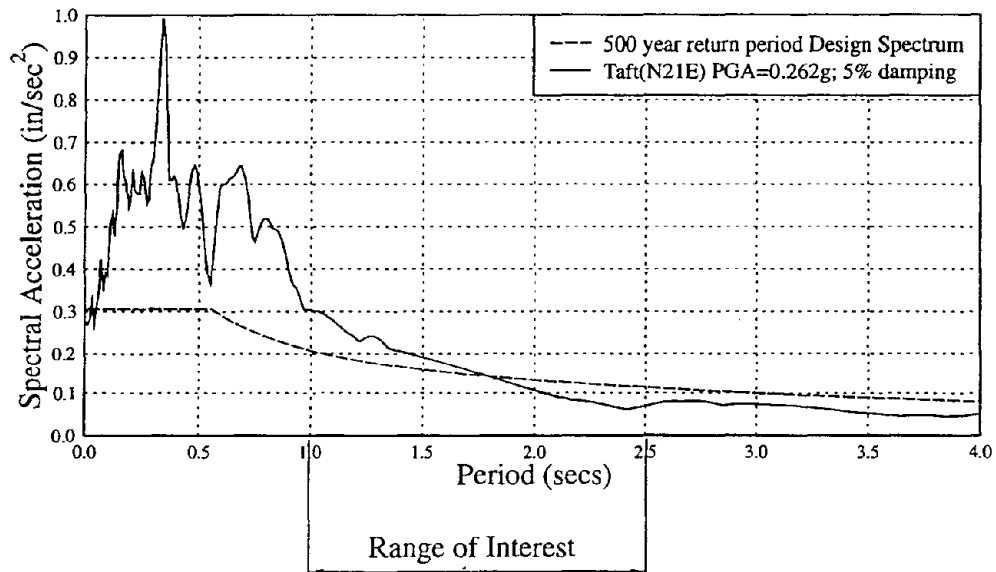


**FIGURE 4-3: Matching response spectra for Taft (N21E) earthquake**

#### 4.2.2 Defining Acceptable Response Limits

For each level of ground motion defined it is necessary to specify an acceptability limit for the structure's response. If the structure has a response level larger than the acceptable limit, the structure would need to be retrofitted (figure 4-2). This brings up the issue of selecting the appropriate response parameter(s). A brief discussion of the various response parameters that can be selected is presented below:

1. Peak Interstory Drift: Maximum interstory drift experienced by a structure when responding to a ground motion is a widely used measure of

structural demand and response. Using the peak drift has the advantage of simplicity and ease in interpretation. This measure however does not capture damage effects due to cyclic loading. If brittle shear failure is precluded in the columns, interstory drift can be used as a sound measure of structural damage state [Toussi and Yao (1983)]. Hasselman and Wiggins (1982), showed some correlation between peak interstory drift and a financial index, defined as the ratio of repair cost to replacement cost. Also, the maximum drift is a reasonably good indication of the non-structural damage experience during the earthquake.

2. Damage Indices: Several damage indices have been proposed over the years to quantify the damage state of a structure or element. Park and Ang (1985), used a combination of peak response and cumulative energy dissipation to define their damage index. Dipasquale and Cakmak (1987) used the ratio of maximum instantaneous period during the earthquake and initial period to obtain the damage index. These and several other damage indices, while based on logically sound principles, suffer from the drawback of difficulty in interpretation of damage index values. Based on regression analyses, attempts have been made to correlate damage indices with visually observed damage. However it has been noted during shake table tests that it is difficult to judge the state of damage in a structure through visual inspection alone.

3. Peak Base Shear: The peak base shear and the peak overturning moment at the base represent the peak demand on the foundations. If the foundations were not designed for large lateral forces or overturning moments, peak shear base overturning moment, and axial force in the footings are important parameters to be monitored to prevent instability.

In light of the above discussion, it was decided to use the maximum interstory drift as a response parameter for the structure. ATC-33 also indirectly uses this parameter to define the acceptability limits. ATC-33 categorizes the overall performance of the structure in terms of the following levels:

- Collapse Prevention (CO): The structure is in a severe damaged state, on the verge of collapse. However the gravity load elements have sufficient integrity to prevent complete collapse and probably the consequent loss of life.
- Life Safety (LS): The structure has undergone some structural and non-structural damage, but there is some margin for collapse. The overall risk of loss of life to occupants is low, i.e. less than CO. The structure is repairable, though it might be economically impractical to do so.
- Immediate Occupancy (IO): The structure has undergone very limited damage. Basic structural elements retain their pre-earthquake capacities. Risk of personal injury is low and the structure can be occupied immediately after minor cleanup.

For different types of structural systems, the damage state corresponding to the three performance levels is given in ATC-33 50% draft. For the three story non-ductile frame under consideration, the peak interstory drifts corresponding to various performance levels was obtained based on observations from tests performed at Cornell, guidelines given by ATC-33, and some analytical studies. To decide the drift levels corresponding to IO and LS, there is a need for input from socioeconomic researchers, since IO and LS are closely related to the perspective of the occupants.

The National Building Code of Canada (1980) considers 0.5% as the drift limit for window damage. Paultre and Mitchell (1991) used a linear log-log relation between window damage and story drift, based on studies by Hasselman et.al. (1980). They found that for a drift level of 0.75%, the window damage ratio was 19 %. From several cyclic tests performed on beam column joints, Beres (1994) obtained the relationship between story shear and interstory drifts. In figure 4-4, story shear vs. drift envelopes are shown for the wide range of specimens tested. It can be noted that for drifts < 0.75% the components were in the linear deformation range. Hence the drift level of 0.75% can be considered as a limit for immediate occupancy. Also, from figure 4-4, the shear reached its maximum level at around 2% drift level, beyond which there was strength deterioration. However, the structure could still sustain several cycles of loading before severe deterioration was noticed at around 3.5% drift level, where the strength loss was around 40% of the maximum strength level. No brittle shear failure was observed during the tests. Based on these observations, it was decided to assign the following values for various performance levels for flexible frames:

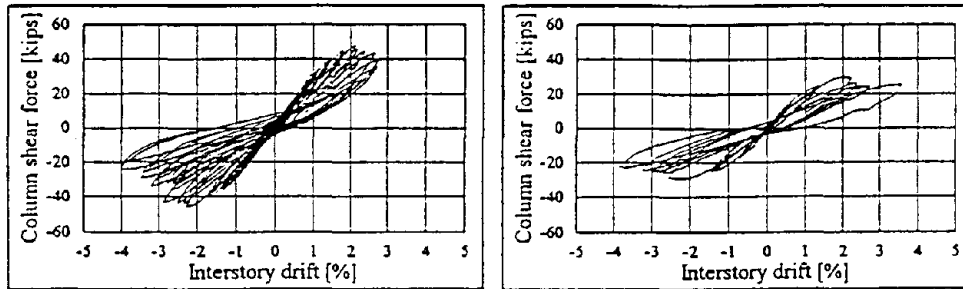
**IO:** max. drift < 0.75%

**LS:** max. drift < 2.0%

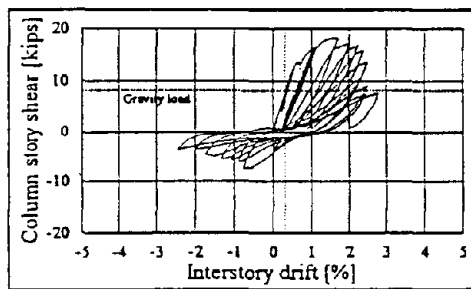
**CO:** max. drift < 3.5%

It must be noted that ATC-33 also explicitly suggests a drift value of 2% for LS, for RC structures. In the tests performed by Beres, the section sizes were larger than those for the three story frame under consideration here. To further verify the rationale of selecting the appropriate drift values for IO, LS, and CO, a non-linear pushover analysis was performed on the three story frame. Details of the pushover analysis are presented in Section 8. Figure 4-5 shows the story shear vs. interstory drift (%) obtained for the first story from the pushover analysis. Figure 4-5 also includes the story shear capacity.

calculated by adding the shear capacities of the columns.  $V_{C+S}$  includes the shear contribution from concrete ( $2\sqrt{f'_c} bd$ ), while  $V_S$  represents the shear capacity

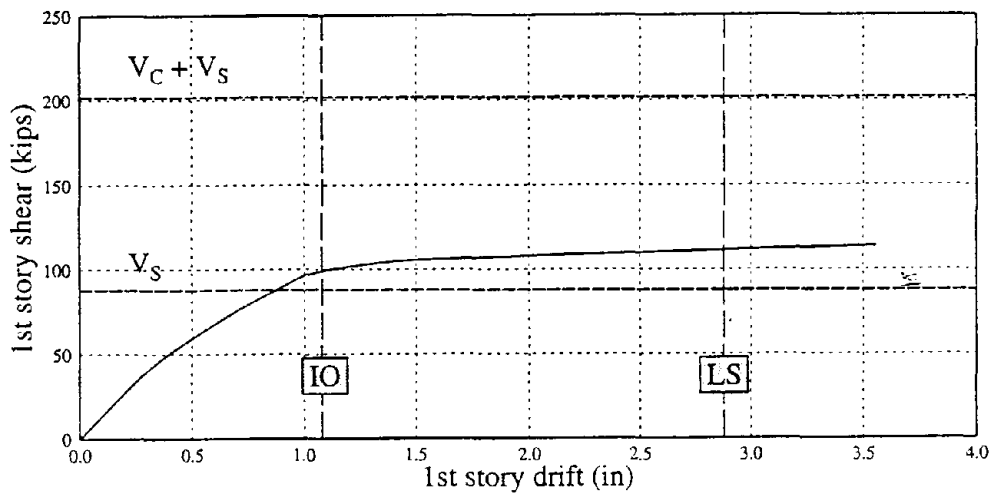


(a) Interior Joint  
Continuous Positive Bars      (b) Interior Joint,  
Discontinuous Positive Bars



(c) Exterior Joint

**FIGURE 4-4: Typical column shear force vs. interstory drift [Beres (1994)]**



IO: Immediate Occupancy, LS: Life Safety

**FIGURE 4-5: Pushover curve for three story frame**

calculated by using only the shear resistance of the stirrups. It can be seen that if concrete shear contribution is considered, no brittle shear failure is possible. In the shake table tests by El-Attar and Bracci et. al., no column shear failure was observed.

### **Desirable Performance Level**

The desirable level of performance of a structure is a highly subjective issue, dependent upon the decision/desire of the owners, the occupants and society as a whole.

Depending on the importance of the structure, to the users, owners or society, one might aim for minimal performance such as CO for 2500 year earthquake, and LS for 500 year earthquake, or one might desire stringent performance such as IO after 500 year earthquake and LS for 2500 year earthquake. For this study, it was decided to aim for collapse prevention under the 2500 year earthquake and substantial damage control (drift < 1.0%) for the 500 year earthquake. Another issue is the foundation capacity. Since it is very expensive to retrofit the foundations, the capacity of foundations, represented by the peak base shear level, should not be exceeded. The foundation capacity depends on several factors such as soil conditions, depth of foundation, foundation details, etc. It was postulated that the capacity of the foundation was about 1.5 times the capacity of the frame. The desired performance level for the frame is schematically shown in figure 4-6.

### **4.3 Modeling the Three Story RC Frame**

The three story frame was analytically modeled in the non-linear dynamic analysis program IDARC(3.0), developed at SUNY (Buffalo). For input motion of Taft (N21E), with PGA of 0.2g, the peak story drifts, displacements and story shears obtained from IDARC analysis were compared with the corresponding Bracci et. al.'s shake table results (scaled to 1/3 scale) (see table 4-VII). The good match indicates that the non-

linear seismic response of the frame can be accurately predicted using IDARC. It must be noted that the results presented are after scaling the test results to represent the full scale frame.

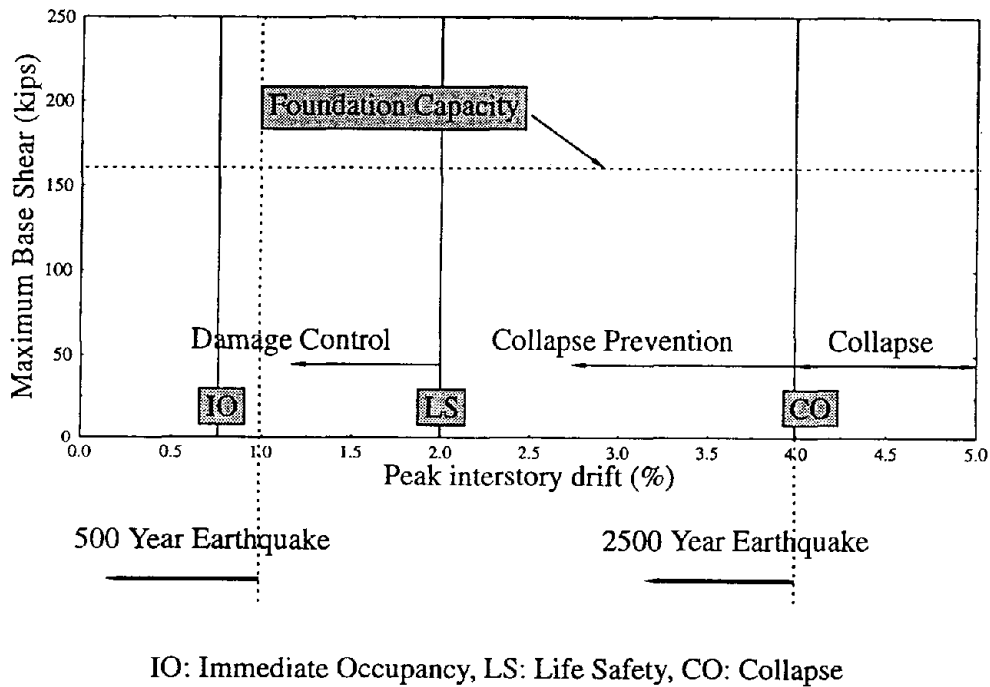


**FIGURE 4-6: Target responses for two levels of earthquake loading**

**TABLE 4-VII Comparison of Analytical and Bracci et. al.'s Test Results**

Story No.	Displ (in)		Shear (kips)	
	Test	Analysis	Test	Analysis
3	1.32	1.35	5.6	5.85
2	1.14	1.07	9.3	9.05
1	0.64	0.49	12.3	11.03

The expected response of the three story bare frame, when subjected to the nine ground motions considered, was analytically calculated using the abovementioned analytical (IDARC) model. Figure 4-7 shows the response of the frame to the two levels of ground motions and the corresponding acceptable limits. It can be seen that except for earthquake nos. 1, 4 and 7, the response of the frame exceeds the acceptable limits for at least one of the two loading levels. The structure is near collapse for a majority of the earthquakes when scaled to 2500 year return period levels. It can hence be concluded that the structure needs to be retrofitted, in order to satisfy the acceptability limits.

#### **4.4 Response with Proposed Retrofit Method**

The response of the structure, when retrofitted with the masonry wall with friction dampers in the central bay of all the stories, was investigated. As discussed in Section 3, a modified version of IDARC(3.0) was used to model the frame with friction dampers. The initial stiffness of the wall before the damper slips is obtained by scaling the stiffness value obtained from shake table tests. The preslip stiffness of the wall was calculated to be 54.0 kips/in and bilinear model used for modeling the wall with dampers for the time history analysis.

##### **4.4.1 Design of Friction Damper Configuration**

The design problem is to select the appropriate slip load values, such that the response of the retrofitted frame satisfies the set performance criterion. Time history analyses were performed for the retrofitted frame with dampers set at different slip load values. For each case all nine earthquakes were considered at the two return period levels. Based on the observed responses of the frame, an appropriate slip load level can be selected.

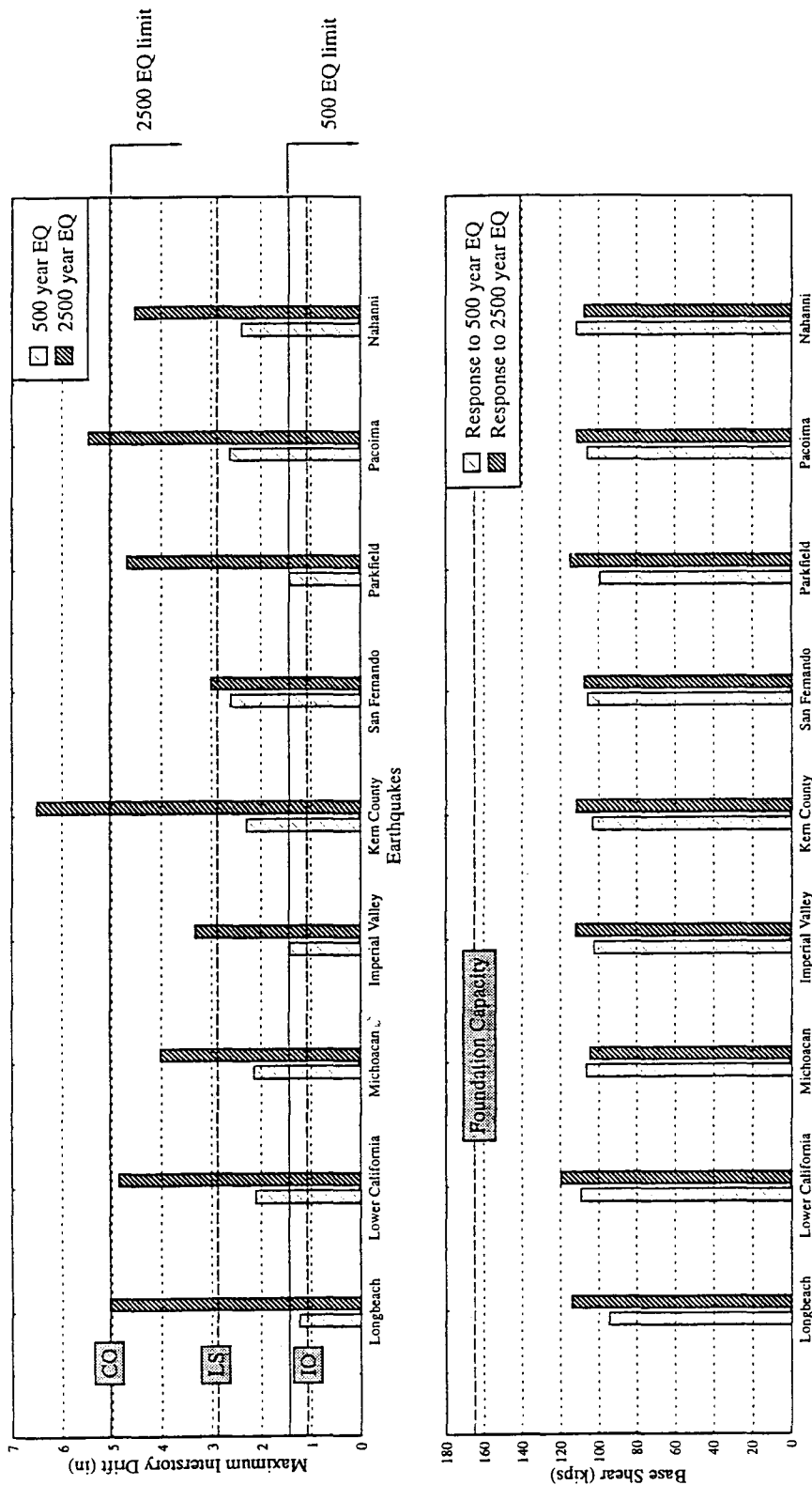


FIGURE 4-7: Response of three story frame to nine ground motions

Another design issue is the distribution of the slip load over the height of the structure. For a given slip load level set for the damper in the first story, one could vary the slip force for the upper stories and get a better performance. It was decided to perform a parametric study to obtain an appropriate slip load distribution. Three slip load distribution patterns were considered:

1. the slip load is same for all levels
2. the slip load is proportional to the shear distribution produced by a laterally applied force having distribution proportional to the first mode shape of the structure
3. the slip load is proportional to the shear distribution produced by a laterally applied force having linear distribution through the height of the frame.

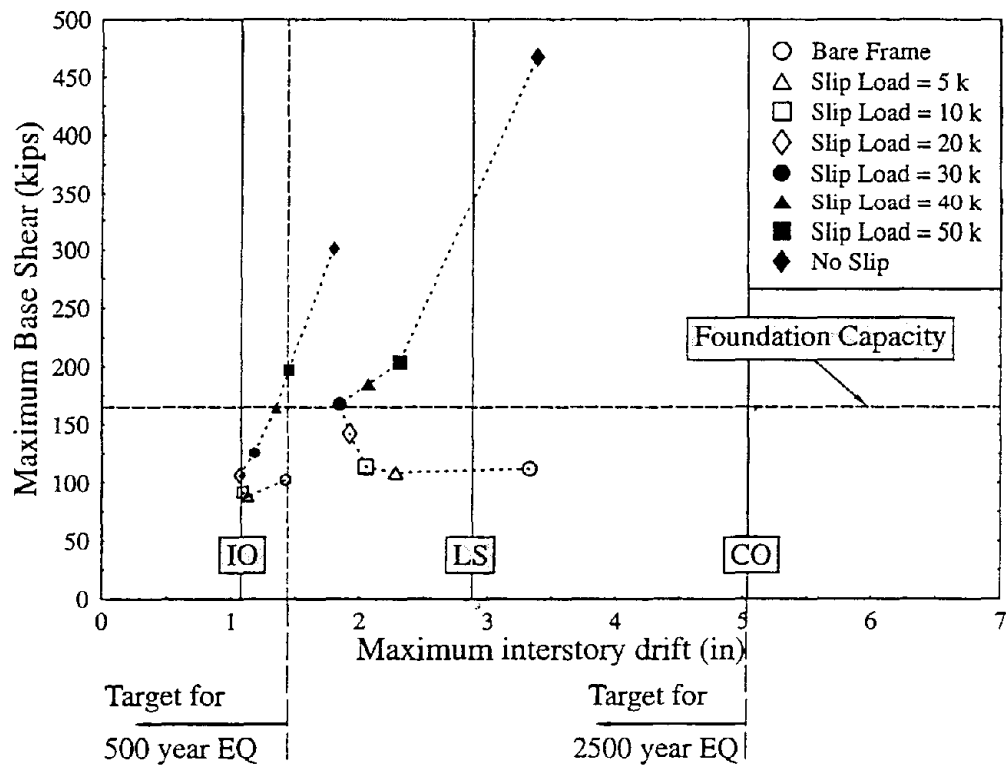
For a ground motion of Taft ( $PGA=0.263g$ ), time history analyses were performed for frames with dampers with different slip load distributions in the three stories. The slip load value in the first story was varied, and the peak responses of the frame for the three patterns compared. It was observed that the slip load distribution pattern (3), where the slip loads are linearly varying over the height is the most efficient in terms of providing lower drifts, displacements and shears in the optimum case. For all the analytical studies in this Section, the distribution pattern (3) will be used.

#### **4.4.2 Results from Time History Analysis**

##### **Comparison of Peak Responses**

From the comprehensive time history analyses performed, peak values of story drifts, displacements and shears were stored and analyzed for each earthquake. Only the results of the analyses for three different ground motions (viz. Taft, Imperial Valley and

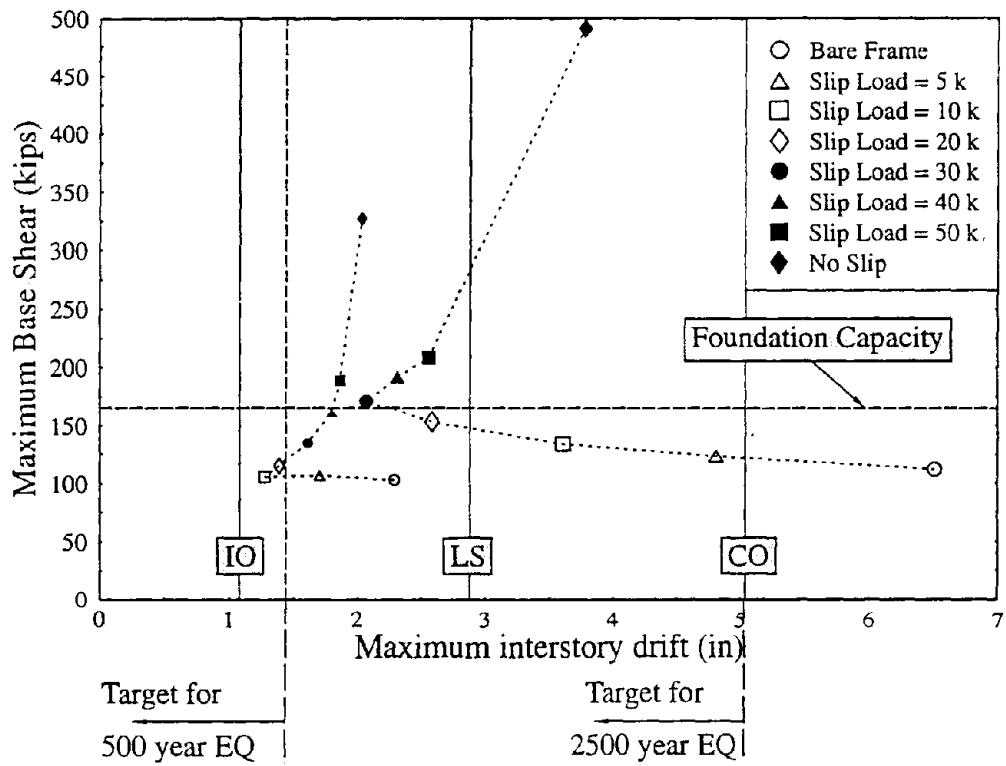
### Earthquake No. 4: Imperial Valley (S00E)



IO: Immediate Occupancy; LS: Life Safety; CO: Collapse

**FIGURE 4-8 (a): Response of three story frame with dampers to Imperial Valley (S00E) Earthquake**

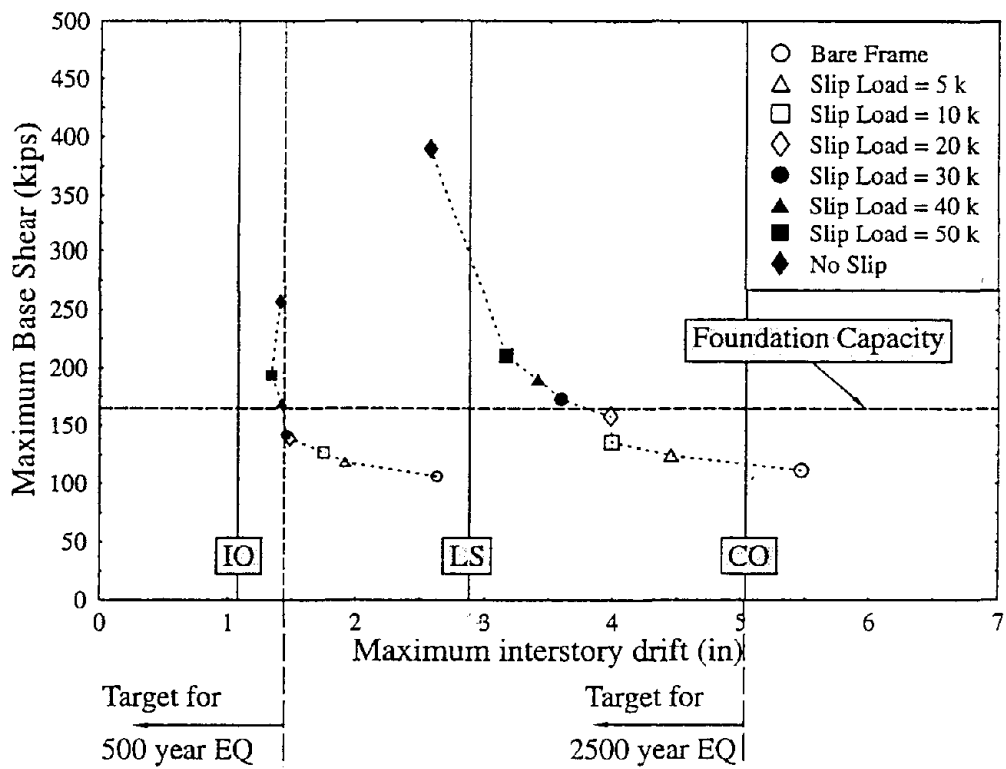
Earthquake No. 5: Kern County (Taft N21E)



IO: Immediate Occupancy; LS: Life Safety; CO: Collapse

**FIGURE 4-8 (b): Response of three story frame with dampers to Taft (N21E) Earthquake**

### Earthquake No. 8: Pacoima (S74W)



IO: Immediate Occupancy; LS: Life Safety; CO: Collapse

**FIGURE 4-8 (c): Response of three story frame with dampers to Pacoima (S74W) Earthquake**

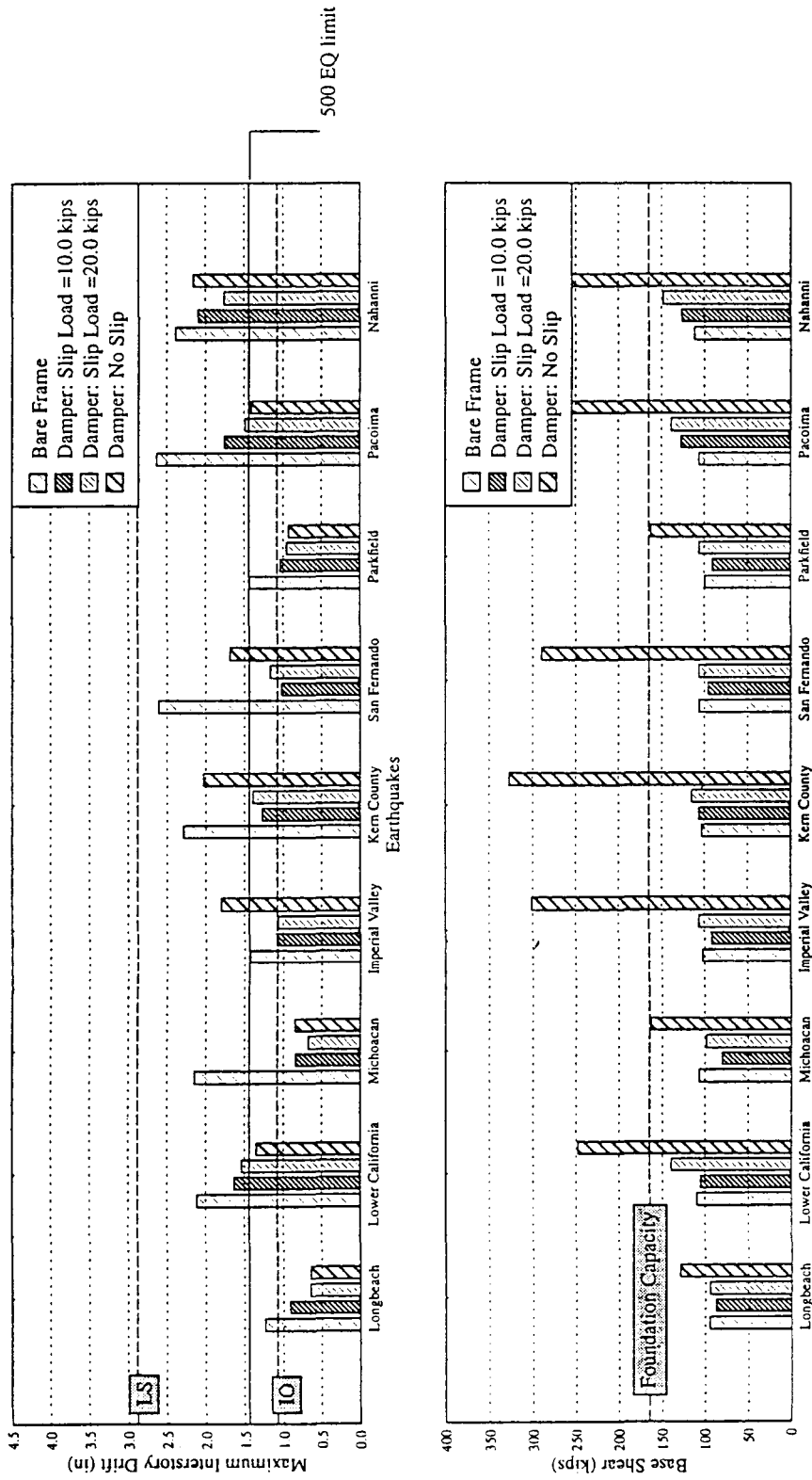


**FIGURE 4-9 Effect of friction dampers for 500 year earthquake**

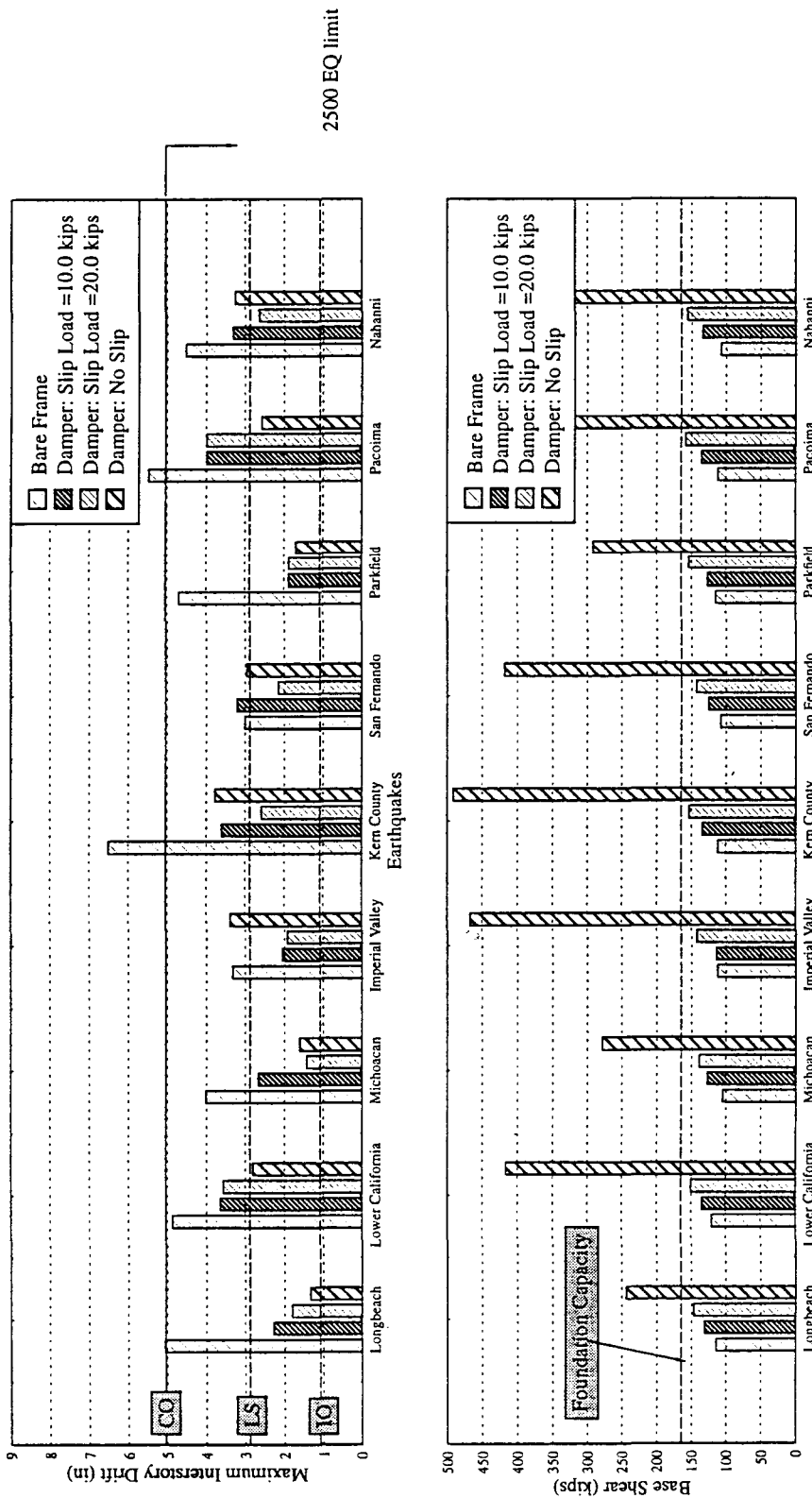


**FIGURE 4-10 Effect of friction for 2500 year earthquake**

Pacoima) are presented in figures 4-8 (a), (b) and (c) in the peak base shear vs. peak story drift plane. The following observations can be made based on the peak responses:

1. Introduction of dampers into the frame can reduce the peak deformations without substantially increasing the base shear.
2. For a given ground motion, there is an optimum slip load level for which the response level is most desirable. For a different slip load level larger drifts and/or shears would be obtained.
3. Optimum slip load for one earthquake is not necessarily optimum for all the ground motions. The frequency content distribution of the individual earthquake influences the response of the structure with dampers.

It can be seen that for damper settings with slip load in the first story set to 10 kips or 20 kips, frame response improved substantially for most ground motions, satisfying the desired performance criterion. figures 4-9 and 4-10 show the responses of the frame before and after retrofitting with friction dampers, for different ground motions.

Figures 4-9 and 4-10 also include the response of the frame with wall which has a large slip load level, such that no slip occurs. This is equivalent to a case of retrofitting with additional stiffeners, which remain elastic during the earthquake.

The following conclusions can be made about the achievements of retrofitting:

1. Installing the friction damper scheme with slip load level of 10.0 kips or 20.0 kips resulted in satisfying the drift performance criteria for all the earthquake loading cases except for Lower California (500 year) and Nahanni (500 year) where none of the slip loads satisfy the drift limits. However, even for these cases the exceedance is not substantial.

2. For most earthquakes, retrofitting with stiffeners with higher strength would, because of lower damping, result in drifts larger than the optimum friction damper case, and for all the earthquakes, the resulting base shears were exceedingly large.

It can be concluded that the retrofit scheme proposed with the appropriate slip load setting (10 kips to 20 kips in the first story) would result in acceptable performance by the structure for the wide range of earthquake loadings considered.

### **Comparison of Time-History Responses**

Success of the retrofit scheme must not be interpreted merely from peak response values. The change in response of the system during the ground motion also reflects the success or otherwise of a retrofit method. In order to illustrate the influence of the wall-damper retrofit over time for the three story frame, one particular ground motion case was considered - Taft (500 year return period). The time history response of the frame in terms of story displacements, story drifts and story shears, with and without the damper retrofit, is shown in figures. 4-11 to 4-13. The retrofitted frame has slip load in the first story set at 10 kips. The time history plots indicate that the dampers are successful in reducing the drifts and displacements throughout the period of motion, while maintaining the shears in the stories at essentially the same levels as those experienced by a bare frame. This is achieved by dissipation of energy through the dampers. Figure 4-14 shows the hysteresis of the wall-damper scheme. In figure 4-15, the hysteresis of each of the stories for the bare frame is compared with that in the retrofitted frame, where the force in the damper is subtracted. It can be seen that while the bare frame RC elements would be subjected to non-linear behavior, and called upon to dissipate hysteretic energy, the RC elements in the retrofitted frame remain largely in the linear range. Hence lesser damage would be expected in the retrofitted frame due to

cyclic effects. Discussions on the energy dissipation aspects are presented in the next section.

### **Comparison of Energy Demand and Dissipation**

The earthquake demand on a structure can be interpreted as energy input by the ground into the system. The energy input has to be dissipated by the structure. When a structure is responding in the linear range, most of the energy gets transformed into recoverable strain and kinetic energy, which result in large instantaneous displacements and forces. The energy is then dissipated mainly by inherent structural damping as a result of interaction with nonstructural components. However, under sufficiently large loading, the structure behaves inelastically. Part of the energy then gets dissipated by the hysteretic behavior of the structural components. While this reduces the earthquake dissipation demand through internal structural damping and kinetic energy, the hysteretic energy dissipated by the components can result in deterioration of the component capacity.

For RC structures it has been shown that repeated cyclic loading in the inelastic range can result in deterioration, especially for poorly detailed components. Damage indices like those proposed by Park and Ang (1985) used the cumulative hysteretic energy dissipated by RC components as a measure of the damage accumulated by a structure as a result of cyclic loading. For the non-ductile three story RC frame under consideration, it is desirable to minimize the hysteretic energy demand on the concrete members. Addition of friction dampers provides a non-destructive path for the energy to be dissipated. Also, as seen in Section 3, adding dampers changes the energy input into the system. Hence energy-time history plots provide another perspective to interpret the success of retrofitting. For the three story frame the various energy components were calculated as follows:

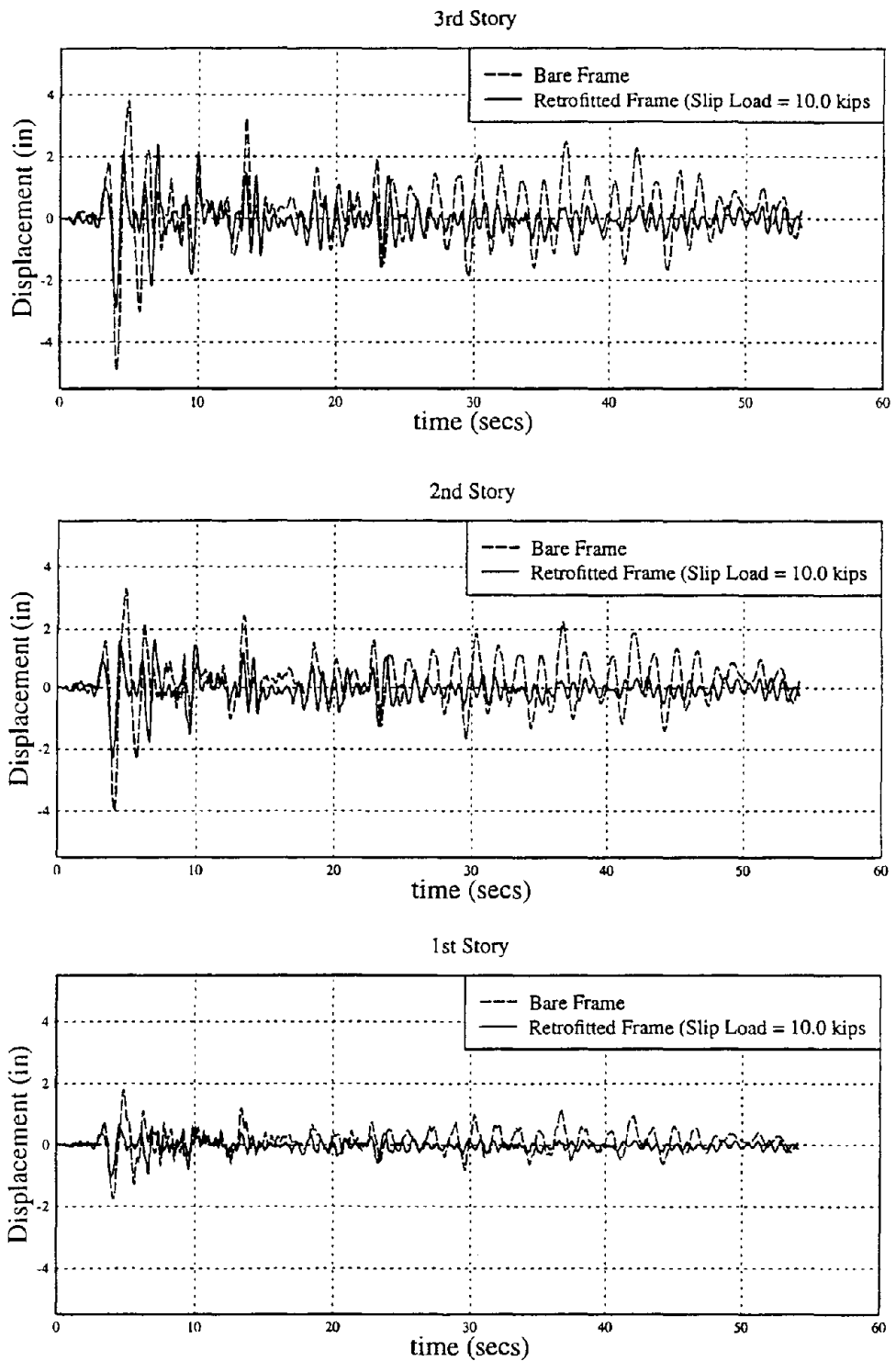


**FIGURE 4-11 Displacement response of frame with and without retrofit under Taft (500 yr)**

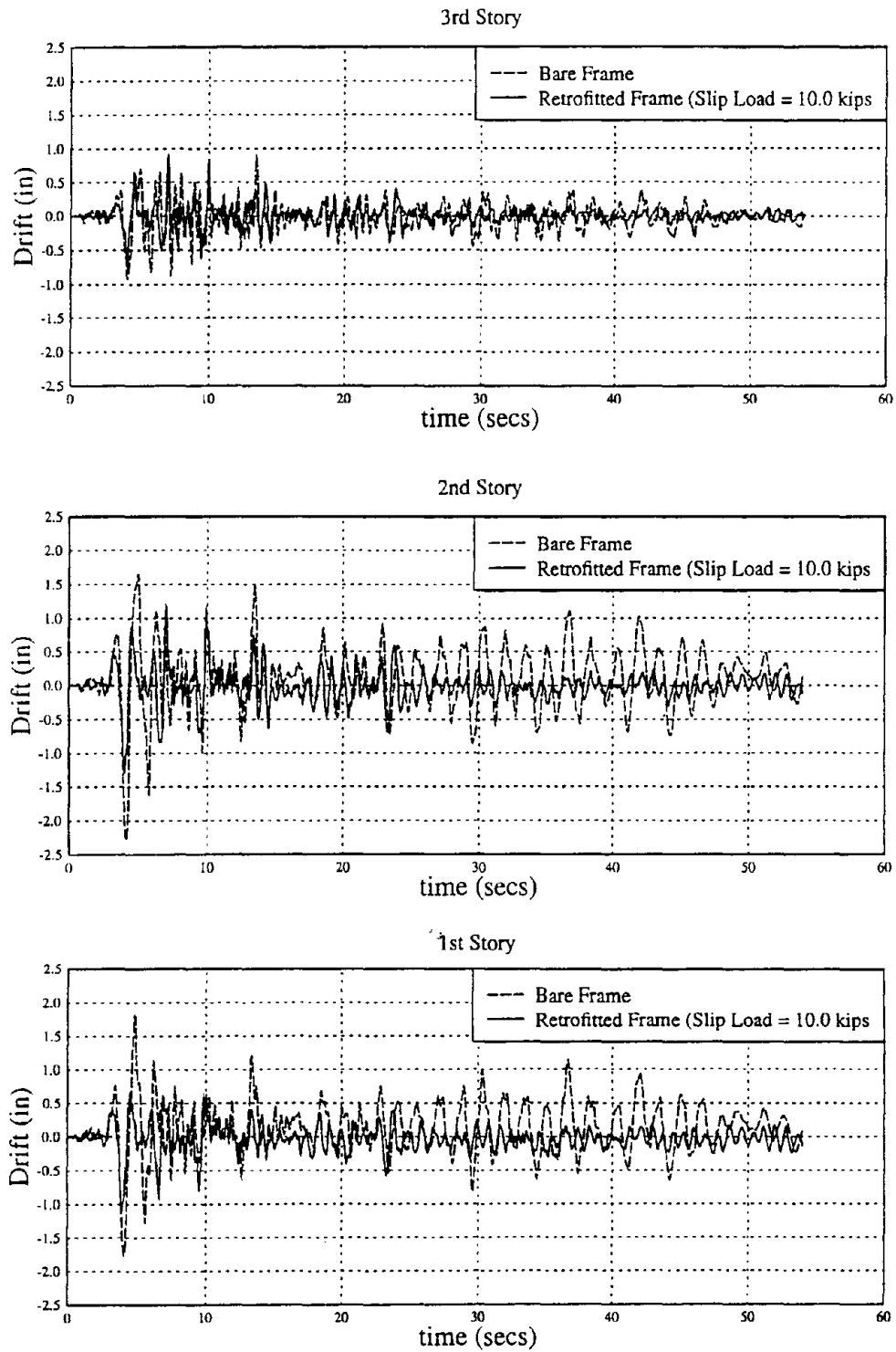


**FIGURE 4-12 Drift response of frame with and without retrofit under Taft (500 year)**

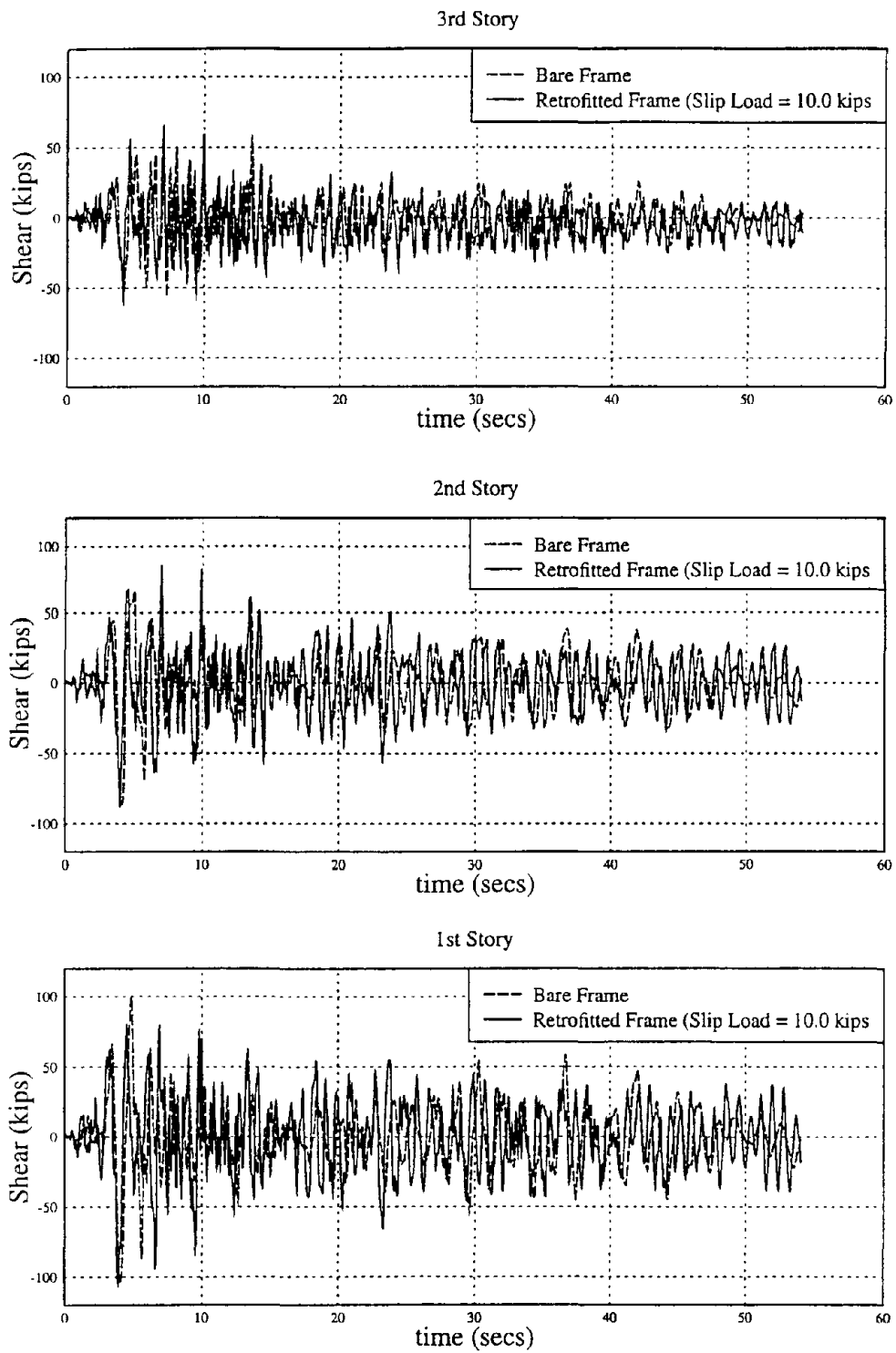


**FIGURE 4-13 Shear response of frame with and without retrofit under Taft (500 yr)**

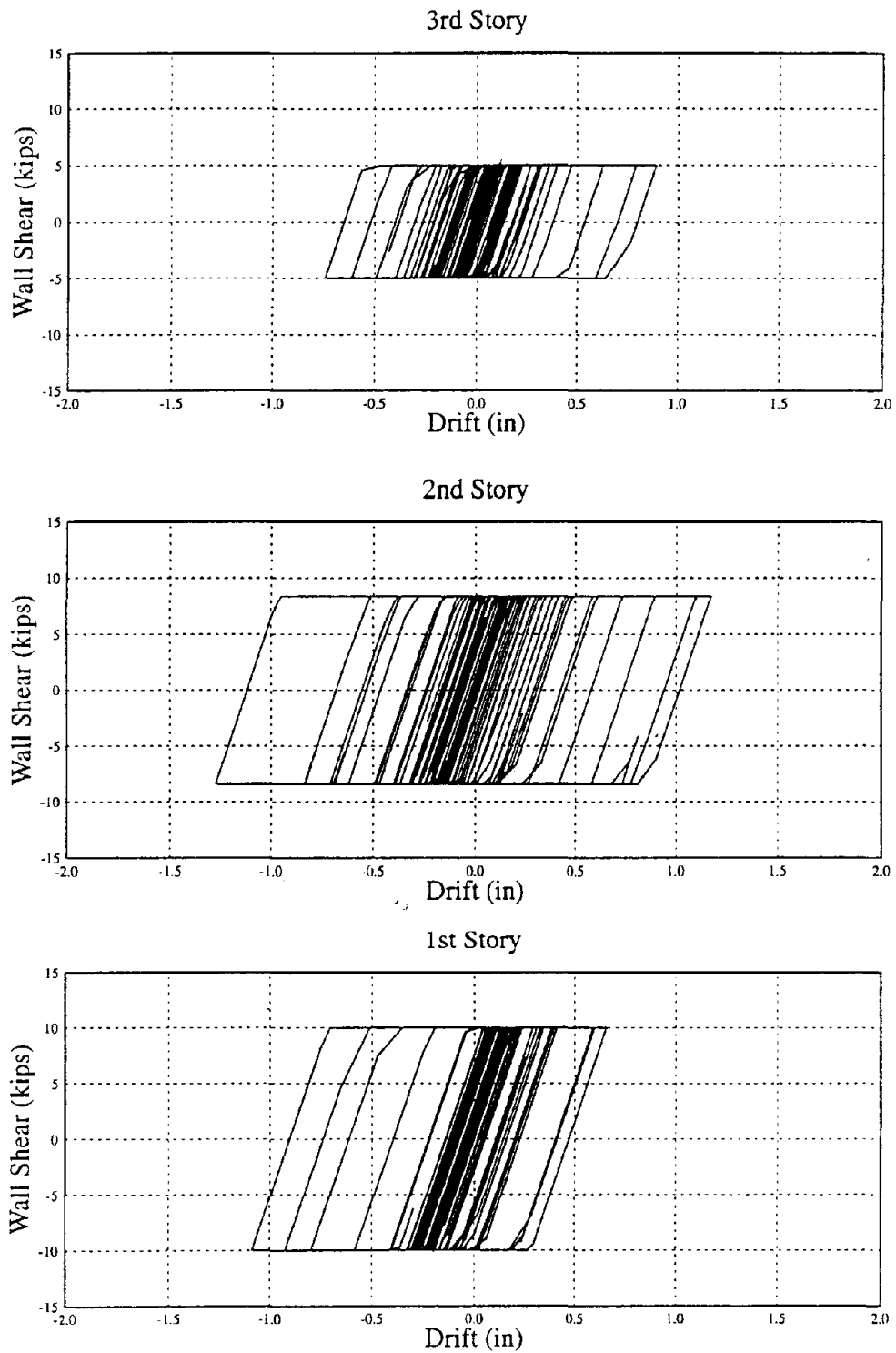


**FIGURE 4-14 Wall-damper hysteresis under Taft (500 yr)**

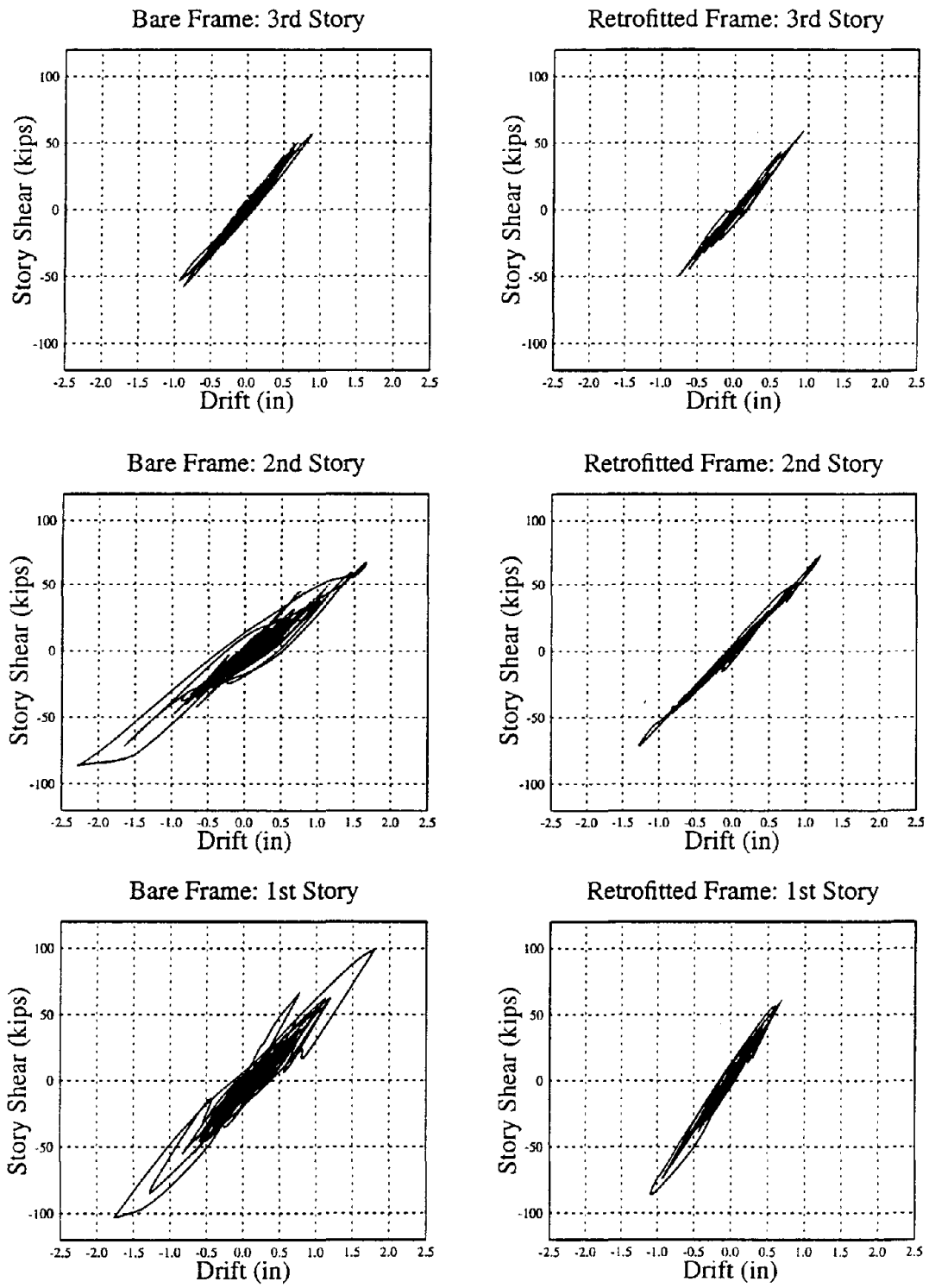


**FIGURE 4-15 Influence of dampers on story hysteresis for Taft (500 yr)**

$$E_I = - \int_0^t \sum_{i=1}^3 m_i \dot{u}_i(t) \ddot{x}_g(t) dt$$

$$E_K = \frac{1}{2} \sum_{i=1}^3 m_i \dot{u}_i(t)^2$$

$$E_{FD} = \int_0^t \sum_{i=1}^3 V_{wi}(t) \delta_i(t) dt - \sum_{i=1}^3 \frac{V_{wi}(t)^2}{2 K_w}$$

$$E_{BAL} = \int_0^t \sum_{i=1}^3 V_i(t) \delta_i(t) dt$$

$$E_{RC} = \int_0^t \sum_{i=1}^3 (V_i(t) - V_{wi}(t)) \delta_i(t) dt$$

$$E_{VD} = E_I - E_{BAL} - E_K$$

where  $E_I$  = total input energy into the system

$E_K$  = total kinetic energy in the system

$E_{FD}$  = total energy dissipated by friction dampers

$E_{BAL}$  = strain + hysteretic energy in the frame + dampers

$E_{RC}$  = strain + hysteretic energy in the RC frame alone

$E_{VD}$  = total energy dissipated by viscous damping

$u_i(t)$  = displacement at story level  $i$

$\ddot{x}_g(t)$  = ground acceleration

$\delta_i(t)$  = interstory drift in story level  $i$

$V_{wi}(t)$  = shear in wall + dampers at story level  $i$

$V_i(t)$  = shear at story level  $i$

The energies calculated are the relative energy values, i.e., the energies relative to the ground. Since the objective of the energy plots is to study the hysteretic energy in the RC components, the relative energy values are appropriate.

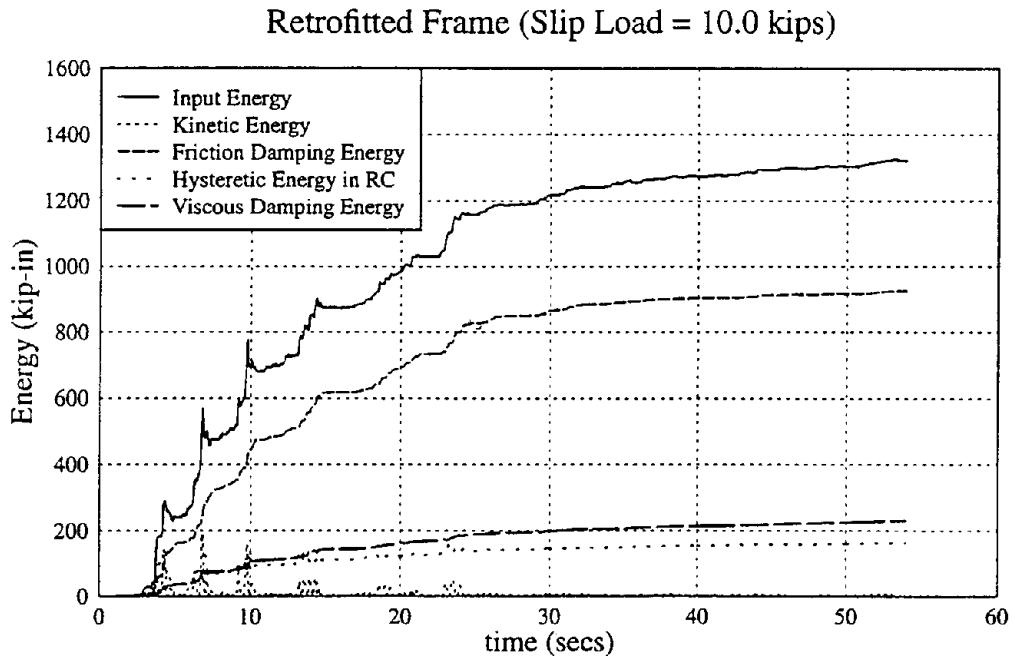
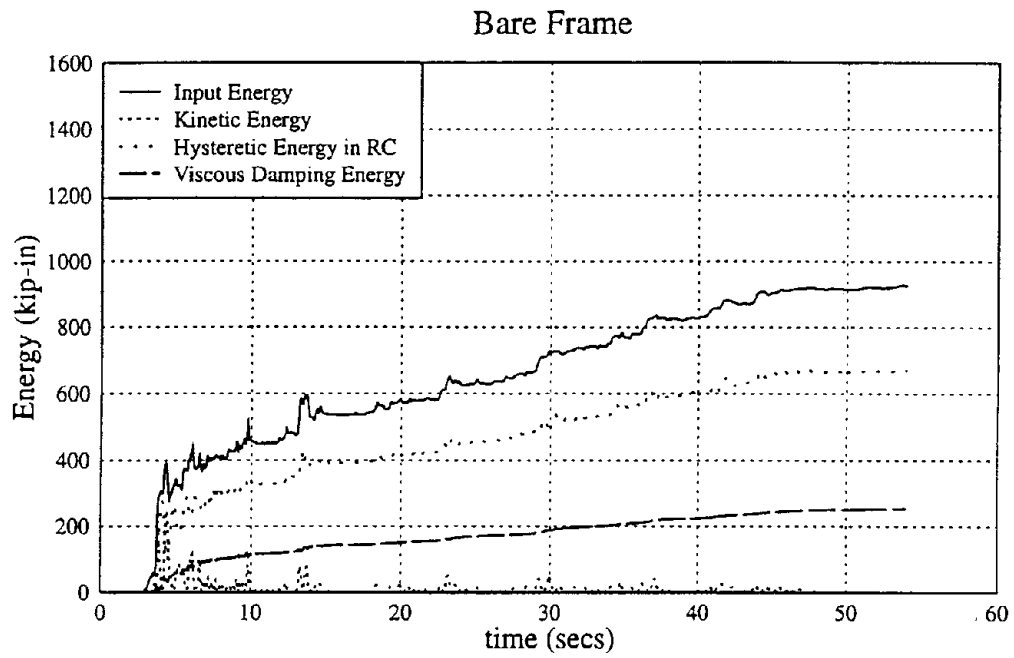


**FIGURE 4-16 Energy time history of frame with and without retrofit to Taft (500 yr)**

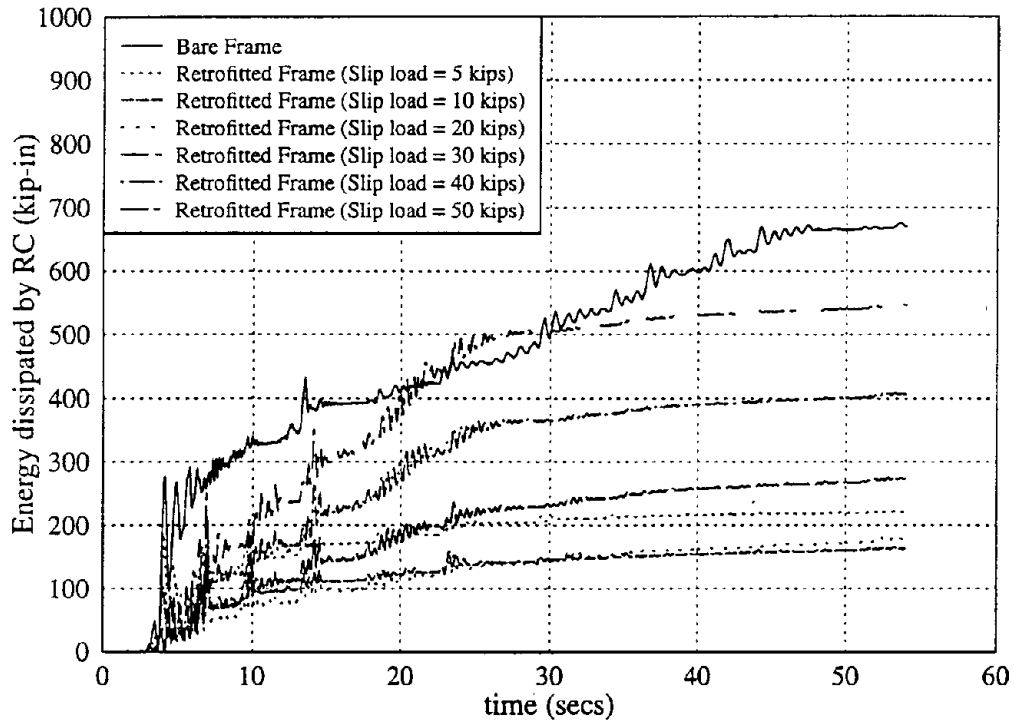


**FIGURE 4-17 Influence of slip load variation on RC hysteretic energy**

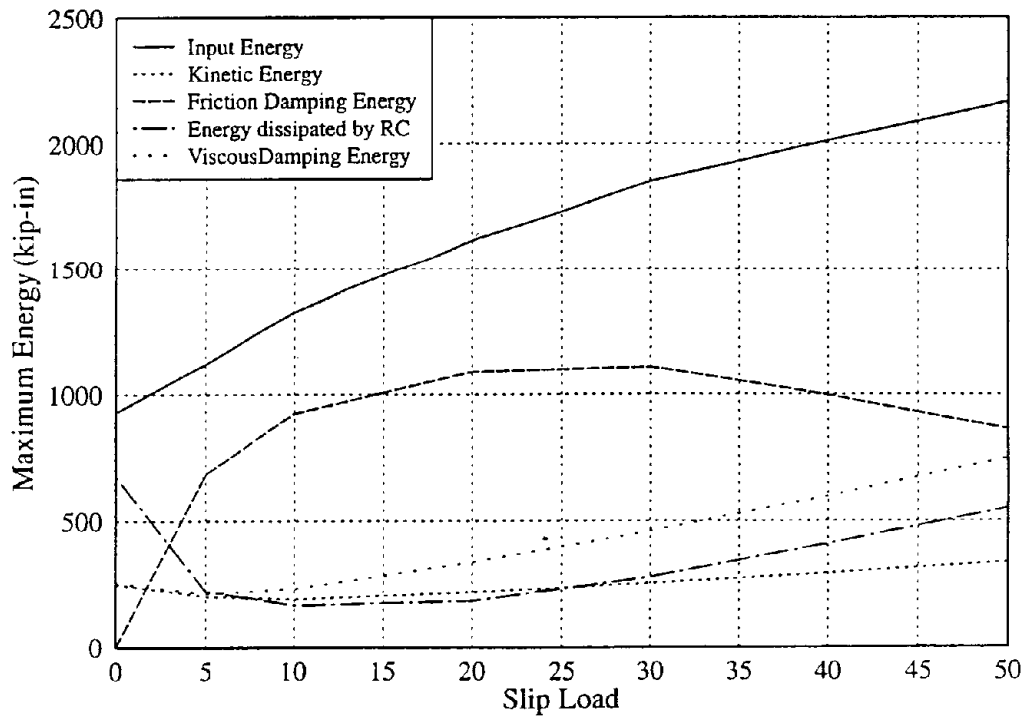


**FIGURE 4-18: Influence of slip load variation on maximum energies**

As in Section 4.4.2.2, only the Taft (500 year) earthquake was considered for this comparative study. Figure 4-16 compares the energy demand and dissipation time histories for the bare frame and the retrofitted frame, with slip load in first story set to 10 kips. Introducing the dampers results in an increase in the input energy (about 40% at maximum level). This is due to the increased stiffness of the system. However, much of the input energy is dissipated through friction dampers (about 70% of input energy). As a result, the energy demand on the RC frame reduces dramatically by about 75% at maximum value. This would result in much lower damage to the RC components. Also, the maximum kinetic energy drops due to retrofitting. In Section 4.4.2, the peak responses in terms of drifts, displacements and shears were compared for the frame with different slip load levels. To further understand the influence of retrofitting with friction dampers on the energy response of the frame, the energy time histories were calculated for various settings of slip load levels in first story viz. 5, 10, 20, 30, 40 and 50 kips. Figure 4-17 compares the time history plots of energy dissipated by RC components for various slip load levels. The variation with slip load, of the maximum values of the input energy, the kinetic energy, friction damping energy, energy demand on the RC frame, and the viscous damping energy is shown in figure 4-18. The following observations can be made based on figures 4-17 and 4-18:

1. For slip load levels in the range of 10 kips and 20 kips, the energy demand on the RC components of the frame are the lowest. It must be noted that even for the maximum drift criterion, the optimum slip load level was in the range of 10 kips to 20 kips.
2. Increasing the slip load level increases the input energy, but the energy dissipated by friction dampers also increases such that the difference between the input and friction damping energy is minimum around 10 to 20 kips slip level. As a result there is lower energy demand on the RC frame.

Hence the optimum energy demand can be obtained, not only by maximizing the friction damping energy, but also by minimizing the difference between the input energy and the friction damping energy.

It can be deduced that the slip load setting of 10 kips in story 1 and the appropriate slip distribution in higher stories (section 4.4.2) would result in an optimum friction damper setting in terms of drift control and energy dissipation demand on the frame. Hence for the three story RC frame, for the friction dampers, the optimum slip load in first story is 3% of the simulated frame weight.

#### **4.5 Summary**

The main objective of this Section was to analytically determine the extent of applicability of the proposed retrofit scheme for a nonductile RC frame for a wide variety of ground motions. For this study, a three bay three story RC frame, which had been experimentally and analytically evaluated earlier, was used. The loading was specified in terms of a set of ground motions with two different levels of return periods. The expected performance criteria, expressed in terms of peak interstory drifts and peak base shears, were specified for each level of loading. The design parameter in the proposed retrofit scheme is the slip load setting in the friction dampers. Large numbers of nonlinear time history analyses were performed to obtain the appropriate slip load setting in the retrofitted frame which would satisfy the expected performance levels.

In the next Section, a simplified design procedure is presented, which can be used to obtain the optimum damper configuration without having to perform a large number of time history analyses.



## SECTION 5

### A NEW DESIGN PROCEDURE FOR RETROFITTING RC FRAMES WITH FRICTION DAMPERS

#### 5.1 Introduction

It was seen in Section 4 that in designing a friction damper retrofit scheme for a three story nonductile RC frame, a large number of time history analyses are required. There is a need for a simplified design procedure which can be used (at least at the preliminary design level) for selecting the required additional stiffness and slip load in the friction damper. In this section, the existing design methodologies for supplemental damping methods are discussed. The existing methods are found to be unsatisfactory for designing friction damper schemes for nonlinear structures. The new design approach involving pushover analysis was developed and is presented in this section.

#### 5.2 Existing design methods

Based on the literature review, two approaches were found to have been proposed for design of friction dampers. These approaches are discussed and critically evaluated in the next sections.

##### 5.2.1 Seismic design spectra for friction-damped structures [Filiatrault and Cherry (1990)]

The first effort towards developing a simplified design procedure for designing friction dampers was that proposed by Filiatrault and Cherry (1990). The method was intended for the friction dampers developed by Pall and Marsh (1982). However, the method can be extended to any friction damper system. For a given structure and a design ground motion, the slip load for the friction dampers can be selected from the design slip-load spectrum shown in figure 5-1. In figure 5-1,  $V_0$  is the total optimum slip shear,  $a_g$  is the peak ground acceleration,  $T_g$  is the predominant ground motion period, and  $T_u$  is

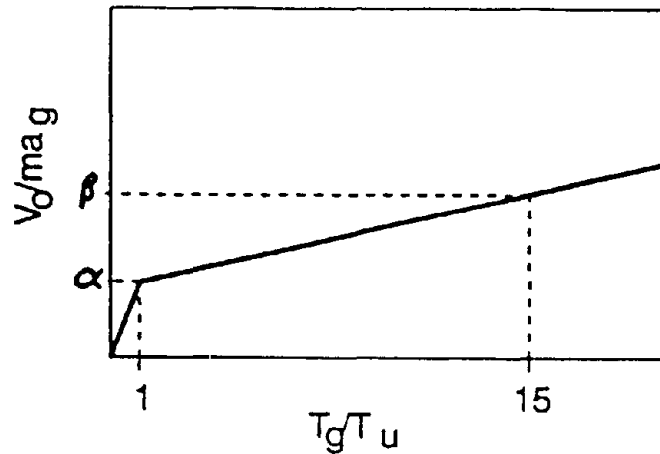


**FIGURE 5-1 Construction of design slip-load spectrum [Filiatrault and Cherry (1990)]**

the period of the bare frame. The spectrum is constructed using the equations given below:

$$\frac{V_0}{ma_g} = \begin{cases} \left\{ \frac{(-1.24NS - 0.31)T_g}{T_u} + 1.04NS + 0.43 \right\} & \text{for } 0 \leq \frac{T_g}{T_u} \leq 1 \\ \left\{ \frac{(0.01NS + 0.02)T_g}{T_u} - 1.25NS - 0.32 \right\} \\ \quad + \frac{(0.002 - 0.002NS)T_g}{T_u} + 1.04NS + 0.42 & \text{for } \frac{T_g}{T_u} > 1 \end{cases}$$

where NS = no. of stories in the structure

$T_b$  = natural period of the structure when fully braced (no slippage)

Hence, given the period and number of stories of the structure, the peak ground acceleration and predominant period of the design ground motion and the size of the stiffeners used with the dampers, the design slip load spectrum can be constructed and the optimum slip load selected. In order to understand the extent of applicability of the method, it is important to detail the approach used by the researchers to obtain the slip load design spectrum. 45 different structures were considered in the parametric study. For each combination of the parametric values, five different sample artificial ground motions were used. For each of the cases, an optimum slip load was calculated by carrying out time history analysis for each case. All the stories in the frame had equal mass. The story stiffnesses of the bare frame however varied through the height, and were proportional to the cumulated mass up to that height, ie.

$$K_{fi} = \frac{\sum_{j=i}^{NS} W_j}{W} K_{f1}$$

where  $K_{fi}$  = stiffness of the  $i$ th story

$W_j$  = weight of the the story

$W$  = total weight of the structure

For the simulation, the dampers were placed in the stories, with the same bracing size and slip load in all the stories. The important aspect of this study to be mentioned is the criterion used for selecting the optimum damper configuration. A relative performance index was defined as follows:

$$RPI = \frac{1}{2} \left( \frac{SEA}{SEA(0)} + \frac{U_{max}}{U_{max}(0)} \right)$$

where SEA is the strain energy area ie. the area under the strain energy time history of a friction damped frame, SEA(0) is the SEA for the identical structure but without bracing

$U_{max}$  = maximum strain energy for a friction damped structure and  $U_{max(0)}$  = maximum strain energy for identical frame with no friction dampers.

The goal for selecting the optimum slip load was to minimize the relative performance index. It was proposed that based on this method, a new frame with friction dampers can be designed or the method could be used to obtain slip loads for retrofitting of existing frames with friction dampers.

The proposed method provides a simple tool for designers to select the appropriate slip load, thereby avoiding the need for a large number of time history analyses. The method however suffers from several shortcomings, as listed below.

1. The frames used in the analyses were assumed to be linear. This assumption could be valid around the optimum level, since the dampers are expected to limit the frame deformations. However the inelastic deformations could be beneficial and reduce the frame deformations at other slip load levels and change the slip load level. In the definition of RPI, the  $SEA(0)$  and  $U_{max(0)}$  were calculated assuming that the frame remains elastic. Clearly, the frame would be expected to go into the inelastic range without the friction dampers. Hence, calculation of RPI by ignoring the inelastic effects is questionable.
2. The analyses were done mainly for steel frames, and hence extension of this method to RC frames is not possible.
3. In a design or retrofit problem, the design parameters are normally the story drifts and the story shears. The interpretation of minimizing RPI is difficult and it is hard to correlate RPI to physical design parameters.

4. The method restricts the use of the spectrum to cases where the friction dampers are used in all stories. However it may not be necessary to use friction dampers in all the stories, in which case the design spectrum from figure 5-1 cannot be used.

On the whole, the slip load design spectrum is an attempt to reduce a rather complicated problem to a very simplified design curve using large number of simulations. Clearly such an approach has its limitations due to the range of parameters used and modeling methods used for the simulation.

### **5.2.2 Method proposed in ATC-33**

As mentioned in section 4, the ATC-33 guidelines and commentary for the seismic rehabilitation of buildings is under preparation. In Chapter 9 of ATC-33, guidelines are proposed for analyzing structures with base isolators and energy dissipating devices (EDD). The guidelines present four different procedures for analysis of a rehabilitated building using EDD. These methods are:

1. Equivalent lateral force procedure (ELF)
2. Elastic dynamic response procedure
3. Simplified nonlinear analysis procedure
4. Nonlinear response history analysis procedure

Guidelines for the first two procedures have not been presented in the 50% submittal draft. The simplified analysis procedure is the method of interest as it avoids nonlinear time history analysis which is the fourth method mentioned above.

The simplified nonlinear analysis procedure involves using static-nonlinear analysis discussed in Section 4.4 of ATC-33. The procedure in Section 4.4 must be modified to account for the damping provided by the EDD. The method involves developing a capacity curve for the frame with the EDD. The intersection of the capacity curve with a demand curve represents the response of the frame. The demand curve is obtained from the 5% damped design elastic response spectrum which is reduced by a factor B to account for the damping provided by the EDDs and the nonlinear response of the frame itself. The factor B is related to the effective viscous damping  $\beta_{\text{eff}}$ , which is given by

$$\beta_{\text{eff}} = f \frac{W_D}{2\pi K_{\text{eff}} D^2}$$

where  $W_D$  = energy dissipated by the frame with EDD

$K_{\text{eff}}$  = effective stiffness of the rehabilitated building at target displacement D

and f is the ratio of the area of actual hysteresis loop divided by area of hysteresis loops associated with idealized bilinear force-deformation relationship.

The document provides further details about calculating  $K_{\text{eff}}$  and damping for different types of devices. For hysteretic devices like friction dampers,

$$K_{\text{eff}} = \frac{|F^+| + |F^-|}{|d^+| + |d^-|}$$

and the damping coefficient is given by:

$$C = \frac{W_D}{\pi \omega d_{\text{ave}}^2}$$

where  $d$  is the displacement of the friction damper

$d^+$  and  $d^-$  are the maximum positive and negative displacements of the damper

$d_{ave}$  is the average displacement of the damper

$F^+$  and  $F^-$  are the maximum positive and negative force in the damper

The commentary section of the guidelines provides further details for using the simplified nonlinear procedure for rehabilitation of structures with EDDs. Figure 5-2 (obtained from ATC-33 50% draft) shows an example of the capacity and demand spectrum curves. The effective damping is given by

$$\beta_{eff} = \frac{2A_f D + 2f(A_y D - D_y A)}{\pi A_2 D}$$

where  $A_f$  = Added base shear due to friction dampers / mass

$A_2$  = Spectral acceleration corresponding to intersection of capacity and demand curves

$D$  = Spectral displacement corresponding to intersection of capacity and demand curves

$A_y$  = Spectral acceleration corresponding to yield computed from the capacity curve

$D_y$  = Spectral displacement corresponding to yield computed from the capacity curve

$f$  = coefficient less than one equal to the ratio of actual loop area to idealized bilinear loop area

The effective period is calculating by using the equation

$$T_{eff} = 2 \pi \sqrt{\frac{D}{A}}$$

which is essentially the secant period of the structure at maximum displacement. The method has to be performed iteratively, calculating  $\beta_{eff}$  and the corresponding demand

spectrum at each stage of the pushover analysis. The iterations are continued until the maximum response in the capacity curve matches the response from the demand curve.

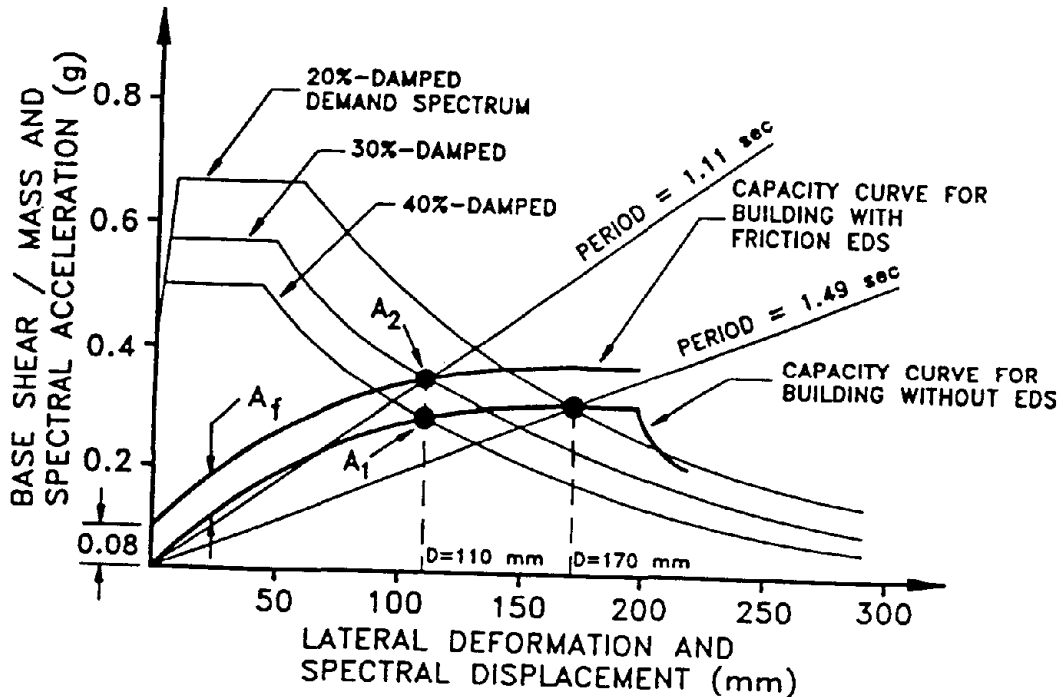


**FIGURE 5-2 Capacity and demand curves for frame with friction dampers [ATC-33 50% submittal draft (1994)]**

Hence the method provides a means of predicting the response of the frame with EDDs for various damper settings without having to perform nonlinear time history analyses. In a design process, the method will have to be repeated for several settings of the friction damper until the estimated frame response is less than the set limits. Following observations can be made about the approach presented in the ATC-33 guidelines (50% submittal draft):

1. The document states “this method must be extended to multi degree of freedom systems”. This indicates that there is still work to be done to reduce the static nonlinear pushover results to a SDOF capacity curve.
2. The capacity curve for the frame with friction dampers in figure 5-2 is conceptually incorrect. The figure indicates that before the damper slips the system has infinite stiffness. Though the damper itself has large stiffness during the “stick” stage, the bracings holding the dampers will have only finite stiffness. Hence a more realistic capacity curve diagram is as shown in figure 5-3.
3. The simplified analysis procedure depends on the concept of reducing a nonlinear MDOF system to a linear SDOF system with equivalent viscous damping. The effective period of the SDOF linear system is taken to be the secant period at the maximum deformation stage. While this approach provides a convenient simplification for analysis of frames with friction dampers, the accuracy of representing hysteretic damping with equivalent viscous damping needs verification, which is not presented in the document.

### 5.2.3 Method Proposed by C. Li and A. Reinhorn

Another study involving the use of capacity vs. demand spectra has been published by Li and Reinhorn (1995). The capacity spectrum is obtained by using an adaptive pushover analysis approach. The demand spectrum for the structure with friction dampers is the elastic response spectrum for an equivalent damping value of  $\xi_{eq}$ .

The proposed equivalent damping is calculated from the following equation:

$$\xi_{eq} = \frac{4\gamma (\mu_{max} - 2)}{\pi\mu_{max} [2 + \alpha (\mu_{max} + 2)]}$$

where  $\gamma$  = ratio of area of enclosed in the actual hysteresis curve of the damper and area of the bounding parallelogram

$\alpha$  = ratio of unloading stiffness and initial stiffness

$\mu_{max}$  = ratio of maximum displacement to equivalent yield displacement

Further details of the method are presented in the referenced NCEER report. Shake table tests for reinforced concrete structure retrofitted with dampers indicate that equivalent viscous damping of up to 20% can be achieved by using the friction dampers.

### **5.3 Proposed Design Procedure: Inelastic Demand Spectrum Method**

It was found that the existing methods were not suitable for providing a simplified yet sufficiently accurate design procedure for designing the friction damper retrofit scheme. A new approach was then developed for this purpose. The method proposed is similar to the approach described in ATC-33 guidelines, but with various modifications. Details of the proposed method are discussed in the following sections.

#### **5.3.1 Pushover analysis to construct the capacity curve**

The method proposed in this section for friction damper design utilizes the lateral pushover analysis approach to obtain the capacity curve of the system. In this section, the pushover analysis approaches used in the past will be discussed. The use of pushover analysis to reduce a MDOF system to a SDOF system has been attempted by Saidi and Sozen (1981) and Freeman (1978). The underlying assumption in obtaining the equivalent SDOF system is that the structure vibrates in its predominant mode. For frames with a large number of stories, the higher modes can increase their influence in the response. In such cases, reducing the multi-story frame to a SDOF system would result in ignoring higher modes.

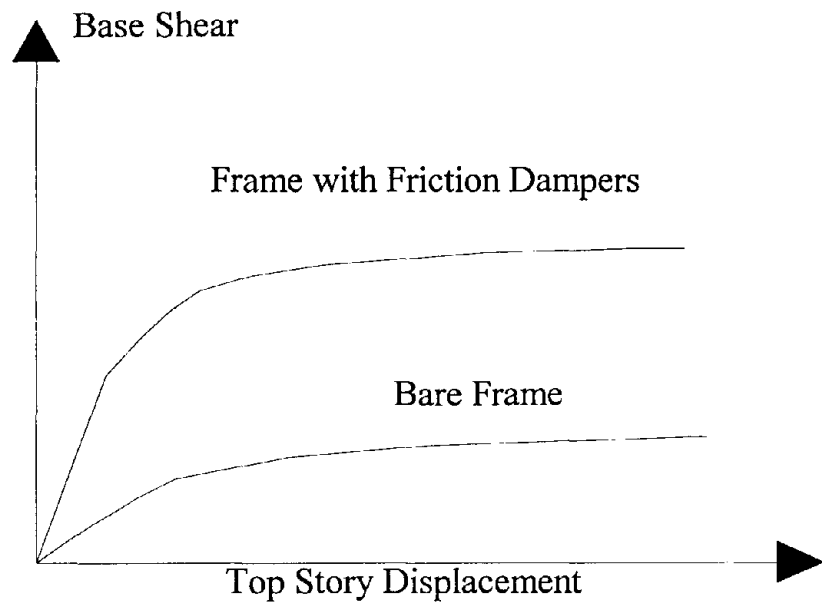


**FIGURE 5-3 Corrected capacity curve for frame with friction dampers**

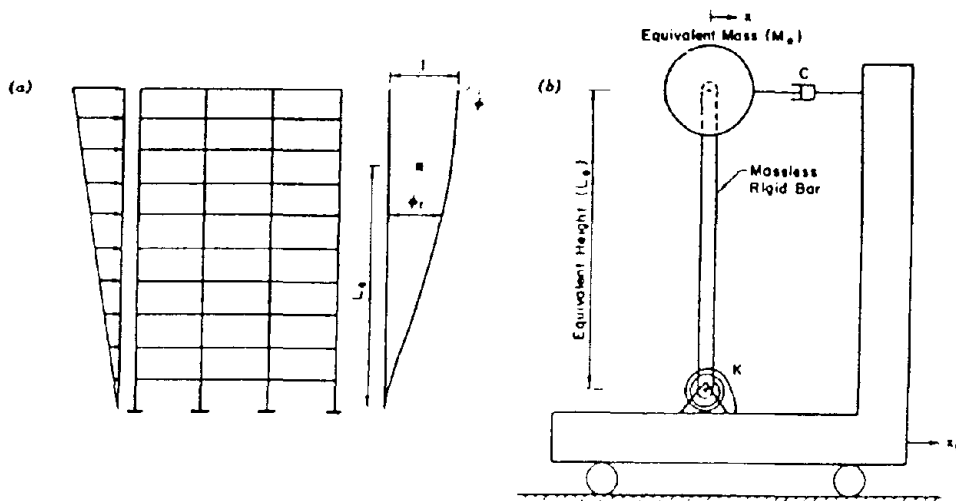


**FIGURE 5-4 Construction of Q-model [Saidi and Sozen (1981)]**

Details of the procedure proposed by Saidi and Sozen to develop the equivalent SDOF system (Q-model) can be inferred from figure 5-4. The nonlinear characteristic of the frame is reflected in the properties assigned to the rotational spring in the SDOF system. The nonlinear behavior of the spring was approximated by a bilinear curve. Pushover analysis was used to obtain the nonlinear spring properties. In this approach, the distribution of lateral forces was taken to be triangular throughout the pushover process.

Another approach to reduce a nonlinear frame to a SDOF system was proposed by Freeman (1978). The capacity spectrum method proposed by Freeman represents the nonlinear frame as a linear SDOF system with equivalent viscous damping. In the capacity spectrum approach, a nonlinear pushover analysis is carried out. The lateral

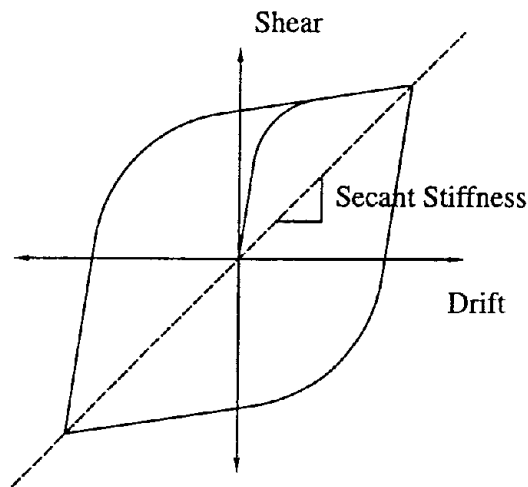


**FIGURE 5-5 Secant stiffness in one cycle**

force in the pushover analysis is to be taken proportional to the first mode shape. At each increment during the analysis, the deformation and force state of the frame is reduced to spectral displacement and spectral acceleration values, respectively. The response of the frame to the design ground motion is obtained from the intersection of

the Sa-Sd spectral curve and demand spectrum (see figure 5-5). The equivalent period of the SDOF system is taken to be the secant period of the system. The equivalent damping is selected graphically between 5% and 20% depending on the extent of inelastic deformation as seen in figure 5-5. The method proposed in ATC-33 very closely represents the CS method, except that the equivalent damping is calculated differently.

Other modifications to the pushover analysis have been published (Lawson et. al. (1994)).

In the methods discussed above, the pushover analysis procedure involves using a lateral force distribution that remains constant throughout the pushover procedure. Such an approach does not account for the change in distribution of the modal forces due to possible variations in the stiffness distribution of the structure during the progression of nonlinear behavior. A pushover analysis procedure is presented here to develop the capacity curve of the frame. In this procedure the lateral forces applied are updated during the pushover process. However for preliminary design, it may be sufficient to use the same lateral force distribution at all stages:

1. Apply a small lateral load at the top story, such that the frame is still in elastic range
2. Calculate story drifts and hence story stiffnesses
3. Construct stiffness matrix and determine the first mode eigenvalue and eigenvector  $\{\phi\}$

4. Select a base shear increment and apply a lateral force to the frame with distribution such that  $\{F\} = \frac{V}{\sum_{i=1}^{NS} \phi_i} \{\phi\}$

5. Calculate secant stiffness matrix using the story shears and story drifts

6. Perform eigenanalysis to obtain secant mode shapes. The spectral displacement and spectral acceleration values on the capacity curve are then given by

$$S_d = \frac{\sum_{i=1}^{NS} m_i \phi_i^2}{\sum_{i=1}^{NS} m_i \phi_i} \frac{v(\text{top})}{\phi(\text{top})}$$

$$S_a = V \frac{\sum_{i=1}^{NS} m_i \phi_i}{\left( \sum_{i=1}^{NS} m_i \phi_i \right)^2}$$

where NS is the number of stories,  $\{\phi\}$  is the first mode, V is the base shear and v is the displacement.

7. Go to step 4 and continue the analysis until failure. The spectral acceleration vs. spectral displacement curve is the required capacity curve of the frame.

The main feature of the procedure presented above is the updating of the lateral load vector using the secant stiffness matrix. At a certain stage in the pushover analysis the forces and deflections in the frame represent the deformed state of the frame during the maximum cycle of dynamic loading. The secant stiffness best represents the average stiffness of the story during that deformation cycle (see figure 5-5). The distribution of the secant stiffnesses would reflect the distribution of the modal forces in the frame.

Updating the lateral force distribution would result in a more accurate representation of the state of forces in the frame, particularly in frames with irregular strength distribution.

### **5.3.2 Equivalent linear SDOF system vs. nonlinear SDOF system**

From the capacity curve obtained from the procedure presented in the earlier section, the response of the MDOF system can be predicted using two approaches:

*1. Equivalent linear system with viscous damping:* This is the approach presented in ATC-33 and also the capacity spectrum method. Initial attempts at using the equivalent viscous damping method resulted in large errors in the predicted response.

Iwan and Gates (1979) statistically compared the accuracy of several linearisation methods for nonlinear systems and found that using secant stiffness and equivalent viscous damping does not provide the most accurate results. The other drawback of this approach is that it is not convenient in a design situation, since it would involve having to perform several pushover analysis procedures with different friction damper settings until the desired response is obtained.

*2. Equivalent nonlinear SDOF system:* The capacity curve was constructed by calculating the spectral response values using the secant stiffness matrix. Hence, the capacity curve is actually an envelope of the secant properties of the MDOF system. Taking mass to be 1.0, the capacity curve represents the force deformation response of an equivalent nonlinear SDOF system. For a given ground motion loading, the response of this equivalent SDOF system can be used to extrapolate the overall frame response. It is proposed here to idealize the nonlinear capacity curve with a bilinear curve, and use this bilinear system to obtain the SDOF response.

To verify the accuracy of this method, a pushover analysis was performed on the three story RC frame, discussed in Section 4. The capacity curve for the frame is shown in figure 5-6. Also shown in the Figure is the idealized bilinear force- displacement response of the equivalent SDOF system. The 500 year Taft (N21E) was used as the design ground motion. Time history analysis of the equivalent bilinear SDOF system was carried out using the program NONSPEC. For the 500 year Taft, the maximum story drifts and shears were obtained by performing nonlinear time history analyses, details of which are discussed in Section 4. The maximum response of the equivalent bilinear SDOF system can be compared to the maximum frame response in the  $S_a - S_d$  plane, as shown in figure 5-7. In figure 5-8 the story drifts and shears obtained from the nonlinear time history analysis are compared with those predicted by the equivalent bilinear SDOF system. The maximum  $S_a$  and  $S_d$  responses for the three story frame were calculated using the equations given below.

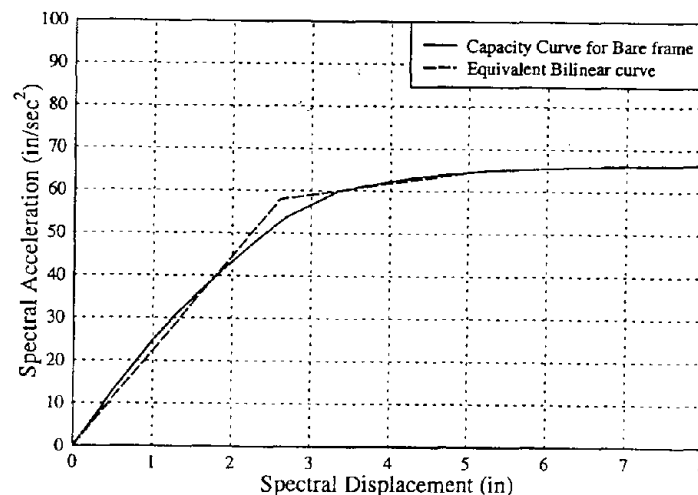


**FIGURE 5-6 Constructing equivalent bilinear SDOF system**

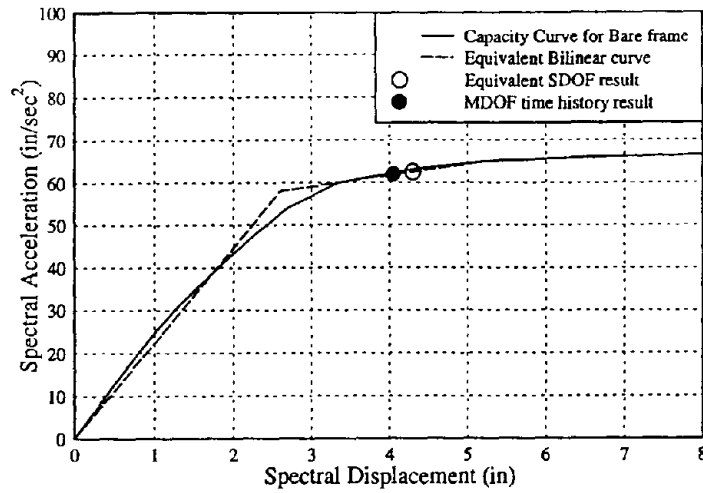


**FIGURE 5-7 Comparison of spectral responses**

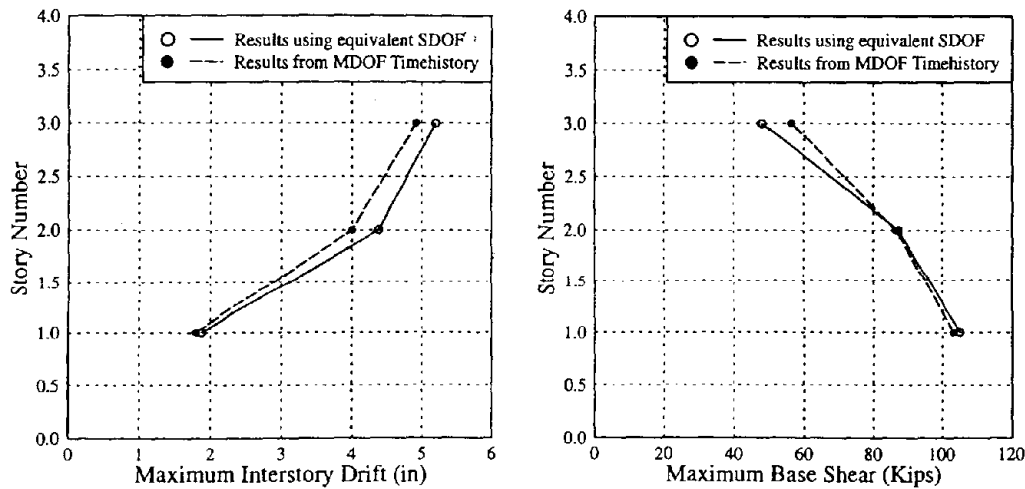


**FIGURE 5-8 Comparison of results from equivalent SDOF and MDOF time history**

The same equations were also used to obtain the story drifts and shears from the maximum response of the equivalent bilinear SDOF system.

$$v_i = S_d|_{BL} \phi_i \left( \frac{\sum_{j=1}^{NS} m_j \phi_j}{\sum_{j=1}^{NS} m_j \phi_j} \right)$$

$$V = S_a|_{BL} \frac{\left( \sum_{j=1}^{NS} m_j \phi_j \right)^2}{\sum_{j=1}^{NS} m_j \phi_j}$$

where BL stands for bilinear spring response,  $\{\phi\}$  is the first mode vector, NS is the number of stories,  $m_i$  is the mass in story  $i$ ,  $v_i$  is the displacement in story  $i$ , and  $V$  is the base shear.

The equivalent bilinear SDOF system constructed from the pushover analysis can hence be used to reliably predict the response of MDOF systems.

### 5.3.3 Inelastic Demand Spectra (IDS)

To study the influence of retrofitting on the response of the MDOF frame, corresponding stiffness and strength changes can be made to the equivalent bilinear SDOF system (EBLSDOF).

An Inelastic Demand Spectrum curve is proposed here to visualize the effect of retrofitting on the overall dynamic response of the frame and to design retrofit schemes using friction dampers. In this section, the method to construct an inelastic demand spectra is presented, using the three story RC frame as an example.

Figure 5-9 shows the  $S_a$ - $S_d$  capacity curve for the three story RC frame. In the retrofit process, the stiffness and strength of the frame can be modified. The corresponding change in the equivalent bilinear SDOF system is shown in figure 5-9. For a given increase in initial stiffness, different strength levels of the EBLSDOF would represent correspondingly different modifications to the RC frame due to retrofit. The peak

displacement and acceleration responses of the different BL systems when plotted on the Sa-Sd plane forms the inelastic demand spectrum. Each inelastic demand spectrum represents the peak response of the systems with a given initial stiffness and with different strength levels.

In figure 5-10, the IDS are plotted for 500 year Taft for the cases when the initial stiffness of the frame was increased by 2.0, 4.0 and 10.0 times the initial stiffness of the bare frame. For the 500 year earthquake, the desired drift and shear limits were decided in Chapter 4. These drift and base shear limits are expressed in terms of Sd and Sa values and superimposed on the inelastic demand spectrum curve and the capacity curve in figure 5-10.

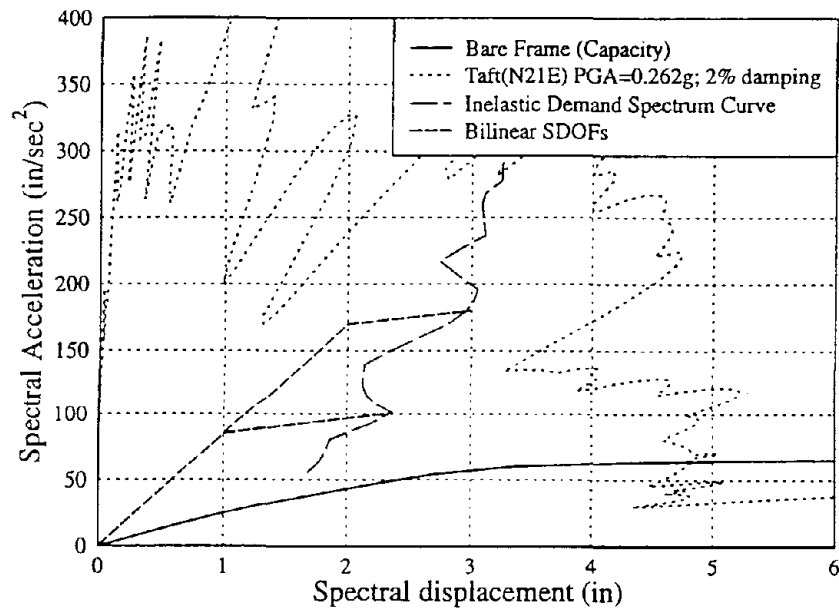


**FIGURE 5-9 Constructing the Inelastic Demand Spectrum curve.**

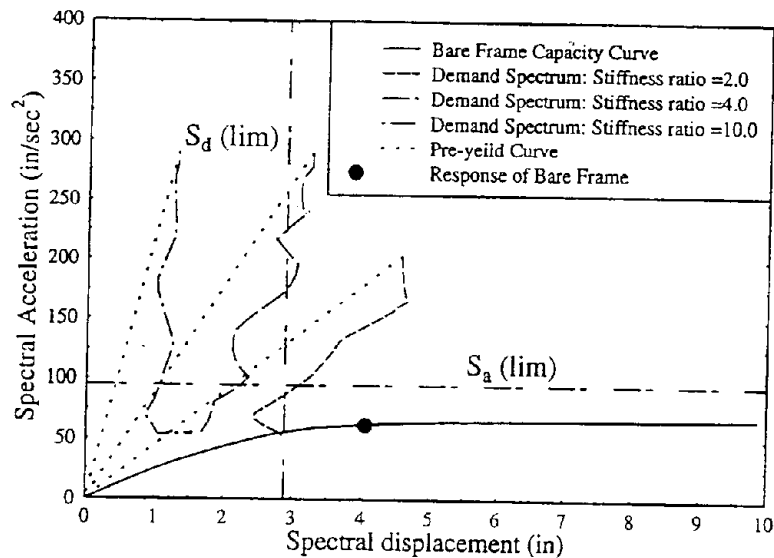


**FIGURE 5-10 Inelastic Demand Spectra for 500 year Taft for different initial stiffnesses**

The IDS curves provide a clear picture about the variation in displacement and shear demand on the structure as a result of the change in stiffness and strength of the structure. Following inferences can be made from the IDS curves in figure 5-10:

1. The drifts can be reduced by increasing initial stiffness.
2. For a given increase in stiffness, higher strength does not necessarily imply lower displacements. There is an optimum strength level for which the displacement levels are the lowest. Hence the strength needs to be controlled.

The strength also needs to be controlled in order to prevent exceeding the base shear capacity of the foundations.

### **5.3.4 Retrofitting with Conventional Methods**

The Inelastic Demand Spectrum method will be used to understand the global effect of introducing conventional retrofit schemes. Consider two conventional retrofit strategies, viz. jacketing of columns and adding shear walls. The jacketing technique is expected to result in a moderate increase in stiffness and strength, while the walls are likely to increase the stiffness and strength of the structure considerably. For argument sake it was surmised that the jacketing method would increase the stiffness and strength of the frame to two times the bare frame values, while the shear wall scheme would increase the stiffness 17 times and the strength to 7 times that of the bare frame. These values were arrived at based on the analytical studies by Jordan and Kreger (1990). Based on this information, the approximate capacity curves for frames with jacketing and frame with shear walls can be constructed as shown in figure 5-11.

For the given design earthquake (500 year Taft), IDS curves were constructed for the cases with initial stiffness of the system being 2.0 times and 17.0 times the stiffness of the bare frame (see figure 5-11). The intersection of the capacity curves with the corresponding IDS curves provides a measure of the displacement and shear response of the retrofitted frame. It can be seen in figure 5-11 that the frame with jacketing would undergo larger displacements and base shears than the bare frame. Also, the frame retrofitted by adding shear walls would have very low drifts compared to the bare frame, but much larger base shears and accelerations, thus jeopardizing the foundations and also increasing demand on building contents due to increased accelerations. From the shapes of the IDS curves, it can be commented that there is a need for a retrofit scheme which would provide an increase in the stiffness but only a limited level of lateral strength increase in the structure. However for conventional retrofit schemes, increasing the stiffness inadvertently leads to uncontrolled increase in strength.

Retrofitting the structure with friction dampers would provide the necessary strength control.

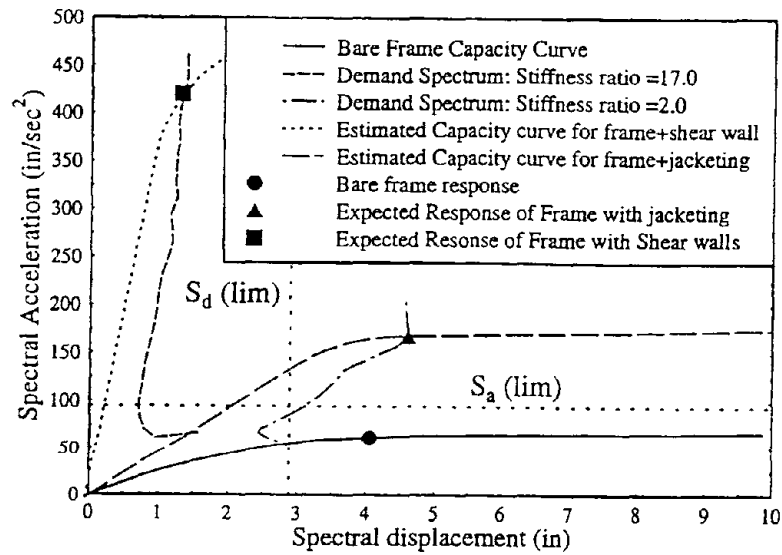


**FIGURE 5-11 Estimating response of frame with conventional retrofit**

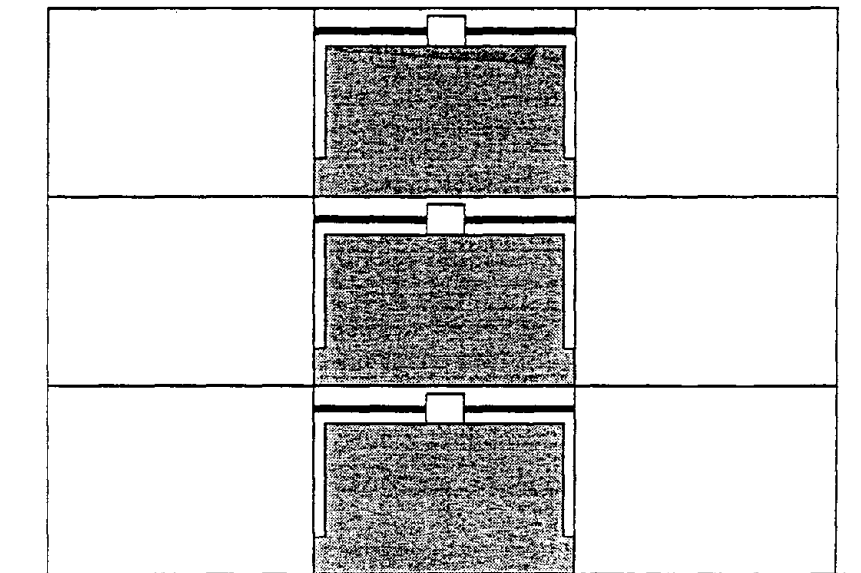


**FIGURE 5-12 Friction damper arrangement for three story RC frame**

### **5.3.5 Design of friction dampers for three story RC frame**

As discussed in Section 4, the slip level setting in the friction dampers in a MDOF frame is an important design parameter. There is a need to select the appropriate slip load so as to have the optimum frame response for the design ground motion and also to prevent overloading of the foundations. The three story RC frame retrofitted with the proposed wall-damper scheme was used to illustrate the use of IDS method to design the friction dampers.

The three story frame was retrofitted by placing the wall-damper system in each of the three stories (figure 5-12). The design problem was to determine the slip load setting in each of the dampers so as to satisfy drift limits and base shear limits for the design earthquakes. Once again, for the case study here, 500 year Taft was used as the design ground motion.

From elastic pushover of the frame with friction dampers it was estimated that introducing the wall-damper scheme increases the stiffness of the structure to 2.0 times that of the bare frame. The analytical model used for the pushover of frame with the wall-damper scheme is same as the one used for analyses described in Section 4. The IDS curve corresponding to this increased initial stiffness is shown in figure 5-13. Also shown in the figure is the  $S_a$  (limit) and  $S_d$  (limit) corresponding to the drift and base shear limits imposed on the structure. As commented earlier, there is an optimum strength level for which the earthquake demand would be less than the displacement demands for other strength levels. From the IDS curve, the bilinear capacity curve corresponding to the optimum strength level can be determined as shown in figure 5-13. The friction damper setting in the retrofitted frame corresponding to the optimum

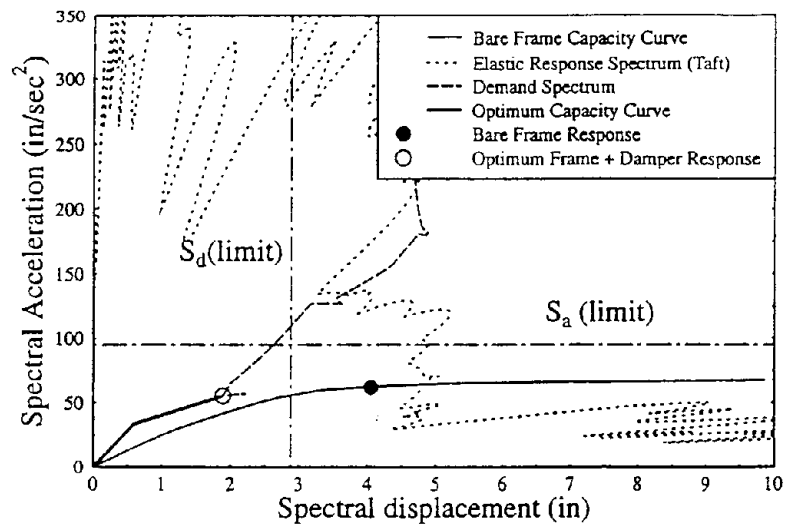


**FIGURE 5-13** Selecting the optimum damper setup

bilinear capacity curve would be the optimum friction damper setting. This can be calculated using the following equation:

$$V(\text{at slip}) = S_a(\text{slip}) \frac{\left( \sum_{i=1}^{NS} m_i \phi_i \right)^2}{\sum_{i=1}^{NS} m_i \phi_i^2}$$

In this case the  $S_a(\text{slip})$  and  $S_d(\text{slip})$  values for the optimum bilinear curve are  $33.4 \text{ in/s}^2$  and 0.6 inches respectively. As a result, the base shear in the frame at slip must be 30.0 kips.

The part of the base shear resisted by the dampers is calculated by subtracting the base shear in the frame from the total base shear when  $S_d = 0.6 \text{ in}$ . This is the level of shear in the first story wall at which the dampers must be set to slip. As shown in Section 4, when the distribution of slip forces in the stories was set to be proportional to the shears developed in each story due to a lateral load with triangular distribution, lower drifts were obtained. Hence the slip force distribution in the dampers from the design procedure presented here must be:

$$\{F_{\text{slip}}\} = \begin{Bmatrix} 7.6 \\ 12.6 \\ 15.0 \end{Bmatrix} \text{ kips}$$

To check if the slip load distribution obtained from the IDS method is close to the optimum slip load levels, several time history analyses were performed with different slip load settings. In figure 5-14, maximum drift and maximum story displacements are plotted for different slip load levels. It can be seen that the slip load distribution obtained from the IDS method is indeed an optimum friction damper setting. Also the retrofitted frame response to 500 year Taft with this slip load setting is within the maximum drift and base shear limits.

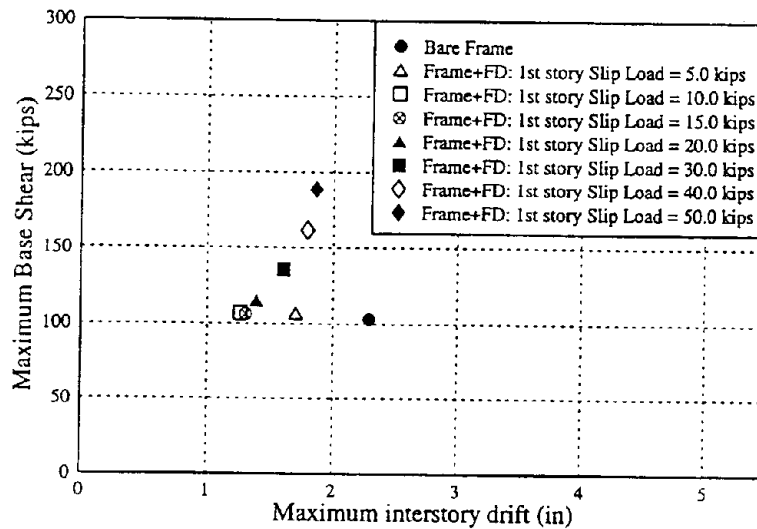


**FIGURE 5-14 Response of structure for different damper settings**

In Section 4, the variation in the frame response (maximum drift and base shear) for different slip load levels was plotted for nine different ground motions. The optimum slip load value and the maximum drift and base shears corresponding to the optimum drifts are different for each of the earthquakes. The IDS method was used to predict the optimum damper slip load and the corresponding maximum responses for this slip load. Figure 5-15 compares these quantities obtained from the two approaches. For the nine earthquakes the IDS method predicted fairly accurately the optimum slip load and the maximum drifts and base shears corresponding to the optimum setting. Hence the IDS method can serve as a powerful tool for obtaining an initial estimate of friction damper slip load levels.

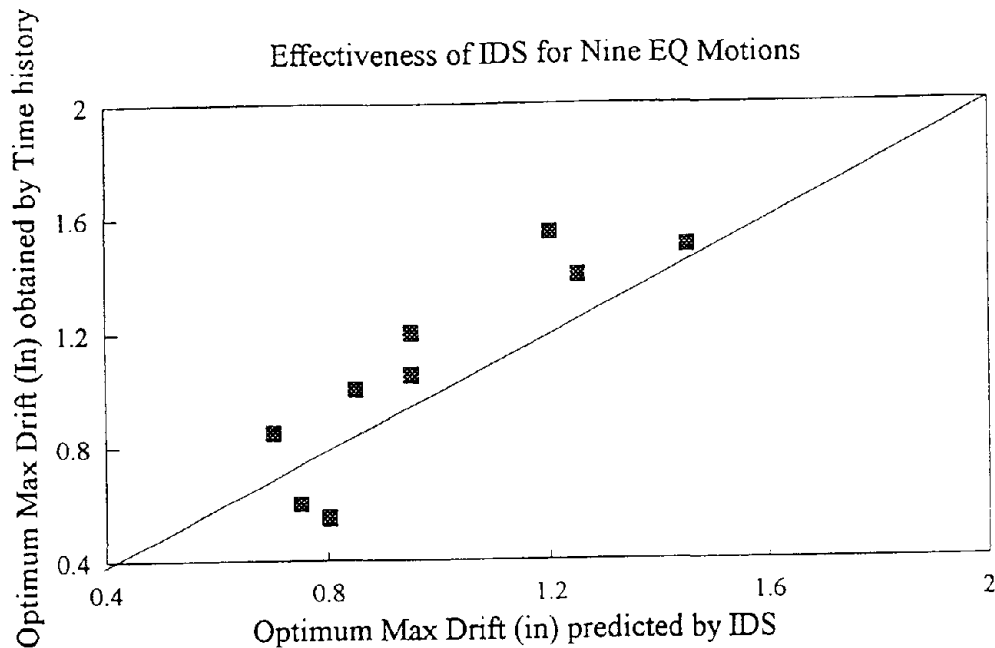


**FIGURE 5-15 Evaluating the accuracy of using IDS method to predict response of frames with friction dampers**

### 5.3.6 Generalized Inelastic Demand Spectra

In design problems, the earthquake loading is often provided in terms of response spectrum and not as a ground acceleration time history. The inelastic demand spectrum curves can be constructed for these design response spectra.

$R_\mu$  factors proposed by several researchers can be used to prepare the IDS curves for a given design response spectra. The  $R_\mu$  factors were developed for design purposes, so that the elastic design loading can be reduced to account for inelastic action. For a given ductility capacity, the  $R_\mu$  factor is the minimum strength factor required so as not to exceed that ductility. The  $R_\mu$  factors are defined as

$$R_{\mu}(\mu, T) = \frac{F(\text{elastic})}{F(\text{yield})}$$

Miranda and Bertero (1994) summarize the various  $R_{\mu}$  factor equations proposed. Significant among them are those published by Newmark and Hall (1973), Nasser and Krawinkler (1991), Lai and Biggs (1980) and Miranda (1993). The most recent of these equations is that proposed by Miranda (1993) and was developed from statistical analysis of group of 124 ground motions. The equations proposed are

$$R_{\mu} = \frac{\mu - 1}{\Phi} + 1 \geq 1$$

where  $\Phi$  is a function of  $\mu$ , period  $T$  and the soil conditions at site

$$\text{For rock sites} \quad \Phi = 1 + \frac{1}{10T - \mu T} - \frac{1}{2T} \exp\left[-\frac{3}{2}\left(\ln T - \frac{3}{5}\right)^2\right]$$

$$\text{For alluvium sites} \quad \Phi = 1 + \frac{1}{12T - \mu T} - \frac{2}{5T} \exp\left[-2\left(\ln T - \frac{1}{5}\right)^2\right]$$

$$\text{For soft soil sites} \quad \Phi = 1 + \frac{T_g}{3T} - \frac{3T_g}{4T} \exp\left[-3\left(\ln \frac{T}{T_g} - \frac{1}{4}\right)^2\right]$$

where  $T_g$  is the predominant period of the ground motion.

The above equations can be used to construct IDS curves for a given elastic response spectrum, by using the following equations:

$$S_d(\text{inelastic}) = \frac{S_d(\text{elastic})}{R(\mu)} \mu$$

$$S_a(\text{inelastic}) = \frac{S_a(\text{elastic})}{R(\mu)} \phi$$

$$\phi = 1 + \alpha (\mu - 1)$$

The factor  $\phi$  in the above equation is to account for the post yield stiffness  $\alpha$ , taken to be 5% in Miranda's work.

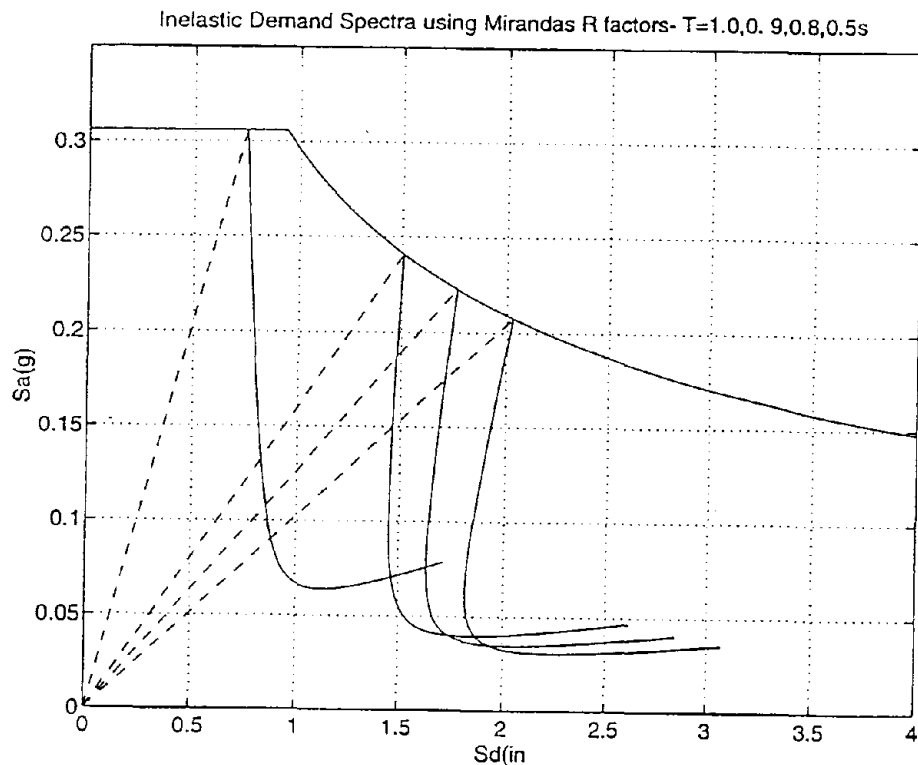


**FIGURE 5-16 Generalized IDS curve using Miranda's R factors**

In Section 4, the 500 year earthquake loading was defined by a response spectrum obtained from criterion provided in the ATC-33 50% submittal draft. Figure 5-15 shows the design response spectrum in the Sa-Sd plane. Generalized IDS curves were developed using Miranda's  $R_{\mu}$  factors for initial periods of  $T = 1.0$  s, 0.5s and 0.1s and are shown in figure 5-16. Based on the generalized IDS curves in figure 5-16, the following observations can be made about the response of inelastic systems and of the effect of retrofitting on the response of structures:

1. For longer initial periods ( $T > 0.8$ secs), increasing the strength initially reduces drift demand. But after a point, the displacement increases for

increased strength levels. This behavior is similar to that observed for the IDS curve generated for Taft 500 year earthquake.

2. For stiff structures, increasing the strength always reduces the displacements.

It is interesting to note that for a given strength level there can be two displacement responses. The explanation comes from the way  $R_{\mu}$  factors were calculated by Miranda. For a given ductility, when there were two strength levels, the higher value was chosen. Hence the low strength systems were excluded. It can be suggested that statistical studies similar to those carried out by Miranda be performed, but aimed towards obtaining averaged IDS curves. Instead of using  $\mu$  as a parameter,  $d = (\Delta(\text{inelastic})/\Delta(\text{elastic}))$  can be obtained in terms of  $R_{\mu}$ .

#### **5.4 Summary**

In this section, existing approaches to designing friction dampers for structures were discussed. The existing methods were found to be inadequate for retrofit design for nonlinear RC frames. An inelastic demand spectrum method was proposed which involved using pushover analysis. The IDS curves reveal that conventional retrofit methods do not provide the required strength control and hence the response of structures conventionally retrofitted may not be satisfactory. The IDS was used to select the optimum slip load setting for a three story RC frame which was retrofitted with the proposed wall-damper scheme. It was then shown that generalized IDS curves can be constructed, when the loading is provided in terms of response spectrum.

In the next section, a design example for the retrofit design of a 10 story RC structure will be presented.

## **SECTION 6**

### **EXAMPLE PROBLEM FOR DESIGN OF FRICTION DAMPER RETROFIT SCHEME USING THE INELASTIC DEMAND SPECTRUM METHOD**

#### **6.1 Introduction**

The Inelastic Demand Spectrum method for the preliminary design of friction dampers was introduced in Section 5. A three story nonductile RC frame was used as an example to illustrate the design methodology. To make the proposed design procedure clearer, it was decided to use another example problem, wherein a step by step procedure would be outlined. To further expedite the preliminary design process, simplifications are made to some parts of the procedure outlined in Section 5.

#### **6.2 Definition of Retrofit Problem**

##### **6.2.1 Ten story nonductile RC frame**

Dimensions of the ten story nonductile RC frame used in this example are shown in figure 6-1. The structure has been analyzed by several researchers in past [Jordan (1991), El-Borgi (1993), Beres (1994)], in an attempt to understand the behavior of medium rise structures with nonductile detailing when subjected to ground motions. While Jordan and El-Borgi used nonlinear time history analyses, Beres used the capacity spectrum method. For details of the section dimensions and reinforcements and for more details the reader is referred to the abovementioned references. Beres (1994) predicted that the structure would undergo widespread inelastic action under 0.2g Taft (S69E), while it would most likely collapse under 0.3g Taft (S69E). Based on these observations it was noted that this frame would need retrofitting.

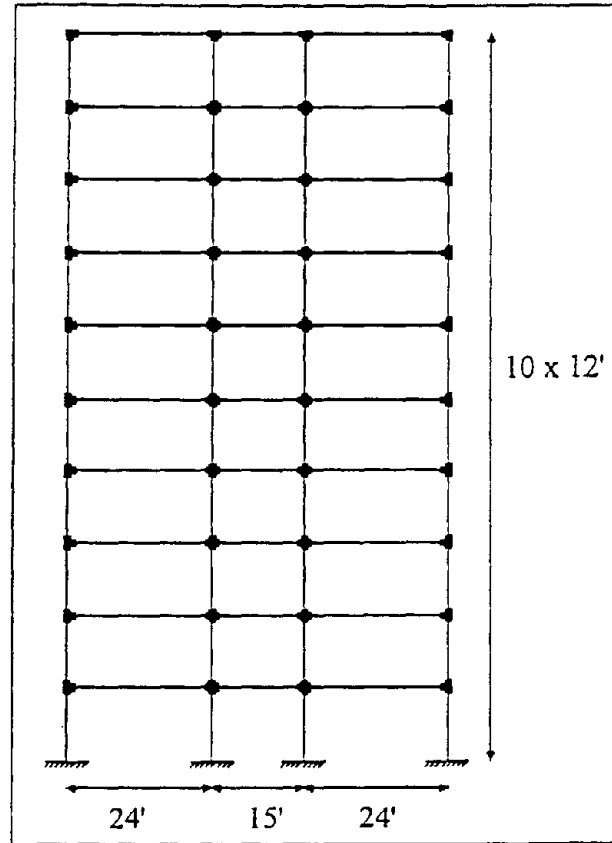


**FIGURE 6-1: Dimensions of ten story RC frame**

**TABLE 6-I: Section properties used for 10 story frame [Beres (1994)]**

Member	Location	I [in <sup>4</sup> ]	EI (reduced) [10 <sup>6</sup> in <sup>2</sup> - kips]	Ultimate Moment [ft-kips]
External Columns	Floor 1-4	88120	165.1	300
	Floor 5-10	84260	157.8	250
Internal Columns	Floor 1-4	51700	96.8	380
	Floor 5-7	49170	92.1	330
	Floor 8-10	46810	87.7	280
Beams	Positive Moment	34400	37.6	80
	Negative Moment	34400	37.6	625

### 6.2.2 Earthquake Loading and Desired Performance Criterion

The loading for the frame was taken to be 500 year Imperial Valley (El Centro) earthquake (S00E component). The 500 year Imperial Valley earthquake was obtained by matching the response spectrum with the 500 year return period design spectrum. Details of the earthquake selection are presented in Section 4.2.1. The PGA corresponding to the 500 year Imperial valley earthquake is 0.237g.

For the defined ground motion loading, the desired performance level was selected as “Collapse Prevention”. As discussed in Section 4, the maximum story drift can be used

as an index to measure the performance of the structures under earthquake loading. Beres (1994) performed a pushover analysis as part of the capacity spectrum method and found that beyond an interstory drift level of 0.5%, the structure would undergo large stiffness deterioration at several joints. For this example, the life safety criterion would be interpreted as having maximum interstory drift to be less than 0.5%. This value is low in comparison to the three story frame, but this could be attributed to the fact that the 10 story frame has large member sizes which would induce more shear and flexural damage at lower drift levels.

### **6.3 Design of Friction Dampers Using the Inelastic Demand Spectrum Method**

Having defined the retrofit problem, viz. ground motion definition and the maximum acceptable drift level, the step by step procedure for carrying out the retrofit design is presented in this section. The major steps involved in the Inelastic Demand Spectrum method can be enumerated as follows:

**Step 1.** The structure is modeled for performing nonlinear pushover analysis

**Step 2.** Pushover analysis is performed on the bare frame as discussed in Section 5.3.1. This step results in the development of the capacity curve for the bare frame.

**Step 3.** The response of the bare frame is estimated by approximating the capacity curve with a bilinear curve, and performing nonlinear timehistory analysis on the equivalent SDOF (see Section 5.3.2). The bare frame response could also be calculated using the nonlinear time history analysis of MDOF frame model.

**Step 4.** If the response of the bare frame is more than the acceptable response, retrofitting is required. For different levels of increased initial stiffnesses,

Inelastic Demand Spectrum curves must be developed. By superimposing the IDS curves with acceptable limits, the required initial stiffness and yield level for the equivalent bilinear SDOF system can be estimated.

**Step 5.** Knowing the required equivalent bilinear SDOF characteristics, pushover analyses is performed on the frame with friction dampers added at different story levels. The properties of the dampers (i.e. initial stiffness and slip load) must be changed until the point when the pushover of the frame results in a capacity curve that matches the desired equivalent SDOF system. This damper setting is the design damper configuration

The procedure outlined below was implemented for the design of friction dampers for the 10 story frame described above.

**Step 1. Modeling the structure:** The model for the ten story frame to be used for pushover analysis in the computer program IDARC was constructed using the section properties calculated by Beres (1994). Details of the structural idealization are given in the reference. The cross sectional properties calculated by Beres for the ten story frame are given in table 6-I. The reduced EI presented in table 6-I were calculated based on gross cross sectional properties, while the modulus of elasticity of concrete was reduced by 40% to account for cracking due to shrinkage and gravity loads.

**Step 2. Pushover analysis and estimating bare frame response:** The pushover analysis for the frame was performed on the 10 story frame using the steps given in Section 5.3.1. However, to speed up the design process, the lateral force distribution shape vector was not modified at every step. The lateral load shape vector was taken to be equal to the first mode shape vector at the beginning of the pushover. Since the structure does not have a large

variation in the strength distribution through the height of the structure, this approximation would not affect the results, while speeding up the calculation process. The resulting capacity curve for the bare frame is shown in figure 6-2.

**Step 3. Estimating the response of the bare frame:** Also shown in figure 6-2 is the estimate of the frame response in the  $S_a$ - $S_d$  plane obtained by performing a time history analysis of the equivalent SDOF system. When the frame response from these two approaches is compared in figure 6-2, it can be seen that the equivalent SDOF underestimates the base shear demand. This can be attributed to the fact that the equivalent SDOF does not account for higher modes of vibration. However, in this design process, the response of the equivalent SDOF system would be used as the reference, since the entire design process is built around the SDOF. The underlying assumption here is that, once the relation between the SDOF and the MDOF response is determined for one case, the same proportion would hold true for other cases. This statement becomes clear in the next steps. The maximum interstory drift in the frame is 0.65% under 500 year Imperial Valley earthquake, which would most likely result in exceeding life safety level of the structure. The desirable response is to have a drift of less than 0.5%. The capacity curve with the prescribed response limits is shown in figure 6-3. This would imply that there is a need for a reduction of around 30% in the frame response. In terms of the equivalent SDOF response, a 30% reduction in  $S_d$  is required. Limits on the foundation shear were not taken into consideration here.

**Step 4. Constructing IDS curves:** Three different initial stiffnesses were considered for the retrofitted equivalent SDOF system. The initial stiffnesses considered were 1.5, 2.0 and 3.0 times the initial stiffness of the bare frame. The IDS curves corresponding to these initial stiffnesses are shown in figure 6-4,

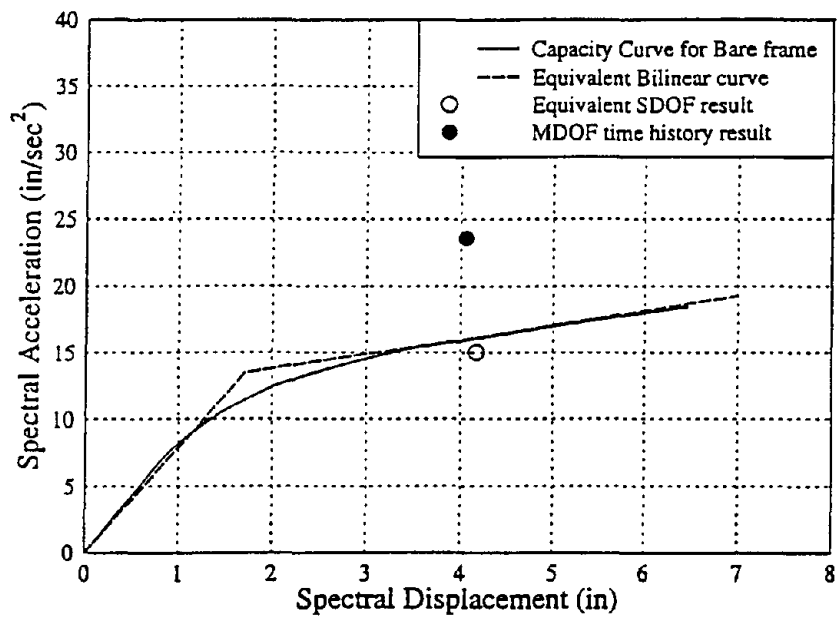


**FIGURE 6-2: Capacity curve and equivalent bilinear curve for 10 story frame**

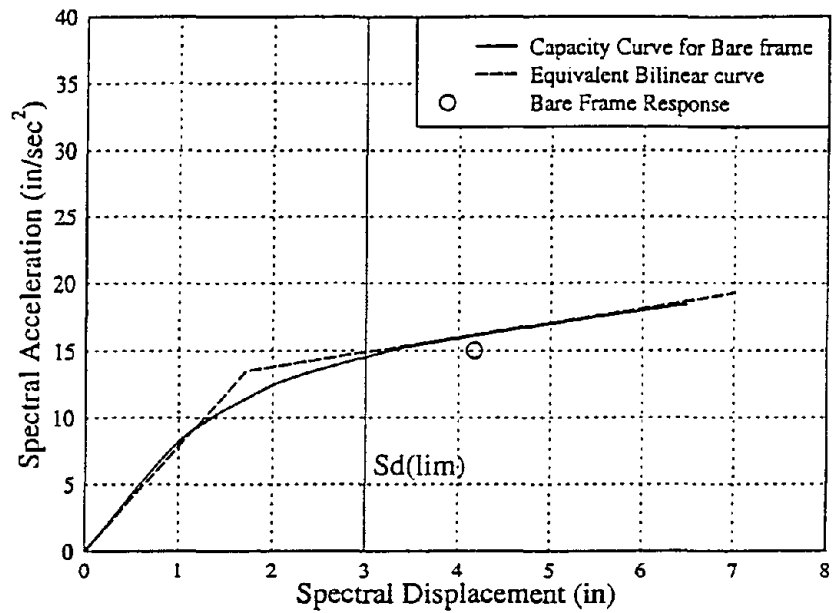


**FIGURE 6-3: Capacity curve and acceptable limit**

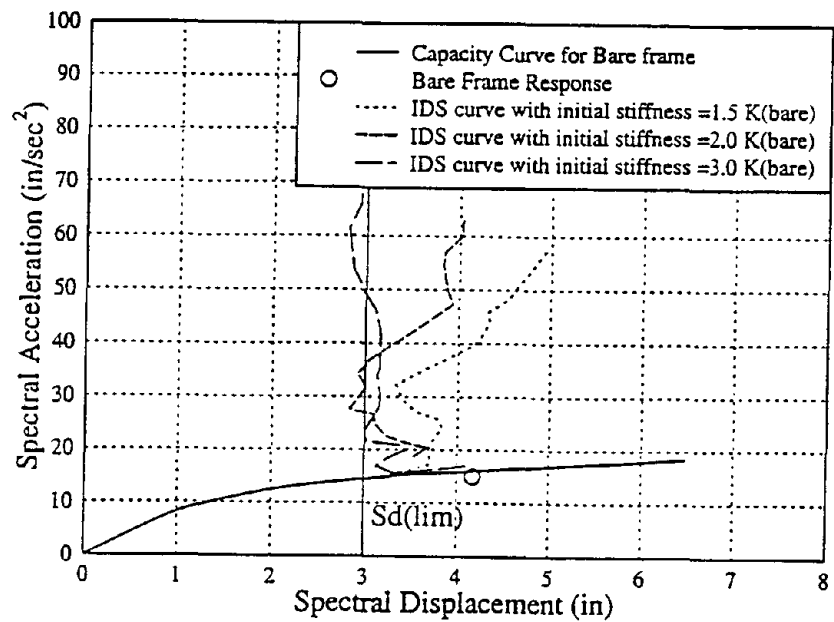


**FIGURE 6-4: IDS curves for K(initial)= 1.5, 2.0 and 3.0 K(bare)**

with the acceptable limits being superimposed in the  $S_a$ - $S_d$  plane. It can be observed that increasing the initial stiffness by 1.5 times is unlikely to reduce frame response to the desired level. Increasing the initial stiffness to twice that of the bare frame would provide the necessary reduction. However, providing a larger initial stiffness to three times the bare frame stiffness is not likely to further improve the performance. Hence initial stiffness of the retrofitted frame must be twice that of the bare frame. In figure 6-5, the equivalent SDOF that would provide the minimum displacement demand, for the given increased initial stiffness, is shown. The  $S_d$  at the point of slip for the optimum equivalent SDOF is 1.4 in. (figure 6-5).

**Step 5. Obtaining the optimum slip load distribution:** In this stage, another pushover analysis, similar to that performed in step 2, was performed, but with the frame having stiffeners. The positions and stiffnesses of the stiffeners can be varied until the initial stiffness matches the required initial stiffness obtained from step 4. The stiffeners can be placed anywhere in the frame, depending on site and architectural requirements. However, in this illustrative example, the stiffeners were placed in all the stories in the central bay. After a few iterations it was determined that in order to double the frame stiffness, stiffeners with stiffness value of 270 kips/in would be required in each story. This value of the required stiffness is much higher than the wall stiffness of 54.0 kips/in. Hence chevron bracings will have to be used in place of the masonry infills to obtain the desired stiffness.

The pushover was carried out until the  $S_d$  of 1.4 in. was reached (see figure 6-6). The force distribution in the stiffeners (dampers) corresponding to this state is the design slip load setting. For the ten story frame the force in the first story damper at this stage was 40 kips. It was decided to have constant slip load

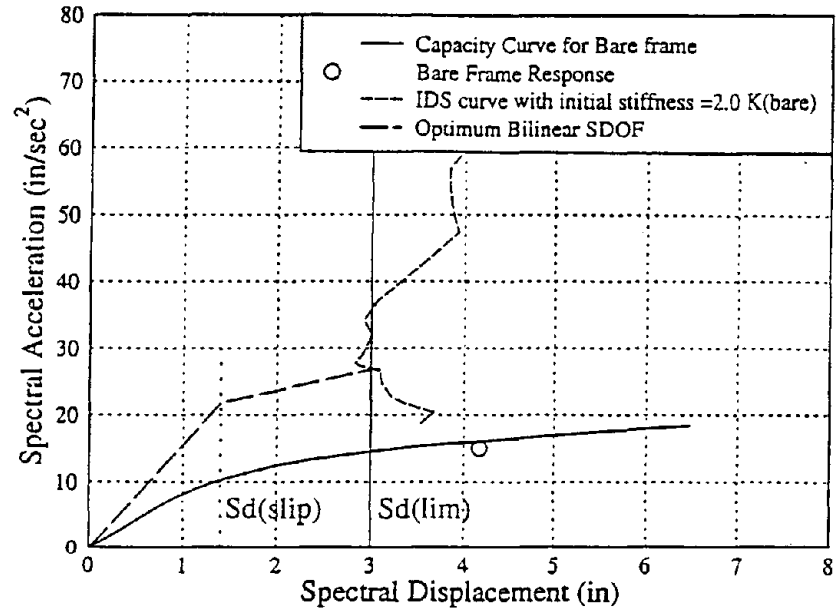


**FIGURE 6-5: Selecting the optimum bilinear SDOF**

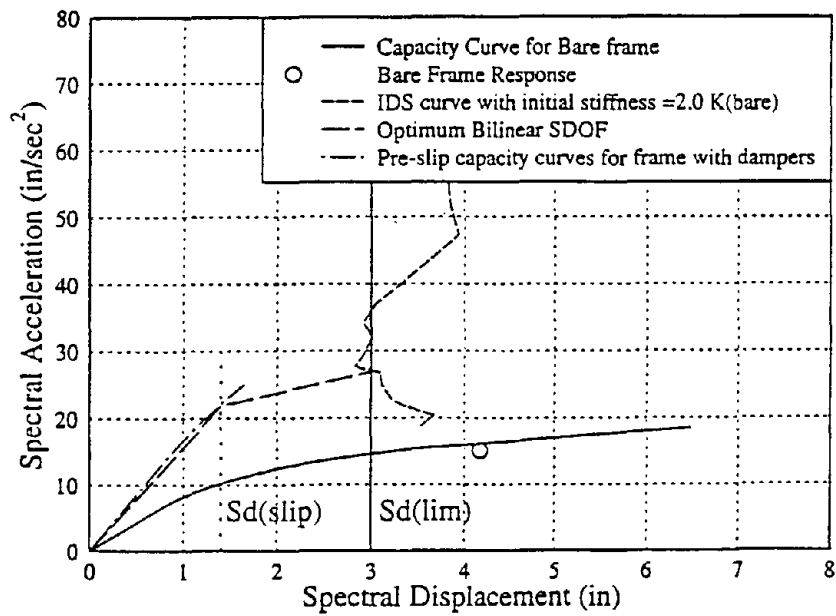


**FIGURE 6-6: Pre-slip capacity curve for frame with dampers**

distribution, since the effect of higher modes has not been accounted in this method. To confirm the results obtained from the preliminary design procedure, nonlinear time history analyses were performed with the frame having dampers with slip load = 40 kips in all the stories. As estimated by the design procedure, the maximum drift in the frame is less than the maximum acceptable drift level. To obtain the most optimum damper setting, time history analyses were performed for different slip load levels around 40 kips. figure 6-7 shows the response of the frame in the maximum drift - maximum base shear plane, for different slip load levels. It is seen that the slip load setting of 30 kips is the optimum slip load; however using slip load of 40 kips still provides the desirable performance.

#### **6.4 Discussion**

A 10 story frame was considered to illustrate the use of the proposed Inelastic Demand Spectrum method for design of friction dampers for nonductile RC frames. It is shown in a step by step manner that by using nonlinear pushover analysis and a series of nonlinear time history analysis of SDOF systems, the friction damper location, initial stiffness and the slip load settings can be estimated. The initial stiffness and the slip load settings calculated by the IDS method for retrofitting the ten story RC frame was confirmed to be accurate by time history analysis. Hence the IDS method can be used as a reliable tool to obtain a preliminary design for friction dampers.

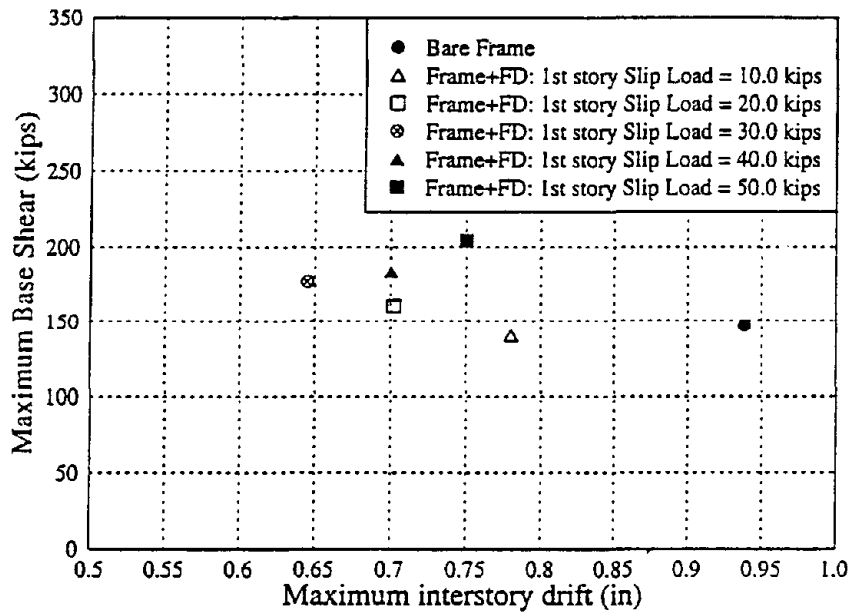


**FIGURE 6-7: Frame response for different slip load settings**

## SECTION 7

### SUMMARY, CONCLUSIONS AND RECOMMENDATIONS FOR FUTURE RESEARCH

#### 7.1 Summary and Conclusions

The research presented in this report was part of a NCEER sponsored research program on (a) evaluating the seismic resistance of RC structures designed for gravity loading alone, and (b) developing seismic rehabilitation methods for these structures. Earlier phases of the research concentrated on the evaluation process, and resulted in the conclusion that structures with nonductile detailing were excessively flexible with large interstory drift response under moderate level earthquakes. The predicted collapse mode of these structures resulted from hinging in the columns due to the strong beam - weak column design.

The main objective of this research was to develop and evaluate a retrofit scheme for these RC frames with nonductile detailing. The retrofit scheme had to satisfy certain constraints viz. (a) the retrofit scheme had to be economically feasible, since it had to be marketed to owners in the central and eastern US, where the level of seismic risk and awareness is low; (b) the proposed scheme must cause the least amount of inconvenience to existing users and; (c) introduction of the retrofit must not alter the characteristics of the structure in a way that would overload the structure's existing foundations.

The main features of this report are:

1. Proposal of a novel retrofit scheme involving friction dampers installed through a masonry infill wall with gaps on the side and top

2. Experimental studies using shake table tests to verify the effectiveness of the proposed scheme
3. Analytical studies using nonlinear time history analyses to evaluate the extent to which the proposed scheme would improve frame response
4. Proposal of a preliminary design method to obtain the damper stiffness and slip load.

First, a background on the various conventional retrofit schemes discussed in literature and supplemental damping methods was presented. Then the new retrofit scheme using friction dampers and masonry infill walls was presented. The method has the features of being constructable and economical compared to conventional schemes. The wall-damper scheme was expected to provide an increase in stiffness which should reduce drift, and the dampers would provide energy dissipation which would limit the force demands on the frame. The friction dampers can be so tuned that the forces being transferred to the foundations are limited, thereby ensuring foundation safety.

To study how the proposed scheme would actually perform when dynamically loaded, an experimental program involving cyclic testing of friction damper specimens and shake table testing of a 1/3 scale one story frame with the retrofit scheme was conducted as described in Section 3. Results from the shake table tests show that the retrofit scheme provides an increase in the initial stiffness and also provides energy dissipation friction action in the slotted bolt connections. It was observed that in case of the Taft earthquake loading, introducing the dampers resulted in reduced drifts and forces. However, when the frame was subjected to the Pacoima earthquake, there was an increase in the maximum drift and shear measured for the frame with the dampers when compared to the bare frame. This was explained using the  $S_a$ - $S_d$  plane response spectrum; the frequency content of Pacoima motion was such that increasing the

stiffness increases the displacement as well as the force demand on the structure. The added damping was not sufficient to bring down the maximum response levels. It was however noted that, even though the dampers did not reduce maximum responses under Pacoima motion, the drifts were reduced for subsequent cycles of motion. This is because the Pacoima motion is an impulse-like motion, with the intense motion confined to a short time frame with the high acceleration spikes arriving at the beginning of the motion. Hence the dampers were not able to dissipate sufficient energy to mitigate this early demand spike; however as more energy was dissipated the subsequent cycles were reduced. The shake table tests also provided the pre-slip stiffness value for the wall-damper scheme.

A three story nonductile RC frame was used in analytical studies to judge the effectiveness of the proposed scheme under a wide variety of ground motions. Section 4 provides details about the analytical studies. The loading was defined in terms of two levels of earthquake motions, defined by design spectrums. Nine recorded earthquake motions were used in the study, scaled to match spectra in the region of interest. Performance objectives were defined in terms of maximum interstory drifts. Time history analyses for these earthquakes for the three story frame for different damper settings showed that by selecting the appropriate slip load in the dampers, the retrofit scheme can improve the frame response and satisfy the performance objectives for different ground motion types.

In the final phase of the research a design methodology for the wall-damper scheme was proposed. The method avoids the need to perform the extensive MDOF time history analyses otherwise required to select the optimum slip loads in the friction dampers. The method involves performing nonlinear pushover analysis and a series of time history analyses for bilinear SDOF systems. A three story and a ten story frame were used to show that the proposed design method can accurately predict the optimum slip

load setting. The method called the Inelastic Demand Spectrum method further showed explicitly that using the friction dampers provides the required strength control to obtain the minimum drift response and to limit the demand on the foundations.

## **7.2 Recommendations for Future Research**

The research discussed in this report aimed to provide a comprehensive evaluation study of a proposed retrofit scheme. However there are certain issues which can be further investigated to make this study more definitive. These include:

1. The performance of energy dissipating devices, and the slotted bolt connections in particular, when subjected to out-of-plane deformations has not been investigated. It can be argued that the structure would be retrofitted in both directions, and hence the out-of-plane deformation demand on the dampers must be low and would not affect their performance. However, an experimental study which would involve subjecting the retrofit scheme to bi-directional dynamic loading, would provide the necessary experimental data on this subject
2. The Inelastic Demand Spectrum method can be extended further to be used as a common design procedure for any retrofit scheme, such as those using viscoelastic dampers, ADAS devices and even conventional retrofit methods. Some ideas in this direction can be obtained from the material given in ATC 33 (50% complete draft). Another improvement to the proposed IDS method would be incorporate the effect of higher modes on frame response.

## SECTION 8

### REFERENCES

Alcocer, A. and Jirsa, J.O., "Assesment of the Response of RC Frame Connections Redesinged by Jacketing", Proceedings of the Fourth U.S. National Conference on Earthquake Engineering, Vol.3, pp.295-304, 1990.

ATC-33 (50% submittal) Guidelines and Commentary for the Seismic Rehabilitaion of Buildings, (1994).

Badoux, M. and Jirsa, J.O., "Steel Bracing of RC Frames for Seismic Retrofitting", ASCE Journal of Structural Engg., Vol. 116, No.1, pp.55-74, 1990.

Beres, A.B., "Experimental and Analytical Evaluation of the Performance of Reinforced Concrete Frames with Non-Ductile Details", Ph.D. Dissertation, Dept. of Civil and Environmental Engineering, Cornell University, Ithaca, NY, 1994.

Bertero, V.V., "Seismic Upgrading of Existing Structures", ", Tenth World Conference on Earthquake Engineering, pp.5101-5106, 1992.

Bracci J.M., Reinhorn, A.M. and Mander, J.B., "Seismic Resistance of R/C Frame Structures Designed Only for Gravity Loads, Part III: Experimental Performance and Analytical Study of Structural Model, Technical Report, NCEER-92-0029, National Center of Earthquake Engineering Research, SUNY, Buffalo, 1992.

Chang, K.K., Soong, T.T., Lai, M.L. and Nielsen, E.J., "Viscoelastic Dampers as Energy Dissipation Devices for Seismic Applications", Earthquake Spectra, Vol. 9, No. 3, pp. 371-387, 1993.

Constantinou, M.C., Reinhorn, A.M., Mokha, A. and Watson, R. (1991), "Displacement Control Device for Base-Isolated Bridges", *Earthquake Spectra*, Vol. 7, No. 2, 1991, p.179-200.

Constantinou, M.C., and Symans, M.D., "Experimental Study of Seismic Response of Buildings with Supplemental Fluid Dampers", *The Structural Design of Tall Buildings*, Vol. (2), pp. 93-132, 1993.

DisPasquale E. and Cakmak, A.S., "Detection and Assessment of Seismic Structural Damage", Technical Report NCEER-87-0015, National Center of Earthquake Engineering, SUNY, Buffalo, NY, (1987).

El-Borgi, S., "Seismic Evaluation and Strengthening of Lightly Reinforced Concrete Structures", Ph.D. Dissertaion, School of Civil and Environmental Engineering, Ithaca, NY, 1993.

Freeman S., "Communications on the Capacity Spectrum Method with Professor Peter Gergely", 1994.

Filiatrault, A. and Cherry, S., "Performance Evaluation of Friction Damped Braced Steel Frames Under Simulated Earthquake Loads", *Earthquake Spectra*, Vol. 3, No. 1, pp.57-87, 1987.

Filiatrault, A. and Cherry, S., "Seismic Design Spectra for Friction-Damped Structures", *Journal of Structural Engineering*, ASCE, Vol. 116, No. 5, pp. 1334-1355, 1990.

Goel S.C. and Lee, H., "Seismic Strengthening of RC Structures by Ductile Steel Bracing Systems", *Proceedings of the Fourth U.S. National Conference on Earthquake Engineering*, Vol.3, pp.323-331, 1990.

Grigorian, C.E. and Popov, E., “Energy Dissipation with Slotted Bolted Connections”, Report No. UCB/EERC-94/02, Earthquake Engineering Research Center Report, 1994.

Hasselman, T.K. and Wiggins, J.H., “Earthquake Damage to High-rise Buildings as a Function of Interstory Drift”, Proceedings of the Third International Earthquake Microzonation Conference, University of Washington, Seattle, Vol. II, pp. 883-894, (1982).

Li C. and Reinhorn A. M., “Experimental and Analytical Investigation of Seismic Retrofit of Structures with Supplemental Damping: Part II - Friction Devices”, Technical Report, NCEER-95-0009, National Center of Earthquake Engineering Research, SUNY, Buffalo, 1995.

Hasselman, T.K., Eguchi, R.T. and Wiggins, J.H., “Assessment of Damageability for Existing Buildings in a Natural Hazards Environment”, Technical Report No. 80-1332, prepared for the National Science Foundation, J.H. Wiggins Company, Redondo Beach, CA, (1980).

Iwan, W.D. and Gates, N.C., “Estimating Earthquake Response of Simple Hysteretic Structures”, Journal of the Engineering, ASCE, Vol. 105, No. EM3, pp. 391-405, 1979.

Jordan, R.M. and Kreger, M.E., “Evaluation of Strengthening Schemes and Effects on Dynamic Characteristics of Reinforced Concrete Frames”, Proceedings of the Fourth U.S. National Conference on Earthquake Engineering, Vol. 3, pp. 363-372, 1990.

Katsumata, H., Kobatake, Y. and Takeda, T., “A study on the strengthening with Carbon Fiber for Earthquake-Resistant Capacity of Existing Reinforced Concrete Columns”, Proceedings of Workshop on Repair and Retrofit of Existing Structures, U.S.-Japan Panel on Wind and Seismic Effects, Tsukuba, Ibaraki, Japan, 1987.

Lai, S.-P. and Biggs, J.M., "Inelastic Response Spectra for Aseismic Building Design", Journal of Structural Division, ASCE, Vol. 106, No. ST6, pp. 1295-1310, 1980.

Miranda, E. and Bertero, V.V., "Evaluation of Strength Reduction Factors for Earthquake- Resistant Design", Earthquake Spectra, Vol. 10, No. 2, pp. 357-379, 1994.

Miranda, E., "Site-Dependent Strength Reduction Factors", Journal of Structural Engineering, ASCE, Vol. 119, No. 12, 1993.

Nassar, A.A. and Krawlinker, H., "Seismic Demands for SDOF and MDOF Systems", Report No. 95, The John A. Blume Earthquake Engineering Center, Stanford University, 1991.

NBCC, National Building Code of Canada and supplement to the National Building Code of Canada, National Research Council of Canada, Ottawa, 1980, 1990.

Newmark N.M. and Hall, W.J., "Seismic Design Criteria for Nuclear Reactor Facilities", Report No. 46, Building Practices for Disaster Mitigation, National Bureau of Standards, U.S. Department of Commerce, pp. 209-236, 1973.

Pall, A., Vezina, S., Proulx, P. and Pall, R., "Friction Dampers for Seismic Control of Canadian Space Agency Headquarters", Earthquake Spectra, Vol. 9, No. 3, pp. 547-557, 1993.

Pall, A.S., and Marsh C., "Response of Friction Damped Braced Frames", Journal of the Structural Division, Vol. 108, No. ST6, ASCE, 1982.

Park, Y.J. and Ang, A.H-S., "Mechanistic Seismic Damage Model for Reinforced Concrete", Journal of Structural Engineering, ASCE, Vol. 111, No. ST4, 722-739, (1985).

Paultre, P. and Mitchell, D., "Assessment of Some Canadian Seismic Code Requirements for Concrete Frame Structures", Canadian Journal of Civil Engineering, Vol. 18, pp. 343-357, (1991).

Pekau, O.A. and Guimond, R., "Controlling Seismic Response of Eccentric Structures by Friction Dampers", Earthquake Engineering and Structural Dynamics, Vol. 20, pp. 505-521, 1991.

Pessiki, S.P., Conley, C., Gergely, P. and White, R.N., "Seismic Behavior of Lightly-Reinforced Concrete Column and Beam Column Joint Details", Technical Report, NCEER-90-0014, National Center of Earthquake Engineering Research, SUNY, Buffalo, 1990.

Pincheira, J.A. and Jirsa, J.O., "Seismic Response of a Strengthened RC Structure", Fifth U.S. Conference on Earthquake Engineering, Vol.3, pp.749-758, 1994

Ramirez-de-Alba, H., Martinez-Rueda, E. and De la Colina-Martinez, J., "Behavior of RC Frame Models Strengthened with Walls", Tenth World Conference on Earthquake Engineering, pp.5257-5260, 1992.

Saidi, M. and Sozen, M.A., "Simple Nonlinear Seismic Analysis of R/C Structures", Journal of Structural Engineering, ASCE, Vol. 107, No. ST5, pp. 937-952, 1981.

Toussi, S. and Yao, J.T.P., "Hysteresis Identification of Existing Structures", Journal of Engineering Mechanics, ASCE, Vol. 109, No. 5, pp. 1189-1202, 1983.

Tso, W.K, Zhu, T.J. and Heidebrecht, A.C., "Engineering Implication of Ground Motion A/V Ratio", Soil Dynamics and Earthquake Engineering, Vol. 11, pp. 133-144, 1992.

Whittaker, A.S., Bertero, V.V., Thompson, C.L. and Alonso, L.J., "Seismic Testing of Steel Plate Energy Dissipation Devices", *Earthquake Spectra*, Vol. 7, No. 4, pp. 563-604, 1991.

**NATIONAL CENTER FOR EARTHQUAKE ENGINEERING RESEARCH  
LIST OF TECHNICAL REPORTS**

The National Center for Earthquake Engineering Research (NCEER) publishes technical reports on a variety of subjects related to earthquake engineering written by authors funded through NCEER. These reports are available from both NCEER Publications and the National Technical Information Service (NTIS). Requests for reports should be directed to NCEER Publications, National Center for Earthquake Engineering Research, State University of New York at Buffalo, Red Jacket Quadrangle, Buffalo, New York 14261. Reports can also be requested through NTIS, 5285 Port Royal Road, Springfield, Virginia 22161. NTIS accession numbers are shown in parenthesis, if available.

- NCEER-87-0001 "First-Year Program in Research, Education and Technology Transfer," 3/5/87, (PB88-134275, A04, MF-A01).
- NCEER-87-0002 "Experimental Evaluation of Instantaneous Optimal Algorithms for Structural Control," by R.C. Lin, T.T. Soong and A.M. Reinhorn, 4/20/87, (PB88-134341, A04, MF-A01).
- NCEER-87-0003 "Experimentation Using the Earthquake Simulation Facilities at University at Buffalo," by A.M. Reinhorn and R.L. Ketter, to be published.
- NCEER-87-0004 "The System Characteristics and Performance of a Shaking Table," by J.S. Hwang, K.C. Chang and G.C. Lee, 6/1/87, (PB88-134259, A03, MF-A01). This report is available only through NTIS (see address given above).
- NCEER-87-0005 "A Finite Element Formulation for Nonlinear Viscoplastic Material Using a Q Model," by O. Gyebi and G. Dasgupta, 11/2/87, (PB88-213764, A08, MF-A01).
- NCEER-87-0006 "Symbolic Manipulation Program (SMP) - Algebraic Codes for Two and Three Dimensional Finite Element Formulations," by X. Lee and G. Dasgupta, 11/9/87, (PB88-218522, A05, MF-A01).
- NCEER-87-0007 "Instantaneous Optimal Control Laws for Tall Buildings Under Seismic Excitations," by J.N. Yang, A. Akbarpour and P. Ghaemmaghami, 6/10/87, (PB88-134333, A06, MF-A01). This report is only available through NTIS (see address given above).
- NCEER-87-0008 "IDARC: Inelastic Damage Analysis of Reinforced Concrete Frame - Shear-Wall Structures," by Y.J. Park, A.M. Reinhorn and S.K. Kunnath, 7/20/87, (PB88-134325, A09, MF-A01). This report is only available through NTIS (see address given above).
- NCEER-87-0009 "Liquefaction Potential for New York State: A Preliminary Report on Sites in Manhattan and Buffalo," by M. Budhu, V. Vijayakumar, R.F. Giese and L. Baumgras, 8/31/87, (PB88-163704, A03, MF-A01). This report is available only through NTIS (see address given above).
- NCEER-87-0010 "Vertical and Torsional Vibration of Foundations in Inhomogeneous Media," by A.S. Veletsos and K.W. Dotson, 6/1/87, (PB88-134291, A03, MF-A01). This report is only available through NTIS (see address given above).
- NCEER-87-0011 "Seismic Probabilistic Risk Assessment and Seismic Margins Studies for Nuclear Power Plants," by Howard H.M. Hwang, 6/15/87, (PB88-134267, A03, MF-A01). This report is only available through NTIS (see address given above).
- NCEER-87-0012 "Parametric Studies of Frequency Response of Secondary Systems Under Ground-Acceleration Excitations," by Y. Yong and Y.K. Lin, 6/10/87, (PB88-134309, A03, MF-A01). This report is only available through NTIS (see address given above).
- NCEER-87-0013 "Frequency Response of Secondary Systems Under Seismic Excitation," by J.A. HoLung, J. Cai and Y.K. Lin, 7/31/87, (PB88-134317, A05, MF-A01). This report is only available through NTIS (see address given above).

- NCEER-87-0014 "Modelling Earthquake Ground Motions in Seismically Active Regions Using Parametric Time Series Methods," by G.W. Ellis and A.S. Cakmak, 8/25/87, (PB88-134283, A08, MF-A01). This report is only available through NTIS (see address given above).
- NCEER-87-0015 "Detection and Assessment of Seismic Structural Damage," by E. DiPasquale and A.S. Cakmak, 8/25/87, (PB88-163712, A05, MF-A01). This report is only available through NTIS (see address given above).
- NCEER-87-0016 "Pipeline Experiment at Parkfield, California," by J. Isenberg and E. Richardson, 9/15/87, (PB88-163720, A03, MF-A01). This report is available only through NTIS (see address given above).
- NCEER-87-0017 "Digital Simulation of Seismic Ground Motion," by M. Shinozuka, G. Deodatis and T. Harada, 8/31/87, (PB88-155197, A04, MF-A01). This report is available only through NTIS (see address given above).
- NCEER-87-0018 "Practical Considerations for Structural Control: System Uncertainty, System Time Delay and Truncation of Small Control Forces," J.N. Yang and A. Akbarpour, 8/10/87, (PB88-163738, A08, MF-A01). This report is only available through NTIS (see address given above).
- NCEER-87-0019 "Modal Analysis of Nonclassically Damped Structural Systems Using Canonical Transformation," by J.N. Yang, S. Sarkani and F.X. Long, 9/27/87, (PB88-187851, A04, MF-A01).
- NCEER-87-0020 "A Nonstationary Solution in Random Vibration Theory," by J.R. Red-Horse and P.D. Spanos, 11/3/87, (PB88-163746, A03, MF-A01).
- NCEER-87-0021 "Horizontal Impedances for Radially Inhomogeneous Viscoelastic Soil Layers," by A.S. Veletsos and K.W. Dotson, 10/15/87, (PB88-150859, A04, MF-A01).
- NCEER-87-0022 "Seismic Damage Assessment of Reinforced Concrete Members," by Y.S. Chung, C. Meyer and M. Shinozuka, 10/9/87, (PB88-150867, A05, MF-A01). This report is available only through NTIS (see address given above).
- NCEER-87-0023 "Active Structural Control in Civil Engineering," by T.T. Soong, 11/11/87, (PB88-187778, A03, MF-A01).
- NCEER-87-0024 "Vertical and Torsional Impedances for Radially Inhomogeneous Viscoelastic Soil Layers," by K.W. Dotson and A.S. Veletsos, 12/87, (PB88-187786, A03, MF-A01).
- NCEER-87-0025 "Proceedings from the Symposium on Seismic Hazards, Ground Motions, Soil-Liquefaction and Engineering Practice in Eastern North America," October 20-22, 1987, edited by K.H. Jacob, 12/87, (PB88-188115, A23, MF-A01).
- NCEER-87-0026 "Report on the Whittier-Narrows, California, Earthquake of October 1, 1987," by J. Pantelic and A. Reinhorn, 11/87, (PB88-187752, A03, MF-A01). This report is available only through NTIS (see address given above).
- NCEER-87-0027 "Design of a Modular Program for Transient Nonlinear Analysis of Large 3-D Building Structures," by S. Srivastav and J.F. Abel, 12/30/87, (PB88-187950, A05, MF-A01). This report is only available through NTIS (see address given above).
- NCEER-87-0028 "Second-Year Program in Research, Education and Technology Transfer," 3/8/88, (PB88-219480, A04, MF-A01).
- NCEER-88-0001 "Workshop on Seismic Computer Analysis and Design of Buildings With Interactive Graphics," by W. McGuire, J.F. Abel and C.H. Conley, 1/18/88, (PB88-187760, A03, MF-A01). This report is only available through NTIS (see address given above).

- NCEER-88-0002 "Optimal Control of Nonlinear Flexible Structures," by J.N. Yang, F.X. Long and D. Wong, 1/22/88, (PB88-213772, A06, MF-A01).
- NCEER-88-0003 "Substructuring Techniques in the Time Domain for Primary-Secondary Structural Systems," by G.D. Manolis and G. Juhn, 2/10/88, (PB88-213780, A04, MF-A01).
- NCEER-88-0004 "Iterative Seismic Analysis of Primary-Secondary Systems," by A. Singhal, L.D. Lutes and P.D. Spanos, 2/23/88, (PB88-213798, A04, MF-A01).
- NCEER-88-0005 "Stochastic Finite Element Expansion for Random Media," by P.D. Spanos and R. Ghanem, 3/14/88, (PB88-213806, A03, MF-A01).
- NCEER-88-0006 "Combining Structural Optimization and Structural Control," by F.Y. Cheng and C.P. Pantelides, 1/10/88, (PB88-213814, A05, MF-A01).
- NCEER-88-0007 "Seismic Performance Assessment of Code-Designed Structures," by H.H-M. Hwang, J-W. Jaw and H-J. Shau, 3/20/88, (PB88-219423, A04, MF-A01). This report is only available through NTIS (see address given above).
- NCEER-88-0008 "Reliability Analysis of Code-Designed Structures Under Natural Hazards," by H.H-M. Hwang, H. Ushiba and M. Shinozuka, 2/29/88, (PB88-229471, A07, MF-A01). This report is only available through NTIS (see address given above).
- NCEER-88-0009 "Seismic Fragility Analysis of Shear Wall Structures," by J-W Jaw and H.H-M. Hwang, 4/30/88, (PB89-102867, A04, MF-A01).
- NCEER-88-0010 "Base Isolation of a Multi-Story Building Under a Harmonic Ground Motion - A Comparison of Performances of Various Systems," by F-G Fan, G. Ahmadi and I.G. Tadjbakhsh, 5/18/88, (PB89-122238, A06, MF-A01). This report is only available through NTIS (see address given above).
- NCEER-88-0011 "Seismic Floor Response Spectra for a Combined System by Green's Functions," by F.M. Lavelle, L.A. Bergman and P.D. Spanos, 5/1/88, (PB89-102875, A03, MF-A01).
- NCEER-88-0012 "A New Solution Technique for Randomly Excited Hysteretic Structures," by G.Q. Cai and Y.K. Lin, 5/16/88, (PB89-102883, A03, MF-A01).
- NCEER-88-0013 "A Study of Radiation Damping and Soil-Structure Interaction Effects in the Centrifuge," by K. Weissman, supervised by J.H. Prevost, 5/24/88, (PB89-144703, A06, MF-A01).
- NCEER-88-0014 "Parameter Identification and Implementation of a Kinematic Plasticity Model for Frictional Soils," by J.H. Prevost and D.V. Griffiths, to be published.
- NCEER-88-0015 "Two- and Three- Dimensional Dynamic Finite Element Analyses of the Long Valley Dam," by D.V. Griffiths and J.H. Prevost, 6/17/88, (PB89-144711, A04, MF-A01).
- NCEER-88-0016 "Damage Assessment of Reinforced Concrete Structures in Eastern United States," by A.M. Reinhorn, M.J. Seidel, S.K. Kunnath and Y.J. Park, 6/15/88, (PB89-122220, A04, MF-A01). This report is only available through NTIS (see address given above).
- NCEER-88-0017 "Dynamic Compliance of Vertically Loaded Strip Foundations in Multilayered Viscoelastic Soils," by S. Ahmad and A.S.M. Israil, 6/17/88, (PB89-102891, A04, MF-A01).
- NCEER-88-0018 "An Experimental Study of Seismic Structural Response With Added Viscoelastic Dampers," by R.C. Lin, Z. Liang, T.T. Soong and R.H. Zhang, 6/30/88, (PB89-122212, A05, MF-A01). This report is available only through NTIS (see address given above).

- NCEER-88-0019 "Experimental Investigation of Primary - Secondary System Interaction," by G.D. Manolis, G. Juhn and A.M. Reinhorn, 5/27/88, (PB89-122204, A04, MF-A01).
- NCEER-88-0020 "A Response Spectrum Approach For Analysis of Nonclassically Damped Structures," by J.N. Yang, S. Sarkani and F.X. Long, 4/22/88, (PB89-102909, A04, MF-A01).
- NCEER-88-0021 "Seismic Interaction of Structures and Soils: Stochastic Approach," by A.S. Veletsos and A.M. Prasad, 7/21/88, (PB89-122196, A04, MF-A01). This report is only available through NTIS (see address given above).
- NCEER-88-0022 "Identification of the Serviceability Limit State and Detection of Seismic Structural Damage," by E. DiPasquale and A.S. Cakmak, 6/15/88, (PB89-122188, A05, MF-A01). This report is available only through NTIS (see address given above).
- NCEER-88-0023 "Multi-Hazard Risk Analysis: Case of a Simple Offshore Structure," by B.K. Bhartia and E.H. Vanmarcke, 7/21/88, (PB89-145213, A05, MF-A01).
- NCEER-88-0024 "Automated Seismic Design of Reinforced Concrete Buildings," by Y.S. Chung, C. Meyer and M. Shinozuka, 7/5/88, (PB89-122170, A06, MF-A01). This report is available only through NTIS (see address given above).
- NCEER-88-0025 "Experimental Study of Active Control of MDOF Structures Under Seismic Excitations," by L.L. Chung, R.C. Lin, T.T. Soong and A.M. Reinhorn, 7/10/88, (PB89-122600, A04, MF-A01).
- NCEER-88-0026 "Earthquake Simulation Tests of a Low-Rise Metal Structure," by J.S. Hwang, K.C. Chang, G.C. Lee and R.L. Ketter, 8/1/88, (PB89-102917, A04, MF-A01).
- NCEER-88-0027 "Systems Study of Urban Response and Reconstruction Due to Catastrophic Earthquakes," by F. Kozin and H.K. Zhou, 9/22/88, (PB90-162348, A04, MF-A01).
- NCEER-88-0028 "Seismic Fragility Analysis of Plane Frame Structures," by H.H-M. Hwang and Y.K. Low, 7/31/88, (PB89-131445, A06, MF-A01).
- NCEER-88-0029 "Response Analysis of Stochastic Structures," by A. Kardara, C. Bucher and M. Shinozuka, 9/22/88, (PB89-174429, A04, MF-A01).
- NCEER-88-0030 "Nonnormal Accelerations Due to Yielding in a Primary Structure," by D.C.K. Chen and L.D. Lutes, 9/19/88, (PB89-131437, A04, MF-A01).
- NCEER-88-0031 "Design Approaches for Soil-Structure Interaction," by A.S. Veletsos, A.M. Prasad and Y. Tang, 12/30/88, (PB89-174437, A03, MF-A01). This report is available only through NTIS (see address given above).
- NCEER-88-0032 "A Re-evaluation of Design Spectra for Seismic Damage Control," by C.J. Turkstra and A.G. Tallin, 11/7/88, (PB89-145221, A05, MF-A01).
- NCEER-88-0033 "The Behavior and Design of Noncontact Lap Splices Subjected to Repeated Inelastic Tensile Loading," by V.E. Sagan, P. Gergely and R.N. White, 12/8/88, (PB89-163737, A08, MF-A01).
- NCEER-88-0034 "Seismic Response of Pile Foundations," by S.M. Mamoon, P.K. Banerjee and S. Ahmad, 11/1/88, (PB89-145239, A04, MF-A01).
- NCEER-88-0035 "Modeling of R/C Building Structures With Flexible Floor Diaphragms (IDARC2)," by A.M. Reinhorn, S.K. Kunnath and N. Panahshahi, 9/7/88, (PB89-207153, A07, MF-A01).

- NCEER-88-0036 "Solution of the Dam-Reservoir Interaction Problem Using a Combination of FEM, BEM with Particular Integrals, Modal Analysis, and Substructuring," by C-S. Tsai, G.C. Lee and R.L. Ketter, 12/31/88, (PB89-207146, A04, MF-A01).
- NCEER-88-0037 "Optimal Placement of Actuators for Structural Control," by F.Y. Cheng and C.P. Pantelides, 8/15/88, (PB89-162846, A05, MF-A01).
- NCEER-88-0038 "Teflon Bearings in Aseismic Base Isolation: Experimental Studies and Mathematical Modeling," by A. Mokha, M.C. Constantinou and A.M. Reinhorn, 12/5/88, (PB89-218457, A10, MF-A01). This report is available only through NTIS (see address given above).
- NCEER-88-0039 "Seismic Behavior of Flat Slab High-Rise Buildings in the New York City Area," by P. Weidlinger and M. Ettouney, 10/15/88, (PB90-145681, A04, MF-A01).
- NCEER-88-0040 "Evaluation of the Earthquake Resistance of Existing Buildings in New York City," by P. Weidlinger and M. Ettouney, 10/15/88, to be published.
- NCEER-88-0041 "Small-Scale Modeling Techniques for Reinforced Concrete Structures Subjected to Seismic Loads," by W. Kim, A. El-Attar and R.N. White, 11/22/88, (PB89-189625, A05, MF-A01).
- NCEER-88-0042 "Modeling Strong Ground Motion from Multiple Event Earthquakes," by G.W. Ellis and A.S. Cakmak, 10/15/88, (PB89-174445, A03, MF-A01).
- NCEER-88-0043 "Nonstationary Models of Seismic Ground Acceleration," by M. Grigoriu, S.E. Ruiz and E. Rosenblueth, 7/15/88, (PB89-189617, A04, MF-A01).
- NCEER-88-0044 "SARCF User's Guide: Seismic Analysis of Reinforced Concrete Frames," by Y.S. Chung, C. Meyer and M. Shinozuka, 11/9/88, (PB89-174452, A08, MF-A01).
- NCEER-88-0045 "First Expert Panel Meeting on Disaster Research and Planning," edited by J. Pantelic and J. Stoye, 9/15/88, (PB89-174460, A05, MF-A01). This report is only available through NTIS (see address given above).
- NCEER-88-0046 "Preliminary Studies of the Effect of Degrading Infill Walls on the Nonlinear Seismic Response of Steel Frames," by C.Z. Chrysostomou, P. Gergely and J.F. Abel, 12/19/88, (PB89-208383, A05, MF-A01).
- NCEER-88-0047 "Reinforced Concrete Frame Component Testing Facility - Design, Construction, Instrumentation and Operation," by S.P. Pessiki, C. Conley, T. Bond, P. Gergely and R.N. White, 12/16/88, (PB89-174478, A04, MF-A01).
- NCEER-89-0001 "Effects of Protective Cushion and Soil Compliancy on the Response of Equipment Within a Seismically Excited Building," by J.A. HoLung, 2/16/89, (PB89-207179, A04, MF-A01).
- NCEER-89-0002 "Statistical Evaluation of Response Modification Factors for Reinforced Concrete Structures," by H.H-M. Hwang and J-W. Jaw, 2/17/89, (PB89-207187, A05, MF-A01).
- NCEER-89-0003 "Hysteretic Columns Under Random Excitation," by G-Q. Cai and Y.K. Lin, 1/9/89, (PB89-196513, A03, MF-A01).
- NCEER-89-0004 "Experimental Study of 'Elephant Foot Bulge' Instability of Thin-Walled Metal Tanks," by Z-H. Jia and R.L. Ketter, 2/22/89, (PB89-207195, A03, MF-A01).
- NCEER-89-0005 "Experiment on Performance of Buried Pipelines Across San Andreas Fault," by J. Isenberg, E. Richardson and T.D. O'Rourke, 3/10/89, (PB89-218440, A04, MF-A01). This report is available only through NTIS (see address given above).

- NCEER-89-0006 "A Knowledge-Based Approach to Structural Design of Earthquake-Resistant Buildings," by M. Subramani, P. Gergely, C.H. Conley, J.F. Abel and A.H. Zaghaw, 1/15/89, (PB89-218465, A06, MF-A01).
- NCEER-89-0007 "Liquefaction Hazards and Their Effects on Buried Pipelines," by T.D. O'Rourke and P.A. Lane, 2/1/89, (PB89-218481, A09, MF-A01).
- NCEER-89-0008 "Fundamentals of System Identification in Structural Dynamics," by H. Imai, C-B. Yun, O. Maruyama and M. Shinozuka, 1/26/89, (PB89-207211, A04, MF-A01).
- NCEER-89-0009 "Effects of the 1985 Michoacan Earthquake on Water Systems and Other Buried Lifelines in Mexico," by A.G. Ayala and M.J. O'Rourke, 3/8/89, (PB89-207229, A06, MF-A01).
- NCEER-89-R010 "NCEER Bibliography of Earthquake Education Materials," by K.E.K. Ross, Second Revision, 9/1/89, (PB90-125352, A05, MF-A01). This report is replaced by NCEER-92-0018.
- NCEER-89-0011 "Inelastic Three-Dimensional Response Analysis of Reinforced Concrete Building Structures (IDARC-3D), Part I - Modeling," by S.K. Kunnath and A.M. Reinhorn, 4/17/89, (PB90-114612, A07, MF-A01).
- NCEER-89-0012 "Recommended Modifications to ATC-14," by C.D. Poland and J.O. Malley, 4/12/89, (PB90-108648, A15, MF-A01).
- NCEER-89-0013 "Repair and Strengthening of Beam-to-Column Connections Subjected to Earthquake Loading," by M. Corazao and A.J. Durrani, 2/28/89, (PB90-109885, A06, MF-A01).
- NCEER-89-0014 "Program EXKAL2 for Identification of Structural Dynamic Systems," by O. Maruyama, C-B. Yun, M. Hoshiya and M. Shinozuka, 5/19/89, (PB90-109877, A09, MF-A01).
- NCEER-89-0015 "Response of Frames With Bolted Semi-Rigid Connections, Part I - Experimental Study and Analytical Predictions," by P.J. DiCorso, A.M. Reinhorn, J.R. Dickerson, J.B. Radzinski and W.L. Harper, 6/1/89, to be published.
- NCEER-89-0016 "ARMA Monte Carlo Simulation in Probabilistic Structural Analysis," by P.D. Spanos and M.P. Mignolet, 7/10/89, (PB90-109893, A03, MF-A01).
- NCEER-89-P017 "Preliminary Proceedings from the Conference on Disaster Preparedness - The Place of Earthquake Education in Our Schools," Edited by K.E.K. Ross, 6/23/89, (PB90-108606, A03, MF-A01).
- NCEER-89-0017 "Proceedings from the Conference on Disaster Preparedness - The Place of Earthquake Education in Our Schools," Edited by K.E.K. Ross, 12/31/89, (PB90-207895, A012, MF-A02). This report is available only through NTIS (see address given above).
- NCEER-89-0018 "Multidimensional Models of Hysteretic Material Behavior for Vibration Analysis of Shape Memory Energy Absorbing Devices, by E.J. Graesser and F.A. Cozzarelli, 6/7/89, (PB90-164146, A04, MF-A01).
- NCEER-89-0019 "Nonlinear Dynamic Analysis of Three-Dimensional Base Isolated Structures (3D-BASIS)," by S. Nagarajah, A.M. Reinhorn and M.C. Constantinou, 8/3/89, (PB90-161936, A06, MF-A01). This report has been replaced by NCEER-93-0011.
- NCEER-89-0020 "Structural Control Considering Time-Rate of Control Forces and Control Rate Constraints," by F.Y. Cheng and C.P. Pantelides, 8/3/89, (PB90-120445, A04, MF-A01).
- NCEER-89-0021 "Subsurface Conditions of Memphis and Shelby County," by K.W. Ng, T-S. Chang and H-H.M. Hwang, 7/26/89, (PB90-120437, A03, MF-A01).
- NCEER-89-0022 "Seismic Wave Propagation Effects on Straight Jointed Buried Pipelines," by K. Elhmadi and M.J. O'Rourke, 8/24/89, (PB90-162322, A10, MF-A02).

- NCEER-89-0023 "Workshop on Serviceability Analysis of Water Delivery Systems," edited by M. Grigoriu, 3/6/89, (PB90-127424, A03, MF-A01).
- NCEER-89-0024 "Shaking Table Study of a 1/5 Scale Steel Frame Composed of Tapered Members," by K.C. Chang, J.S. Hwang and G.C. Lee, 9/18/89, (PB90-160169, A04, MF-A01).
- NCEER-89-0025 "DYNA1D: A Computer Program for Nonlinear Seismic Site Response Analysis - Technical Documentation," by Jean H. Prevost, 9/14/89, (PB90-161944, A07, MF-A01). This report is available only through NTIS (see address given above).
- NCEER-89-0026 "1:4 Scale Model Studies of Active Tendon Systems and Active Mass Dampers for Aseismic Protection," by A.M. Reinhorn, T.T. Soong, R.C. Lin, Y.P. Yang, Y. Fukao, H. Abe and M. Nakai, 9/15/89, (PB90-173246, A10, MF-A02).
- NCEER-89-0027 "Scattering of Waves by Inclusions in a Nonhomogeneous Elastic Half Space Solved by Boundary Element Methods," by P.K. Hadley, A. Askar and A.S. Cakmak, 6/15/89, (PB90-145699, A07, MF-A01).
- NCEER-89-0028 "Statistical Evaluation of Deflection Amplification Factors for Reinforced Concrete Structures," by H.H.M. Hwang, J-W. Jaw and A.L. Ch'ng, 8/31/89, (PB90-164633, A05, MF-A01).
- NCEER-89-0029 "Bedrock Accelerations in Memphis Area Due to Large New Madrid Earthquakes," by H.H.M. Hwang, C.H.S. Chen and G. Yu, 11/7/89, (PB90-162330, A04, MF-A01).
- NCEER-89-0030 "Seismic Behavior and Response Sensitivity of Secondary Structural Systems," by Y.Q. Chen and T.T. Soong, 10/23/89, (PB90-164658, A08, MF-A01).
- NCEER-89-0031 "Random Vibration and Reliability Analysis of Primary-Secondary Structural Systems," by Y. Ibrahim, M. Grigoriu and T.T. Soong, 11/10/89, (PB90-161951, A04, MF-A01).
- NCEER-89-0032 "Proceedings from the Second U.S. - Japan Workshop on Liquefaction, Large Ground Deformation and Their Effects on Lifelines, September 26-29, 1989," Edited by T.D. O'Rourke and M. Hamada, 12/1/89, (PB90-209388, A22, MF-A03).
- NCEER-89-0033 "Deterministic Model for Seismic Damage Evaluation of Reinforced Concrete Structures," by J.M. Bracci, A.M. Reinhorn, J.B. Mander and S.K. Kunnath, 9/27/89, (PB91-108803, A06, MF-A01).
- NCEER-89-0034 "On the Relation Between Local and Global Damage Indices," by E. DiPasquale and A.S. Cakmak, 8/15/89, (PB90-173865, A05, MF-A01).
- NCEER-89-0035 "Cyclic Undrained Behavior of Nonplastic and Low Plasticity Silts," by A.J. Walker and H.E. Stewart, 7/26/89, (PB90-183518, A10, MF-A01).
- NCEER-89-0036 "Liquefaction Potential of Surficial Deposits in the City of Buffalo, New York," by M. Budhu, R. Giese and L. Baumgrass, 1/17/89, (PB90-208455, A04, MF-A01).
- NCEER-89-0037 "A Deterministic Assessment of Effects of Ground Motion Incoherence," by A.S. Veletsos and Y. Tang, 7/15/89, (PB90-164294, A03, MF-A01).
- NCEER-89-0038 "Workshop on Ground Motion Parameters for Seismic Hazard Mapping," July 17-18, 1989, edited by R.V. Whitman, 12/1/89, (PB90-173923, A04, MF-A01).
- NCEER-89-0039 "Seismic Effects on Elevated Transit Lines of the New York City Transit Authority," by C.J. Costantino, C.A. Miller and E. Heymsfield, 12/26/89, (PB90-207887, A06, MF-A01).
- NCEER-89-0040 "Centrifugal Modeling of Dynamic Soil-Structure Interaction," by K. Weissman, Supervised by J.H. Prevost, 5/10/89, (PB90-207879, A07, MF-A01).

- NCEER-89-0041 "Linearized Identification of Buildings With Cores for Seismic Vulnerability Assessment," by I-K. Ho and A.E. Aktan, 11/1/89, (PB90-251943, A07, MF-A01).
- NCEER-90-0001 "Geotechnical and Lifeline Aspects of the October 17, 1989 Loma Prieta Earthquake in San Francisco," by T.D. O'Rourke, H.E. Stewart, F.T. Blackburn and T.S. Dickerman, 1/90, (PB90-208596, A05, MF-A01).
- NCEER-90-0002 "Nonnormal Secondary Response Due to Yielding in a Primary Structure," by D.C.K. Chen and L.D. Lutes, 2/28/90, (PB90-251976, A07, MF-A01).
- NCEER-90-0003 "Earthquake Education Materials for Grades K-12," by K.E.K. Ross, 4/16/90, (PB91-251984, A05, MF-A05). This report has been replaced by NCEER-92-0018.
- NCEER-90-0004 "Catalog of Strong Motion Stations in Eastern North America," by R.W. Busby, 4/3/90, (PB90-251984, A05, MF-A01).
- NCEER-90-0005 "NCEER Strong-Motion Data Base: A User Manual for the GeoBase Release (Version 1.0 for the Sun3)," by P. Friberg and K. Jacob, 3/31/90 (PB90-258062, A04, MF-A01).
- NCEER-90-0006 "Seismic Hazard Along a Crude Oil Pipeline in the Event of an 1811-1812 Type New Madrid Earthquake," by H.H.M. Hwang and C-H.S. Chen, 4/16/90, (PB90-258054, A04, MF-A01).
- NCEER-90-0007 "Site-Specific Response Spectra for Memphis Sheahan Pumping Station," by H.H.M. Hwang and C.S. Lee, 5/15/90, (PB91-108811, A05, MF-A01).
- NCEER-90-0008 "Pilot Study on Seismic Vulnerability of Crude Oil Transmission Systems," by T. Ariman, R. Dobry, M. Grigoriu, F. Kozin, M. O'Rourke, T. O'Rourke and M. Shinozuka, 5/25/90, (PB91-108837, A06, MF-A01).
- NCEER-90-0009 "A Program to Generate Site Dependent Time Histories: EQGEN," by G.W. Ellis, M. Srinivasan and A.S. Cakmak, 1/30/90, (PB91-108829, A04, MF-A01).
- NCEER-90-0010 "Active Isolation for Seismic Protection of Operating Rooms," by M.E. Talbott, Supervised by M. Shinozuka, 6/8/9, (PB91-110205, A05, MF-A01).
- NCEER-90-0011 "Program LINEARID for Identification of Linear Structural Dynamic Systems," by C-B. Yun and M. Shinozuka, 6/25/90, (PB91-110312, A08, MF-A01).
- NCEER-90-0012 "Two-Dimensional Two-Phase Elasto-Plastic Seismic Response of Earth Dams," by A.N. Yiagos, Supervised by J.H. Prevost, 6/20/90, (PB91-110197, A13, MF-A02).
- NCEER-90-0013 "Secondary Systems in Base-Isolated Structures: Experimental Investigation, Stochastic Response and Stochastic Sensitivity," by G.D. Manolis, G. Juhn, M.C. Constantinou and A.M. Reinhorn, 7/1/90, (PB91-110320, A08, MF-A01).
- NCEER-90-0014 "Seismic Behavior of Lightly-Reinforced Concrete Column and Beam-Column Joint Details," by S.P. Pessiki, C.H. Conley, P. Gergely and R.N. White, 8/22/90, (PB91-108795, A11, MF-A02).
- NCEER-90-0015 "Two Hybrid Control Systems for Building Structures Under Strong Earthquakes," by J.N. Yang and A. Danielians, 6/29/90, (PB91-125393, A04, MF-A01).
- NCEER-90-0016 "Instantaneous Optimal Control with Acceleration and Velocity Feedback," by J.N. Yang and Z. Li, 6/29/90, (PB91-125401, A03, MF-A01).
- NCEER-90-0017 "Reconnaissance Report on the Northern Iran Earthquake of June 21, 1990," by M. Mehrain, 10/4/90, (PB91-125377, A03, MF-A01).

- NCEER-90-0018 "Evaluation of Liquefaction Potential in Memphis and Shelby County," by T.S. Chang, P.S. Tang, C.S. Lee and H. Hwang, 8/10/90, (PB91-125427, A09, MF-A01).
- NCEER-90-0019 "Experimental and Analytical Study of a Combined Sliding Disc Bearing and Helical Steel Spring Isolation System," by M.C. Constantinou, A.S. Mokha and A.M. Reinhorn, 10/4/90, (PB91-125385, A06, MF-A01). This report is available only through NTIS (see address given above).
- NCEER-90-0020 "Experimental Study and Analytical Prediction of Earthquake Response of a Sliding Isolation System with a Spherical Surface," by A.S. Mokha, M.C. Constantinou and A.M. Reinhorn, 10/11/90, (PB91-125419, A05, MF-A01).
- NCEER-90-0021 "Dynamic Interaction Factors for Floating Pile Groups," by G. Gazetas, K. Fan, A. Kaynia and E. Kausel, 9/10/90, (PB91-170381, A05, MF-A01).
- NCEER-90-0022 "Evaluation of Seismic Damage Indices for Reinforced Concrete Structures," by S. Rodriguez-Gomez and A.S. Cakmak, 9/30/90, PB91-171322, A06, MF-A01).
- NCEER-90-0023 "Study of Site Response at a Selected Memphis Site," by H. Desai, S. Ahmad, E.S. Gazetas and M.R. Oh, 10/11/90, (PB91-196857, A03, MF-A01).
- NCEER-90-0024 "A User's Guide to Strongmo: Version 1.0 of NCEER's Strong-Motion Data Access Tool for PCs and Terminals," by P.A. Friberg and C.A.T. Susch, 11/15/90, (PB91-171272, A03, MF-A01).
- NCEER-90-0025 "A Three-Dimensional Analytical Study of Spatial Variability of Seismic Ground Motions," by L-L. Hong and A.H.-S. Ang, 10/30/90, (PB91-170399, A09, MF-A01).
- NCEER-90-0026 "MUMOID User's Guide - A Program for the Identification of Modal Parameters," by S. Rodriguez-Gomez and E. DiPasquale, 9/30/90, (PB91-171298, A04, MF-A01).
- NCEER-90-0027 "SARCF-II User's Guide - Seismic Analysis of Reinforced Concrete Frames," by S. Rodriguez-Gomez, Y.S. Chung and C. Meyer, 9/30/90, (PB91-171280, A05, MF-A01).
- NCEER-90-0028 "Viscous Dampers: Testing, Modeling and Application in Vibration and Seismic Isolation," by N. Makris and M.C. Constantinou, 12/20/90 (PB91-190561, A06, MF-A01).
- NCEER-90-0029 "Soil Effects on Earthquake Ground Motions in the Memphis Area," by H. Hwang, C.S. Lee, K.W. Ng and T.S. Chang, 8/2/90, (PB91-190751, A05, MF-A01).
- NCEER-91-0001 "Proceedings from the Third Japan-U.S. Workshop on Earthquake Resistant Design of Lifeline Facilities and Countermeasures for Soil Liquefaction, December 17-19, 1990," edited by T.D. O'Rourke and M. Hamada, 2/1/91, (PB91-179259, A99, MF-A04).
- NCEER-91-0002 "Physical Space Solutions of Non-Proportionally Damped Systems," by M. Tong, Z. Liang and G.C. Lee, 1/15/91, (PB91-179242, A04, MF-A01).
- NCEER-91-0003 "Seismic Response of Single Piles and Pile Groups," by K. Fan and G. Gazetas, 1/10/91, (PB92-174994, A04, MF-A01).
- NCEER-91-0004 "Damping of Structures: Part 1 - Theory of Complex Damping," by Z. Liang and G. Lee, 10/10/91, (PB92-197235, A12, MF-A03).
- NCEER-91-0005 "3D-BASIS - Nonlinear Dynamic Analysis of Three Dimensional Base Isolated Structures: Part II," by S. Nagarajaiah, A.M. Reinhorn and M.C. Constantinou, 2/28/91, (PB91-190553, A07, MF-A01). This report has been replaced by NCEER-93-0011.

- NCEER-91-0006 "A Multidimensional Hysteretic Model for Plasticity Deforming Metals in Energy Absorbing Devices," by E.J. Graesser and F.A. Cozzarelli, 4/9/91, (PB92-108364, A04, MF-A01).
- NCEER-91-0007 "A Framework for Customizable Knowledge-Based Expert Systems with an Application to a KBES for Evaluating the Seismic Resistance of Existing Buildings," by E.G. Ibarra-Anaya and S.J. Fenves, 4/9/91, (PB91-210930, A08, MF-A01).
- NCEER-91-0008 "Nonlinear Analysis of Steel Frames with Semi-Rigid Connections Using the Capacity Spectrum Method," by G.G. Deierlein, S-H. Hsieh, Y-J. Shen and J.F. Abel, 7/2/91, (PB92-113828, A05, MF-A01).
- NCEER-91-0009 "Earthquake Education Materials for Grades K-12," by K.E.K. Ross, 4/30/91, (PB91-212142, A06, MF-A01). This report has been replaced by NCEER-92-0018.
- NCEER-91-0010 "Phase Wave Velocities and Displacement Phase Differences in a Harmonically Oscillating Pile," by N. Makris and G. Gazetas, 7/8/91, (PB92-108356, A04, MF-A01).
- NCEER-91-0011 "Dynamic Characteristics of a Full-Size Five-Story Steel Structure and a 2/5 Scale Model," by K.C. Chang, G.C. Yao, G.C. Lee, D.S. Hao and Y.C. Yeh, 7/2/91, (PB93-116648, A06, MF-A02).
- NCEER-91-0012 "Seismic Response of a 2/5 Scale Steel Structure with Added Viscoelastic Dampers," by K.C. Chang, T.T. Soong, S-T. Oh and M.L. Lai, 5/17/91, (PB92-110816, A05, MF-A01).
- NCEER-91-0013 "Earthquake Response of Retaining Walls; Full-Scale Testing and Computational Modeling," by S. Alampalli and A-W.M. Elgamal, 6/20/91, to be published.
- NCEER-91-0014 "3D-BASIS-M: Nonlinear Dynamic Analysis of Multiple Building Base Isolated Structures," by P.C. Tsopelas, S. Nagarajaiah, M.C. Constantinou and A.M. Reinhorn, 5/28/91, (PB92-113885, A09, MF-A02).
- NCEER-91-0015 "Evaluation of SEAOC Design Requirements for Sliding Isolated Structures," by D. Theodossiou and M.C. Constantinou, 6/10/91, (PB92-114602, A11, MF-A03).
- NCEER-91-0016 "Closed-Loop Modal Testing of a 27-Story Reinforced Concrete Flat Plate-Core Building," by H.R. Somaprasad, T. Toksoy, H. Yoshiyuki and A.E. Aktan, 7/15/91, (PB92-129980, A07, MF-A02).
- NCEER-91-0017 "Shake Table Test of a 1/6 Scale Two-Story Lightly Reinforced Concrete Building," by A.G. El-Attar, R.N. White and P. Gergely, 2/28/91, (PB92-222447, A06, MF-A02).
- NCEER-91-0018 "Shake Table Test of a 1/8 Scale Three-Story Lightly Reinforced Concrete Building," by A.G. El-Attar, R.N. White and P. Gergely, 2/28/91, (PB93-116630, A08, MF-A02).
- NCEER-91-0019 "Transfer Functions for Rigid Rectangular Foundations," by A.S. Veletsos, A.M. Prasad and W.H. Wu, 7/31/91, to be published.
- NCEER-91-0020 "Hybrid Control of Seismic-Excited Nonlinear and Inelastic Structural Systems," by J.N. Yang, Z. Li and A. Danielians, 8/1/91, (PB92-143171, A06, MF-A02).
- NCEER-91-0021 "The NCEER-91 Earthquake Catalog: Improved Intensity-Based Magnitudes and Recurrence Relations for U.S. Earthquakes East of New Madrid," by L. Seeber and J.G. Armbruster, 8/28/91, (PB92-176742, A06, MF-A02).
- NCEER-91-0022 "Proceedings from the Implementation of Earthquake Planning and Education in Schools: The Need for Change - The Roles of the Changemakers," by K.E.K. Ross and F. Winslow, 7/23/91, (PB92-129998, A12, MF-A03).
- NCEER-91-0023 "A Study of Reliability-Based Criteria for Seismic Design of Reinforced Concrete Frame Buildings," by H.H.M. Hwang and H-M. Hsu, 8/10/91, (PB92-140235, A09, MF-A02).

- NCEER-91-0024 "Experimental Verification of a Number of Structural System Identification Algorithms," by R.G. Ghanem, H. Gavin and M. Shinozuka, 9/18/91, (PB92-176577, A18, MF-A04).
- NCEER-91-0025 "Probabilistic Evaluation of Liquefaction Potential," by H.H.M. Hwang and C.S. Lee," 11/25/91, (PB92-143429, A05, MF-A01).
- NCEER-91-0026 "Instantaneous Optimal Control for Linear, Nonlinear and Hysteretic Structures - Stable Controllers," by J.N. Yang and Z. Li, 11/15/91, (PB92-163807, A04, MF-A01).
- NCEER-91-0027 "Experimental and Theoretical Study of a Sliding Isolation System for Bridges," by M.C. Constantinou, A. Kartoum, A.M. Reinhorn and P. Bradford, 11/15/91, (PB92-176973, A10, MF-A03).
- NCEER-92-0001 "Case Studies of Liquefaction and Lifeline Performance During Past Earthquakes, Volume 1: Japanese Case Studies," Edited by M. Hamada and T. O'Rourke, 2/17/92, (PB92-197243, A18, MF-A04).
- NCEER-92-0002 "Case Studies of Liquefaction and Lifeline Performance During Past Earthquakes, Volume 2: United States Case Studies," Edited by T. O'Rourke and M. Hamada, 2/17/92, (PB92-197250, A20, MF-A04).
- NCEER-92-0003 "Issues in Earthquake Education," Edited by K. Ross, 2/3/92, (PB92-222389, A07, MF-A02).
- NCEER-92-0004 "Proceedings from the First U.S. - Japan Workshop on Earthquake Protective Systems for Bridges," Edited by I.G. Buckle, 2/4/92, (PB94-142239, A99, MF-A06).
- NCEER-92-0005 "Seismic Ground Motion from a Haskell-Type Source in a Multiple-Layered Half-Space," A.P. Theoharis, G. Deodatis and M. Shinozuka, 1/2/92, to be published.
- NCEER-92-0006 "Proceedings from the Site Effects Workshop," Edited by R. Whitman, 2/29/92, (PB92-197201, A04, MF-A01).
- NCEER-92-0007 "Engineering Evaluation of Permanent Ground Deformations Due to Seismically-Induced Liquefaction," by M.H. Baziar, R. Dobry and A-W.M. Elgamal, 3/24/92, (PB92-222421, A13, MF-A03).
- NCEER-92-0008 "A Procedure for the Seismic Evaluation of Buildings in the Central and Eastern United States," by C.D. Poland and J.O. Malley, 4/2/92, (PB92-222439, A20, MF-A04).
- NCEER-92-0009 "Experimental and Analytical Study of a Hybrid Isolation System Using Friction Controllable Sliding Bearings," by M.Q. Feng, S. Fujii and M. Shinozuka, 5/15/92, (PB93-150282, A06, MF-A02).
- NCEER-92-0010 "Seismic Resistance of Slab-Column Connections in Existing Non-Ductile Flat-Plate Buildings," by A.J. Durrani and Y. Du, 5/18/92, (PB93-116812, A06, MF-A02).
- NCEER-92-0011 "The Hysteretic and Dynamic Behavior of Brick Masonry Walls Upgraded by Ferrocement Coatings Under Cyclic Loading and Strong Simulated Ground Motion," by H. Lee and S.P. Prawel, 5/11/92, to be published.
- NCEER-92-0012 "Study of Wire Rope Systems for Seismic Protection of Equipment in Buildings," by G.F. Demetriades, M.C. Constantinou and A.M. Reinhorn, 5/20/92, (PB93-116655, A08, MF-A02).
- NCEER-92-0013 "Shape Memory Structural Dampers: Material Properties, Design and Seismic Testing," by P.R. Witting and F.A. Cozzarelli, 5/26/92, (PB93-116663, A05, MF-A01).
- NCEER-92-0014 "Longitudinal Permanent Ground Deformation Effects on Buried Continuous Pipelines," by M.J. O'Rourke, and C. Nordberg, 6/15/92, (PB93-116671, A08, MF-A02).
- NCEER-92-0015 "A Simulation Method for Stationary Gaussian Random Functions Based on the Sampling Theorem," by M. Grigoriu and S. Balopoulou, 6/11/92, (PB93-127496, A05, MF-A01).

- NCEER-92-0016 "Gravity-Load-Designed Reinforced Concrete Buildings: Seismic Evaluation of Existing Construction and Detailing Strategies for Improved Seismic Resistance," by G.W. Hoffmann, S.K. Kunnath, A.M. Reinhorn and J.B. Mander, 7/15/92, (PB94-142007, A08, MF-A02).
- NCEER-92-0017 "Observations on Water System and Pipeline Performance in the Limón Area of Costa Rica Due to the April 22, 1991 Earthquake," by M. O'Rourke and D. Ballantyne, 6/30/92, (PB93-126811, A06, MF-A02).
- NCEER-92-0018 "Fourth Edition of Earthquake Education Materials for Grades K-12," Edited by K.E.K. Ross, 8/10/92, (PB93-114023, A07, MF-A02).
- NCEER-92-0019 "Proceedings from the Fourth Japan-U.S. Workshop on Earthquake Resistant Design of Lifeline Facilities and Countermeasures for Soil Liquefaction," Edited by M. Hamada and T.D. O'Rourke, 8/12/92, (PB93-163939, A99, MF-E11).
- NCEER-92-0020 "Active Bracing System: A Full Scale Implementation of Active Control," by A.M. Reinhorn, T.T. Soong, R.C. Lin, M.A. Riley, Y.P. Wang, S. Aizawa and M. Higashino, 8/14/92, (PB93-127512, A06, MF-A02).
- NCEER-92-0021 "Empirical Analysis of Horizontal Ground Displacement Generated by Liquefaction-Induced Lateral Spreads," by S.F. Bartlett and T.L. Youd, 8/17/92, (PB93-188241, A06, MF-A02).
- NCEER-92-0022 "IDARC Version 3.0: Inelastic Damage Analysis of Reinforced Concrete Structures," by S.K. Kunnath, A.M. Reinhorn and R.F. Lobo, 8/31/92, (PB93-227502, A07, MF-A02).
- NCEER-92-0023 "A Semi-Empirical Analysis of Strong-Motion Peaks in Terms of Seismic Source, Propagation Path and Local Site Conditions, by M. Kamiyama, M.J. O'Rourke and R. Flores-Berrones, 9/9/92, (PB93-150266, A08, MF-A02).
- NCEER-92-0024 "Seismic Behavior of Reinforced Concrete Frame Structures with Nonductile Details, Part I: Summary of Experimental Findings of Full Scale Beam-Column Joint Tests," by A. Beres, R.N. White and P. Gergely, 9/30/92, (PB93-227783, A05, MF-A01).
- NGEER-92-0025 "Experimental Results of Repaired and Retrofitted Beam-Column Joint Tests in Lightly Reinforced Concrete Frame Buildings," by A. Beres, S. El-Borgi, R.N. White and P. Gergely, 10/29/92, (PB93-227791, A05, MF-A01).
- NCEER-92-0026 "A Generalization of Optimal Control Theory: Linear and Nonlinear Structures," by J.N. Yang, Z. Li and S. Vongchavalitkul, 11/2/92, (PB93-188621, A05, MF-A01).
- NCEER-92-0027 "Seismic Resistance of Reinforced Concrete Frame Structures Designed Only for Gravity Loads: Part I - Design and Properties of a One-Third Scale Model Structure," by J.M. Bracci, A.M. Reinhorn and J.B. Mander, 12/1/92, (PB94-104502, A08, MF-A02).
- NCEER-92-0028 "Seismic Resistance of Reinforced Concrete Frame Structures Designed Only for Gravity Loads: Part II - Experimental Performance of Subassemblages," by L.E. Aycardi, J.B. Mander and A.M. Reinhorn, 12/1/92, (PB94-104510, A08, MF-A02).
- NCEER-92-0029 "Seismic Resistance of Reinforced Concrete Frame Structures Designed Only for Gravity Loads: Part III - Experimental Performance and Analytical Study of a Structural Model," by J.M. Bracci, A.M. Reinhorn and J.B. Mander, 12/1/92, (PB93-227528, A09, MF-A01).
- NCEER-92-0030 "Evaluation of Seismic Retrofit of Reinforced Concrete Frame Structures: Part I - Experimental Performance of Retrofitted Subassemblages," by D. Choudhuri, J.B. Mander and A.M. Reinhorn, 12/8/92, (PB93-198307, A07, MF-A02).

- NCEER-92-0031 "Evaluation of Seismic Retrofit of Reinforced Concrete Frame Structures: Part II - Experimental Performance and Analytical Study of a Retrofitted Structural Model," by J.M. Bracci, A.M. Reinhorn and J.B. Mander, 12/8/92, (PB93-198315, A09, MF-A03).
- NCEER-92-0032 "Experimental and Analytical Investigation of Seismic Response of Structures with Supplemental Fluid Viscous Dampers," by M.C. Constantinou and M.D. Symans, 12/21/92, (PB93-191435, A10, MF-A03).
- NCEER-92-0033 "Reconnaissance Report on the Cairo, Egypt Earthquake of October 12, 1992," by M. Khater, 12/23/92, (PB93-188621, A03, MF-A01).
- NCEER-92-0034 "Low-Level Dynamic Characteristics of Four Tall Flat-Plate Buildings in New York City," by H. Gavin, S. Yuan, J. Grossman, E. Pekelis and K. Jacob, 12/28/92, (PB93-188217, A07, MF-A02).
- NCEER-93-0001 "An Experimental Study on the Seismic Performance of Brick-Infilled Steel Frames With and Without Retrofit," by J.B. Mander, B. Nair, K. Wojtkowski and J. Ma, 1/29/93, (PB93-227510, A07, MF-A02).
- NCEER-93-0002 "Social Accounting for Disaster Preparedness and Recovery Planning," by S. Cole, E. Pantoja and V. Razak, 2/22/93, (PB94-142114, A12, MF-A03).
- NCEER-93-0003 "Assessment of 1991 NEHRP Provisions for Nonstructural Components and Recommended Revisions," by T.T. Soong, G. Chen, Z. Wu, R-H. Zhang and M. Grigoriu, 3/1/93, (PB93-188639, A06, MF-A02).
- NCEER-93-0004 "Evaluation of Static and Response Spectrum Analysis Procedures of SEAOC/UBC for Seismic Isolated Structures," by C.W. Winters and M.C. Constantinou, 3/23/93, (PB93-198299, A10, MF-A03).
- NCEER-93-0005 "Earthquakes in the Northeast - Are We Ignoring the Hazard? A Workshop on Earthquake Science and Safety for Educators," edited by K.E.K. Ross, 4/2/93, (PB94-103066, A09, MF-A02).
- NCEER-93-0006 "Inelastic Response of Reinforced Concrete Structures with Viscoelastic Braces," by R.F. Lobo, J.M. Bracci, K.L. Shen, A.M. Reinhorn and T.T. Soong, 4/5/93, (PB93-227486, A05, MF-A02).
- NCEER-93-0007 "Seismic Testing of Installation Methods for Computers and Data Processing Equipment," by K. Kosar, T.T. Soong, K.L. Shen, J.A. HoLung and Y.K. Lin, 4/12/93, (PB93-198299, A07, MF-A02).
- NCEER-93-0008 "Retrofit of Reinforced Concrete Frames Using Added Dampers," by A. Reinhorn, M. Constantinou and C. Li, to be published.
- NCEER-93-0009 "Seismic Behavior and Design Guidelines for Steel Frame Structures with Added Viscoelastic Dampers," by K.C. Chang, M.L. Lai, T.T. Soong, D.S. Hao and Y.C. Yeh, 5/1/93, (PB94-141959, A07, MF-A02).
- NCEER-93-0010 "Seismic Performance of Shear-Critical Reinforced Concrete Bridge Piers," by J.B. Mander, S.M. Waheed, M.T.A. Chaudhary and S.S. Chen, 5/12/93, (PB93-227494, A08, MF-A02).
- NCEER-93-0011 "3D-BASIS-TABS: Computer Program for Nonlinear Dynamic Analysis of Three Dimensional Base Isolated Structures," by S. Nagarajaiah, C. Li, A.M. Reinhorn and M.C. Constantinou, 8/2/93, (PB94-141819, A09, MF-A02).
- NCEER-93-0012 "Effects of Hydrocarbon Spills from an Oil Pipeline Break on Ground Water," by O.J. Helweg and H.H.M. Hwang, 8/3/93, (PB94-141942, A06, MF-A02).
- NCEER-93-0013 "Simplified Procedures for Seismic Design of Nonstructural Components and Assessment of Current Code Provisions," by M.P. Singh, L.E. Suarez, E.E. Matheu and G.O. Maldonado, 8/4/93, (PB94-141827, A09, MF-A02).
- NCEER-93-0014 "An Energy Approach to Seismic Analysis and Design of Secondary Systems," by G. Chen and T.T. Soong, 8/6/93, (PB94-142767, A11, MF-A03).

- NCEER-93-0015 "Proceedings from School Sites: Becoming Prepared for Earthquakes - Commemorating the Third Anniversary of the Loma Prieta Earthquake," Edited by F.E. Winslow and K.E.K. Ross, 8/16/93, (PB94-154275, A16, MF-A02).
- NCEER-93-0016 "Reconnaissance Report of Damage to Historic Monuments in Cairo, Egypt Following the October 12, 1992 Dahshur Earthquake," by D. Sykora, D. Look, G. Croci, E. Karaesmen and E. Karaesmen, 8/19/93, (PB94-142221, A08, MF-A02).
- NCEER-93-0017 "The Island of Guam Earthquake of August 8, 1993," by S.W. Swan and S.K. Harris, 9/30/93, (PB94-141843, A04, MF-A01).
- NCEER-93-0018 "Engineering Aspects of the October 12, 1992 Egyptian Earthquake," by A.W. Elgamal, M. Amer, K. Adalier and A. Abul-Fadl, 10/7/93, (PB94-141983, A05, MF-A01).
- NCEER-93-0019 "Development of an Earthquake Motion Simulator and its Application in Dynamic Centrifuge Testing," by I. Krstelj, Supervised by J.H. Prevost, 10/23/93, (PB94-181773, A-10, MF-A03).
- NCEER-93-0020 "NCEER-Taisei Corporation Research Program on Sliding Seismic Isolation Systems for Bridges: Experimental and Analytical Study of a Friction Pendulum System (FPS)," by M.C. Constantinou, P. Tsopelas, Y-S. Kim and S. Okamoto, 11/1/93, (PB94-142775, A08, MF-A02).
- NCEER-93-0021 "Finite Element Modeling of Elastomeric Seismic Isolation Bearings," by L.J. Billings, Supervised by R. Shepherd, 11/8/93, to be published.
- NCEER-93-0022 "Seismic Vulnerability of Equipment in Critical Facilities: Life-Safety and Operational Consequences," by K. Porter, G.S. Johnson, M.M. Zadeh, C. Scawthorn and S. Eder, 11/24/93, (PB94-181765, A16, MF-A03).
- NCEER-93-0023 "Hokkaido Nansei-oki, Japan Earthquake of July 12, 1993, by P.I. Yanev and C.R. Scawthorn, 12/23/93, (PB94-181500, A07, MF-A01).
- NCEER-94-0001 "An Evaluation of Seismic Serviceability of Water Supply Networks with Application to the San Francisco Auxiliary Water Supply System," by I. Markov, Supervised by M. Grigoriu and T. O'Rourke, 1/21/94, (PB94-204013, A07, MF-A02).
- NCEER-94-0002 "NCEER-Taisei Corporation Research Program on Sliding Seismic Isolation Systems for Bridges: Experimental and Analytical Study of Systems Consisting of Sliding Bearings, Rubber Restoring Force Devices and Fluid Dampers," Volumes I and II, by P. Tsopelas, S. Okamoto, M.C. Constantinou, D. Ozaki and S. Fujii, 2/4/94, (PB94-181740, A09, MF-A02 and PB94-181757, A12, MF-A03).
- NCEER-94-0003 "A Markov Model for Local and Global Damage Indices in Seismic Analysis," by S. Rahman and M. Grigoriu, 2/18/94, (PB94-206000, A12, MF-A03).
- NCEER-94-0004 "Proceedings from the NCEER Workshop on Seismic Response of Masonry Infills," edited by D.P. Abrams, 3/1/94, (PB94-180783, A07, MF-A02).
- NCEER-94-0005 "The Northridge, California Earthquake of January 17, 1994: General Reconnaissance Report," edited by J.D. Goltz, 3/11/94, (PB193943, A10, MF-A03).
- NCEER-94-0006 "Seismic Energy Based Fatigue Damage Analysis of Bridge Columns: Part I - Evaluation of Seismic Capacity," by G.A. Chang and J.B. Mander, 3/14/94, (PB94-219185, A11, MF-A03).
- NCEER-94-0007 "Seismic Isolation of Multi-Story Frame Structures Using Spherical Sliding Isolation Systems," by T.M. Al-Hussaini, V.A. Zayas and M.C. Constantinou, 3/17/94, (PB193745, A09, MF-A02).

- NCEER-94-0008 "The Northridge, California Earthquake of January 17, 1994: Performance of Highway Bridges," edited by I.G. Buckle, 3/24/94, (PB94-193851, A06, MF-A02).
- NCEER-94-0009 "Proceedings of the Third U.S.-Japan Workshop on Earthquake Protective Systems for Bridges," edited by I.G. Buckle and I. Friedland, 3/31/94, (PB94-195815, A99, MF-A06).
- NCEER-94-0010 "3D-BASIS-ME: Computer Program for Nonlinear Dynamic Analysis of Seismically Isolated Single and Multiple Structures and Liquid Storage Tanks," by P.C. Tsopelas, M.C. Constantinou and A.M. Reinhorn, 4/12/94, (PB94-204922, A09, MF-A02).
- NCEER-94-0011 "The Northridge, California Earthquake of January 17, 1994: Performance of Gas Transmission Pipelines," by T.D. O'Rourke and M.C. Palmer, 5/16/94, (PB94-204989, A05, MF-A01).
- NCEER-94-0012 "Feasibility Study of Replacement Procedures and Earthquake Performance Related to Gas Transmission Pipelines," by T.D. O'Rourke and M.C. Palmer, 5/25/94, (PB94-206638, A09, MF-A02).
- NCEER-94-0013 "Seismic Energy Based Fatigue Damage Analysis of Bridge Columns: Part II - Evaluation of Seismic Demand," by G.A. Chang and J.B. Mander, 6/1/94, (PB95-18106, A08, MF-A02).
- NCEER-94-0014 "NCEER-Taisei Corporation Research Program on Sliding Seismic Isolation Systems for Bridges: Experimental and Analytical Study of a System Consisting of Sliding Bearings and Fluid Restoring Force/Damping Devices," by P. Tsopelas and M.C. Constantinou, 6/13/94, (PB94-219144, A10, MF-A03).
- NCEER-94-0015 "Generation of Hazard-Consistent Fragility Curves for Seismic Loss Estimation Studies," by H. Hwang and J-R. Huo, 6/14/94, (PB95-181996, A09, MF-A02).
- NCEER-94-0016 "Seismic Study of Building Frames with Added Energy-Absorbing Devices," by W.S. Pong, C.S. Tsai and G.C. Lee, 6/20/94, (PB94-219136, A10, A03).
- NCEER-94-0017 "Sliding Mode Control for Seismic-Excited Linear and Nonlinear Civil Engineering Structures," by J. Yang, J. Wu, A. Agrawal and Z. Li, 6/21/94, (PB95-138483, A06, MF-A02).
- NCEER-94-0018 "3D-BASIS-TABS Version 2.0: Computer Program for Nonlinear Dynamic Analysis of Three Dimensional Base Isolated Structures," by A.M. Reinhorn, S. Nagarajaiah, M.C. Constantinou, P. Tsopelas and R. Li, 6/22/94, (PB95-182176, A08, MF-A02).
- NCEER-94-0019 "Proceedings of the International Workshop on Civil Infrastructure Systems: Application of Intelligent Systems and Advanced Materials on Bridge Systems," Edited by G.C. Lee and K.C. Chang, 7/18/94, (PB95-252474, A20, MF-A04).
- NCEER-94-0020 "Study of Seismic Isolation Systems for Computer Floors," by V. Lambrou and M.C. Constantinou, 7/19/94, (PB95-138533, A10, MF-A03).
- NCEER-94-0021 "Proceedings of the U.S.-Italian Workshop on Guidelines for Seismic Evaluation and Rehabilitation of Unreinforced Masonry Buildings," Edited by D.P. Abrams and G.M. Calvi, 7/20/94, (PB95-138749, A13, MF-A03).
- NCEER-94-0022 "NCEER-Taisei Corporation Research Program on Sliding Seismic Isolation Systems for Bridges: Experimental and Analytical Study of a System Consisting of Lubricated PTFE Sliding Bearings and Mild Steel Dampers," by P. Tsopelas and M.C. Constantinou, 7/22/94, (PB95-182184, A08, MF-A02).
- NCEER-94-0023 "Development of Reliability-Based Design Criteria for Buildings Under Seismic Load," by Y.K. Wen, H. Hwang and M. Shinozuka, 8/1/94, (PB95-211934, A08, MF-A02).

- NCEER-94-0024 "Experimental Verification of Acceleration Feedback Control Strategies for an Active Tendon System," by S.J. Dyke, B.F. Spencer, Jr., P. Quast, M.K. Sain, D.C. Kaspari, Jr. and T.T. Soong, 8/29/94, (PB95-212320, A05, MF-A01).
- NCEER-94-0025 "Seismic Retrofitting Manual for Highway Bridges," Edited by I.G. Buckle and I.F. Friedland, to be published.
- NCEER-94-0026 "Proceedings from the Fifth U.S.-Japan Workshop on Earthquake Resistant Design of Lifeline Facilities and Countermeasures Against Soil Liquefaction," Edited by T.D. O'Rourke and M. Hamada, 11/7/94, (PB95-220802, A99, MF-E08).
- NCEER-95-0001 "Experimental and Analytical Investigation of Seismic Retrofit of Structures with Supplemental Damping: Part 1 - Fluid Viscous Damping Devices," by A.M. Reinhorn, C. Li and M.C. Constantinou, 1/3/95, (PB95-266599, A09, MF-A02).
- NCEER-95-0002 "Experimental and Analytical Study of Low-Cycle Fatigue Behavior of Semi-Rigid Top-And-Seat Angle Connections," by G. Pekcan, J.B. Mander and S.S. Chen, 1/5/95, (PB95-220042, A07, MF-A02).
- NCEER-95-0003 "NCEER-ATC Joint Study on Fragility of Buildings," by T. Anagnos, C. Rojahn and A.S. Kiremidjian, 1/20/95, (PB95-220026, A06, MF-A02).
- NCEER-95-0004 "Nonlinear Control Algorithms for Peak Response Reduction," by Z. Wu, T.T. Soong, V. Gattulli and R.C. Lin, 2/16/95, (PB95-220349, A05, MF-A01).
- NCEER-95-0005 "Pipeline Replacement Feasibility Study: A Methodology for Minimizing Seismic and Corrosion Risks to Underground Natural Gas Pipelines," by R.T. Eguchi, H.A. Seligson and D.G. Honegger, 3/2/95, (PB95-252326, A06, MF-A02).
- NCEER-95-0006 "Evaluation of Seismic Performance of an 11-Story Frame Building During the 1994 Northridge Earthquake," by F. Naeim, R. DiSulio, K. Benuska, A. Reinhorn and C. Li, to be published.
- NCEER-95-0007 "Prioritization of Bridges for Seismic Retrofitting," by N. Basöz and A.S. Kiremidjian, 4/24/95, (PB95-252300, A08, MF-A02).
- NCEER-95-0008 "Method for Developing Motion Damage Relationships for Reinforced Concrete Frames," by A. Singhal and A.S. Kiremidjian, 5/11/95, (PB95-266607, A06, MF-A02).
- NCEER-95-0009 "Experimental and Analytical Investigation of Seismic Retrofit of Structures with Supplemental Damping: Part II - Friction Devices," by C. Li and A.M. Reinhorn, 7/6/95, (PB96-128087, A11, MF-A03).
- NCEER-95-0010 "Experimental Performance and Analytical Study of a Non-Ductile Reinforced Concrete Frame Structure Retrofitted with Elastomeric Spring Dampers," by G. Pekcan, J.B. Mander and S.S. Chen, 7/14/95, (PB96-137161, A08, MF-A02).
- NCEER-95-0011 "Development and Experimental Study of Semi-Active Fluid Damping Devices for Seismic Protection of Structures," by M.D. Symans and M.C. Constantinou, 8/3/95, (PB96-136940, A23, MF-A04).
- NCEER-95-0012 "Real-Time Structural Parameter Modification (RSPM): Development of Innervated Structures," by Z. Liang, M. Tong and G.C. Lee, 4/11/95, (PB96-137153, A06, MF-A01).
- NCEER-95-0013 "Experimental and Analytical Investigation of Seismic Retrofit of Structures with Supplemental Damping: Part III - Viscous Damping Walls," by A.M. Reinhorn and C. Li, 10/1/95, (PB96-176409, A11, MF-A03).
- NCEER-95-0014 "Seismic Fragility Analysis of Equipment and Structures in a Memphis Electric Substation," by J-R. Huo and H.H.M. Hwang, (PB96-128087, A09, MF-A02), 8/10/95.

- NCEER-95-0015 "The Hanshin-Awaji Earthquake of January 17, 1995: Performance of Lifelines," Edited by M. Shinozuka, 11/3/95, (PB96-176383, A15, MF-A03).
- NCEER-95-0016 "Highway Culvert Performance During Earthquakes," by T.L. Youd and C.J. Beckman, 11/6/95, to be published.
- NCEER-95-0017 "The Hanshin-Awaji Earthquake of January 17, 1995: Performance of Highway Bridges," Edited by I.G. Buckle, 12/1/95, to be published.
- NCEER-95-0018 "Modeling of Masonry Infill Panels for Structural Analysis," by A.M. Reinhorn, A. Madan, R.E. Valles, Y. Reichmann and J.B. Mander, 12/8/95.
- NCEER-95-0019 "Optimal Polynomial Control for Linear and Nonlinear Structures," by A.K. Agrawal and J.N. Yang, 12/11/95, (PB96-168737, A07, MF-A02).
- NCEER-95-0020 "Retrofit of Non-Ductile Reinforced Concrete Frames Using Friction Dampers," by R.S. Rao, P. Gergely and R.N. White, 12/22/95.





<b>REPORT DOCUMENTATION PAGE</b>		1. REPORT NO. NCEER-95-0020	2.
4. Title and Subtitle  Retrofit of Non-Ductile Reinforced Concrete Frames Using Friction Dampers		5. Report Date December 22, 1995	
7. Author(s) R.S. Rao, P. Gergely and R.N. White		6.	
9. Performing Organization Name and Address Cornell University School of Civil and Environmental Engineering Hollister Hall Ithaca, New York 14853-3501		8. Performing Organization Rept. No.	
		10. Project/Task/Work Unit No.	
		11. Contract(C) or Grant(G) No. (C) BCS 90-25010 (G) NEC-91029	
12. Sponsoring Organization Name and Address National Center for Earthquake Engineering Research State University of New York at Buffalo Red Jacket Quadrangle Buffalo, New York 14261		13. Type of Report & Period Covered Technical report	
		14.	
15. Supplementary Notes This research was conducted at Cornell University and was supported in whole or in part by the National Science Foundation under Grant No. BCS 90-25010 and the New York State Science and Technology Foundation under Grant No. NEC-91029.			
16. Abstract (Limit: 200 words)  A comprehensive study of evaluation of damping systems using shaking table studies and subsequent modeling has been completed and initial design recommendations were proposed at NCEER. This report extends the knowledge base concerning friction damping devices, suggests design solutions that are feasible from both engineering and economic perspectives, and evaluates the performance of these designs. Moreover, design procedures based on capacity-demand spectra developed in numerous NCEER projects were extended to procedure-specific design guidelines for friction dampers. The experience gained from this project will further enhance newer developments in seismic codes for retrofit of lightly reinforced concrete frames.			
17. Document Analysis a. Descriptors			
b. Identifiers/Open-Ended Terms Earthquake engineering. Friction dampers. Slotted bolted bracing systems. Retrofitting. Friction damped bracing systems. Nonductile concrete frames. Gravity load design. Reinforced concrete frames. Masonry infill walls. Inelastic demand spectra method. Shaking table tests. Time history analysis. Simplified design methods.			
c. COSATI Field/Group			
18. Availability Statement Release unlimited		19. Security Class (This Report) Unclassified	21. No. of Pages 192
		20. Security Class (This Page) Unclassified	22. Price

